N73-18041
NASA TM X-2749

NASA TECHNICAL MEMORANDUM

NASA TM X-2749

ACOUSTIC CHARACTERISTICS OF A SEMISPAN WING EQUIPPED WITH AN EXTERNALLY BLOWN JET FLAP INCLUDING RESULTS AT FORWARD SPEED

by Michael D. Falarski

Ames Research Center

and

U.S. Army Air Mobility R&D Laboratory

Moffett Field, Calif. 94035

NATIONAL AERONAUTICS AND SPACE ADMINISTRATION • WASHINGTON, D. C. • MARCH 1973

1. Report No. NASA TM X-2749	2. Government Accession No.	3. Recipient's Catalog No.
4. Title and Subtitle ACOUSTIC CHARACTERISTICS OF A SEMISPAN WING EQUIPPED WITH AN EXTERNALLY BLOWN JET FLAP INCLUDING RESULTS AT FORWARD SPEED		5. Report Date March 1973 6. Performing Organization Code
7. Author(s) Michael D. Falarski		8. Performing Organization Report No. A–4469
9. Performing Organization Name and Address NASA Ames Research Center and U.S. Army Air Mobility R&D Laboratory Moffett Field, Calif. 94035		10. Work Unit No. 760-72-01-05-00-21 11. Contract or Grant No.
12. Sponsoring Agency Name and Address National Aeronautics and Space Administration Washington, D. C. 20546		13. Type of Report and Period Covered Technical Memorandum 14. Sponsoring Agency Code
15. Supplementary Notes		

16. Abstract

A wind-tunnel investigation was made of the noise characteristics of a 4.42-m (14.5-ft) semispan, externally blown jet flap model. The model was equipped with a single 76.2-cm (30-in.) diameter, ducted fan with a 1.03 pressure ratio. The effects of flap size, fan vertical location, and forward speed on the noise characteristics were studied.

With the ducted fan mounted 0.79 or 1.24 diameters below the wing and a flap chord greater than 50 percent, the peak perceived noise level increased 2 to 3 PndB when the flap was deflected to 90°. The jet scrubbing noise increased 3 to 4 dB when the flap was deflected 90°. Installation of the fan on the wing was responsible for 1 to 2 dB of this change. Forward speed did not have a significant effect on the perceived noise level, although it did cause a reduction in the sound pressure levels of the first and second fan harmonics.

17. Key Words (Suggested by Author(s)) STOL noise EBF STOL Externally blown flap	18. Distribution Statement Unclassified – Unlimited		
19. Security Classif. (of this report) Unclassified	20. Security Classif. (of this page) Unclassified	21. No. of Pages 85	22. Price* $3.00

* For sale by the National Technical Information Service, Springfield, Virginia 22151

NOTATION

b	wing semispan measured from the end plate, m (ft)
$C\mu$	gross thrust coefficient, gross thrust/qS
c_f	flap chord, streamwise, m (ft)
c_w	wing chord, streamwise, m (ft)
D	ducted fan exit diameter, m (ft)
L	lift, N (lb)
PNL	perceived noise level, PNdB
q	free-stream dynamic pressure, N/sq m (lb/sq ft)
R	resultant force, $\sqrt{L^2 + X^2}$, N (lb)
S	wing area, m^2 (ft^2)
SPL	sound pressure level, decibels referenced to 0.0002 microbar
T	ducted fan gross thrust, N (lb)
V_∞	free-stream velocity, knots
X	longitudinal force parallel to thrust axis, N (lb)
Z	vertical location of fan axis with respect to wing chord, cm (in.)
α	angle of attack referenced to wing chord, deg
δ_f	deflection of last flap element referenced to wing chord, deg
θ	angle of the static resultant force vector with respect to the thrust axis, deg

ACOUSTIC CHARACTERISTICS OF A SEMISPAN WING EQUIPPED WITH AN EXTERNALLY BLOWN JET FLAP INCLUDING RESULTS AT FORWARD SPEED

Michael D. Falarski

Ames Research Center
and
U.S. Army Air Mobility R&D Laboratory

SUMMARY

A wind-tunnel investigation was made of the noise characteristics of a 4.42-m (14.5-ft) semispan, externally blown jet flap model. The model was equipped with a single 76.2-cm (30-in.) diameter, ducted fan with a 1.03 pressure ratio. The effects of flap size, fan vertical location, and forward speed on the noise characteristics were studied.

With the ducted fan mounted 0.79 or 1.24 diameters below the wing and a flap chord greater than 50 percent, the peak perceived noise level increased 2 to 3 PNdB when the flap was deflected to 90°. The jet scrubbing noise increased 3 to 4 dB when the flap was deflected 90°. Installation of the fan on the wing was responsible for 1 to 2 dB of this change. Forward speed did not have a significant effect on the perceived noise level, although it did cause a reduction in the sound pressure levels of the first and second fan harmonics.

INTRODUCTION

STOL aircraft will operate from airports within areas of high density population. They will therefore be required to operate at noise levels substantially lower than todays commercial aircraft. For this reason the acoustic as well as the aerodynamic characteristics of the externally blown jet flap (EBF) STOL concept are being investigated. The results of small scale investigation of the noise characteristics of the EBF and several other STOL concepts are reported in reference 1.

This paper presents the results of an investigation undertaken to study the effects of forward speed, flap size, and vertical fan location on the acoustic characteristics of an EBF powered by a low pressure ratio fan. As an acoustic source this type of propulsive device is dominated by the blade-passage tones and not jet exhaust noise.

The model was a 4.42-m (14.5-ft) semispan wing powered by a 76.2-cm (30-in.) diameter ducted fan with a pressure ratio of 1.03. The tests were performed in the Ames 40- by 80-Foot Wind Tunnel.

The longitudinal aerodynamic characteristics were also investigated. They are reported in reference 2.

MODEL DESCRIPTION

Basic Model

Photographs of the model installed in the wind tunnel and model preparation area are shown in figure 1. The basic geometry of the model is presented in figure 2 and table 1. The end plate was attached to the wing, while the fairing was isolated from the model.

The geometry of the ducted fan is presented in figure 3(a) and table 1. The blade plan-form curves for the eight-bladed, 1.03 pressure ratio fan are presented in figure 3(b). The static thrust as a function of fan speed is given in figure 3(c), while the variation of fan gross thrust coefficient with free-stream dynamic pressure is shown in figure 3(d).

Flap System

The three flap systems tested are shown in figure 4(a), and their reference dimensions are given in table 1. Flap I is a large-chord, triple-slotted flap. The geometric details are shown in figure 4(b). This system was made by attaching a modification to the aft flap of flap III. Flap II is a large-chord, double-slotted flap. For this system, the first element of flap I was set at 0°, the first slot sealed, and the remaining two elements deflected. Flap III is a smaller chord, double-slotted flap. Its basic geometry is shown in figure 4(c), and its coordinates are given in tables 2 and 3. This system is very similar to the flap used on the propeller-driven, deflected-slipstream STOL model reported in reference 3.

Ducted Fan Pylons

The model was tested with the ducted fan mounted at three vertical distances below the wing. The duct positions are described in figure 5. Mounted on the long pylon, the fan was 1.25 diameters below the wing chord line. The medium pylon positioned the fan 0.79 diameters below the wing. The cross section of the pylon is also shown in figure 5. With the pylon removed, the fan was mounted 0.33 diameters below the wing, allowing a portion of the fan slipstream to flow over the top of the wing.

TESTS

The tests at forward speed were performed at 0° angle of attack; limited tests were performed at other angles of attack. Gross thrust coefficient $C\mu$ was varied from 0 to 6 by varying free-stream dynamic pressure with the fan rotational speed set at 5000 rpm. The gross thrust was determined from a calibration of fan exit total pressure versus static ducted fan thrust.

The other test variable was flap deflection. Data were recorded at deflections of 0°, 30°, 60°, and 90° for each flap system and pylon.

The static (q = 0 N/m^2) noise characteristics were investigated with the model installed in the 40– by 80-foot wind tunnel model preparation area, as shown in figure 1(b). The microphones were mounted in the spanwise plane of the ducted fan and spaced at 20° increments in a semicircle around the undersurface of the wing (fig. 6). For the wind-tunnel tests, the semicircle radius was 6.1-m (20-ft), while for the static tests it was of 7.62-m (25-ft).

The isolated ducted fan was also tested statically as shown in figure 1(c). In this case, the ducted fan was mounted on the long pylon, which was attached to a steel spar. The upper portion of the spar was wrapped with sound-absorption material to prevent sound reflection.

The noise data was measured with Bruel and Kjaer 1.27-cm (1/2-in.) diameter, type 4133, condenser microphones and recorded on an Ampex F1300A multichannel tape recorder. For the wind-tunnel tests, the microphones were equipped with wind-shield nose cones and oriented into the wind. During the static tests, microphones 1 through 5 were also equipped with the nose cones. In this case, all the microphones were directed at the fan.

CORRECTIONS

The data have been corrected for reverberations in the wind-tunnel test section and model preparation area. The test-section corrections were derived from an acoustic investigation reported in reference 4. Reverberation in the model preparation area was measured with the dodecahedron sound system described in reference 4. These results were used to correct the static test data. The data recorded in the wind tunnel have been extrapolated to 7.62-m (25-ft), equivalent to the static test distance.

Microphones immersed in the relatively high velocity turbulent fan slipstream had high sound pressure levels at low frequency due to the turbulent airflow and vibration. The data reflect this false sound source, so care must be taken in the interpretation of data at low frequencies.

The one-third octave band frequency analysis was computed with a Bruel and Kjaer Real-Time Analyzer. The data were integrated over a period of 30 sec or longer.

RESULTS AND DISCUSSION

Aerodynamic Performance

The static aerodynamic characteristics of the model are presented in figure 7. The configuration with flap I and no pylon had the best static performance. It showed both the highest turning effectiveness and efficiency. Flap II had essentially the same performance up to δ_f = 75, where the upper surface airflow separated, causing a large loss in lift.

Acoustic Characteristics

A complete listing of the acoustic data from this investigation has been reported in reference 5 in the form of tabulated one-third octave band frequency spectrum, overall SPL, and PNL for each microphone of a given test condition. The results of the acoustic studies are given in figures 7 through 21 and described in table 4.

The static ($q = 0$) noise investigation was performed in both the wind tunnel and the model preparation area. The results are compared in figures 8 and 9. Figure 8 compares the PNL directivity patterns for the two tests. In general, the comparison is good, although there is a small loss in directivity due to the wind tunnel reverberant field. There is also good agreement between the one-third octave band frequency spectra of the two tests, as shown in figure 9. Below 500 Hz, the wind-tunnel results tend to be 2 to 3 dB higher than the data recorded in the model preparation area, partly because of the wind-tunnel background noise.

Effect of configuration, $V_\infty = 0$– Figures 10 and 11 show the PNL directivity patterns of the isolated ducted fan and the various configurations investigated. On all configurations deflecting the flap tended to focus the noise and increase the acoustic directivity. Since the fan is pure tone dominated (fig. 12), this is probably caused by the reflections of the pure tones from the wing surface. The major noise lobe was centered at approximately 60° for all flap deflections. The change in peak PNL with flap deflection is presented in figure 13. With no pylon installed, deflection of either flap II or III had no significant effect on peak PNL. With the medium pylon and flap II, the noise increased continuously with δ_f to a ΔPNL = 4 PNdB at $\delta_f = 90°$. Deflecting flaps I and II 60° or more caused an increase of 1 to 2 PNdB when the ducted fan was mounted on the long pylon. With either the medium or long pylon, deflecting flap III caused no change. These increases in PNL with flap deflection are probably the result of noise focusing and reflection from the wing and flap. In general, the data show that PNL can be reduced by moving the fan away from the lower surface, and eliminated by reducing the flap chord or moving the fan so that a portion of its slipstream flows over the wing upper surface.

The primary acoustic source of the low-pressure fan is rotational in nature; therefore, the PNL will be dominated by the fundamental blade passage frequency and its harmonics. This can readily be seen in the one-third octave spectrum in figure 12. Therefore, any change in PNL caused by flap deflection must result from a change in SPL at these frequencies. Figure 14 shows the change in the fundamental and the first two harmonics with δ_f. Variation of PNL with flap deflection was caused by a proportional variation in the fundamental and second harmonic. For the most part the change occurred in the second harmonic because the higher frequency sound contributes more to the PNL. This also results from the fact that reflection is a function of chord to wavelength ratio; therefore, the higher frequency sounds will be directed more than the lower frequency sounds.

Effect of configuration on broadband noise– It can be seen in figure 12 that the broadband noise below 500 Hz increases when the ducted fan is installed on the wing and the flap is deflected. Commonly called "jet scrubbing noise," this noise results from the impingement of the fan exhaust on the wing and flap, and it would become dominant if the fan rotational noise were attenuated. To study this noise source, an overall SPL was computed over only the 12.5- to 500-Hz portion of the spectrum. Figure 15 shows the directivity patterns of the jet scrubbing noise. It can be seen that there is very little directivity. These results are summarized in figure 16. Installation of the fan on

the wing resulted in an increase of 1 to 2 dB. The increases with δ_f were approximately linear. For all configurations the overall increase at $\delta_f = 90°$ was 3 to 4 dB.

Effect of forward speed– The effect of forward speed on the acoustic characteristics was determined in the wind tunnel. The variation of the perceived noise level directivity patterns and boardband noise frequency spectrum are presented in figures 17 and 18, respectively. In the range of forward speeds investigated, there was no discernible trend on either the PNL directivity or broadband frequency spectrum, although SPL of the first and second fan harmonics decreased with increasing forward speed, the greatest change being in the first harmonic (figs. 19 and 20). The reduction tends to be the same for all flap deflections, indicating that it results from an unloading of the fan blades and improvement in inlet flow conditions rather than any influence of the wing.

A limited sample of acoustic data was recorded at angles of attack up to 18°. These results are presented in figure 21 as the variation of PNL and SPL of the fundamental and harmonic tones with angle of attack. The effect on acoustic directivity was investigated with several model azimuthal positions taken with respect to the fan thrust line rather than the microphone position. In the range of angle of attack and forward speeds investigated, there was no evident trend of the effect of angle of attack on the acoustics of the semispan wing, although there were significant changes in the level of the fundamental and harmonic tone sound pressure.

CONCLUDING REMARKS

There is good agreement between static data taken in the model preparation area and in the wind tunnel. There was a slight loss in directivity due to the tunnel reverberant field. This could be more of a problem with a highly directional acoustic source.

When the ducted fan was mounted 0.79 diameter below the wing, the peak PNL increased 4 PndB with flap deflection. This increase was the result of an increase in SPL of the blade-passage frequency and its second harmonic. This effect was eliminated by either reducing the flap chord or moving the ducted fan to a position 0.33 diameter below the wing.

The increase in jet noise due to scrubbing was 3 to 4 dB at $\delta_f = 90°$ for all configurations. Installation of the ducted fan on the wing accounted for 1 to 2 dB of this increase.

Forward speed had no discernible effect on the perceived noise level directivity pattern or the broadband noise of the model. The SPL of the first and second fan harmonics was reduced by the lower fan blade loading and improved inlet flow created by forward speed. This trend was not seen at the fan fundamental frequency.

Ames Research Center
National Aeronautics and Space Administration
and
U. S. Army Air Mobility R & D Laboratory
Moffett Field, Calif. 94035, June 20, 1972

REFERENCES

1. Dorsch, R. G.; Krejsa, E. A.; and Olsen, W. A.: Blown Flap Noise Research. AIAA paper 71-745, 1971.

2. Falarski, M. D.; and Aiken, T. N.: Large-Scale Wind-Tunnel Investigation of a Semispan Wing Equipped With an Externally-Blown Jet Flap. NASA TM X-62,079, 1971.

3. Page, V. R.; Dickinson, S. O.; and Deckert, W. H.: Large-Scale Wind-Tunnel Tests of a Deflected Slipstream STOL Model With Wings of Various Aspect Ratios. NASA TN D-4448, 1968.

4. Bies, David Alan: Investigation of the Feasibility of Making Acoustic Measurements in the NASA Ames 40- by 80-Foot Wind Tunnel. NASA CR-114352, 1971.

5. Falarski, Michael D.: Large-Scale Wind-Tunnel Investigation of the Noise Characteristics of a Semispan Wing Equipped With an Externally-Blown Jet Flap. NASA TM X-62, 154, 1972.

TABLE 1.– REFERENCE DIMENSIONS

Flap I		
Wing area, S, $m^2(ft^2)$		11.0(118.4)
Wing chord, c_w, m(ft)		2.49(8.17)
Flap chord, c_f, m(ft)		1.62(5.30)
c_f/c_w		0.65
c_f/D_S		2.12
Flap II		
Wing area, S, $m^2(ft^2)$		11.0(118.4)
Wing chord, c_w, m(ft)		2.49(8.17)
Flap chord, c_f, m(ft)		1.28(4.19)
c_f/c_w		0.514
c_f/D_S		1.68
Flap III		
Wing area, S, $m^2(ft^2)$		7.40(79.8)
Wing chord, c_w, m(ft)		1.68(5.5)
Flap chord, c_f, m(ft)		0.71(2.31)
c_f/c_w		0.42
c_f/D_S		0.93
Semispan, b, m(ft)		4.42(14.5)
Ducted fan		
Duct		
Inside diameter, m(ft)		0.762(2.5)
Exit diameter, m(ft)		0.762(2.5)
Chord, m(ft)		0.655(2.146)
Fan station, percent of duct chord		35.13
Fan		
Planform curves		See figure 3(b)
Number of blades		8
Hub-to-tip diameter ratio		0.533
Blade angle at tip, deg		30
Approximately blade tip clearance, cm(in)		0.81(0.032)
Pressure ratio		1.03
Pylons	Z, m(ft)	Z/D
Long pylon	0.96(3.13)	1.24
Medium pylon	0.604(1.98)	0.79
No pylon	0.253(0.83)	0.33

TABLE 2.– COORDINATES FOR FLAP III

Fore flap			Aft flap		
Chordwise station	Upper ordinate	Lower ordinate	Chordwise station	Upper ordinate	Lower ordinate
0	0	0	0	0	0
.75	4.50	-6.25	1.16	5.21	-4.18
1.50	6.60	-8.10	2.32	7.36	-5.77
2.50	8.64	-10.00	3.49	8.95	-6.76
3.75	10.75	-11.74	4.65	10.03	-7.54
5.00	12.50	-13.02	6.90	11.61	-8.28
10.00	17.20	-15.75	9.30	12.91	-8.53
15.00	20.70	-16.65	11.61	13.72	-8.39
20.00	23.10	-16.44	13.95	14.37	-8.17
25.00	24.85	-15.90	18.60	14.92	-7.71
30.00	26.15	-15.45	23.22	15.14	-7.29
35.00	26.90	-15.00	34.85	13.24	-6.19
40.00	27.41	-14.55	46.50	10.91	-5.04
45.00	27.72	-14.09	58.10	8.59	-3.94
50.00	27.63	-13.63	69.70	6.19	-2.89
62.10	26.65	-12.88	81.40	3.87	-1.72
63.70	26.50	0	93.00	1.48	-.69
75.00	24.61	12.50	100.00	-.09	-.14
87.50	22.10	17.65			
100.00	19.24	19.00			
L.E. radius = 15.00 Chord = 33.52 cm (13.2 in.)			L.E. radius = 8.39 Chord = 36.06 cm (14.2 in.)		

All dimensions in percent chord

TABLE 3.– BASIC WING COORDINATES

Upper surface		Lower surface	
Chordwise station	Ordinate	Chordwise station	Ordinate
0	0	0	0
.42	1.93	.985	-1.63
.74	2.38	1.37	-1.96
1.39	3.11	2.12	-2.47
3.10	4.45	3.94	-3.33
6.57	6.40	7.52	-4.50
10.05	7.90	11.05	-5.35
13.57	9.13	14.57	-6.01
20.61	11.01	21.55	-6.98
27.75	12.41	28.55	-7.65
34.80	13.41	35.30	-8.05
42.00	14.05	42.47	-8.22
49.00	14.35	49.45	-8.16
57.40	14.30	56.40	-7.87
63.25	13.95	63.35	-7.37
70.25	13.33	70.30	-6.73
77.50	12.49	77.30	-5.88
84.60	11.40	78.70	-5.74
93.80	10.19	84.30	3.94
100.00	8.52	91.30	8.19
		100.00	8.40

Leading-edge radius = 1.171

Chord = 1.194 m (47.0 in.)

All dimensions in percent chord

TABLE IV.– INDEX TO DATA FIGURES

Figure	Pylon	Flap	δ_f	Figure type	Variable	Remarks
7(a)	Medium and long	I-III	~	Aero. char.	δ_f	
(b)	No	↓	↓	↓	↓	
8(a)	↓	II	30	PNL directivity	Test area	
(b)		III	↓	↓	↓	
(c)	Medium	II	↓	↓	↓	
(d)	↓	↓	60	↓	↓	
9(a)	No	↓	30	Spectrum	↓	100° azimuth
(b)	↓	↓	↓	↓	↓	60° azimuth
(c)	↓	III	↓	↓	↓	120° azimuth
(d)	Medium	II	↓	↓	↓	↓
(e)	↓	↓	60	↓	↓	60° azimuth
10	Long	Isolated fan	–	PNL directivity	rpm	
11(a)	No	II	~	↓	δ_f	
(b)	↓	III	↓	↓	↓	
(c)	Medium	II	↓	↓	↓	
(d)	↓	III	↓	↓	↓	
(e)	Long	I	↓	↓	↓	
(f)	↓	II	↓	↓	↓	
(g)	↓	III	↓	↓	↓	
12(a)	Medium	II	↓	Spectrum	↓	60° azimuth
(b)	No	III	↓	↓	↓	↓
13	No, medium, long	I-III	↓	Δpeak PNL	↓	
14(a)	No	III	↓	ΔSPL-harmonic	↓	
(b)	Medium	II	↓	↓	↓	
(c)	↓	III	↓	↓	↓	
(d)	Long	II	↓	↓	↓	
15(a)	Long	Isolated fan	–	Jet noise directivity	rpm	
(b)	No	II	~	↓	δ_f	
(c)	↓	III	↓	↓	↓	
(d)	Medium	II	↓	↓	↓	
(e)	↓	III	↓	↓	↓	
(f)	Long	I	↓	↓	↓	
(g)	↓	III	↓	↓	↓	
16	No, medium, long	I-III	↓	Δjet OASPL	↓	80° azimuth
17(a)	No	II	30	PNL directivity	Forward speed	5000 rpm
(b)	↓	↓	↓	↓	↓	4000 rpm
(c)	↓	↓	60	↓	↓	5000 rpm
(d)	↓	↓	90	↓	↓	4000 rpm
(e)	Medium	↓	30	↓	↓	5000 rpm
(f)	↓	↓	↓	↓	↓	4000 rpm
(g)	↓	↓	60	↓	↓	4000 rpm
(h)	No	III	30	↓	↓	5000 rpm
18(a)	No	II	30	60° azimuth spectrum	↓	5000 rpm
(b)	↓	↓	60	↓	↓	4000 rpm
(c)	↓	↓	90	↓	↓	
(d)	Medium	↓	30	↓	↓	5000 rpm
(e)	↓	↓	60	↓	↓	4000 rpm
(f)	Power off	III	0	↓	↓	–
19(a)	Medium	II	~	–	Forward speed	Fundamental
(b)	↓	↓	↓	↓	↓	First harmonic
(c)	↓	↓	↓	↓	↓	Second harmonic
20(a)	No	↓	↓	↓	↓	Fundamental
(b)	↓	↓	↓	↓	↓	First harmonic
(c)	↓	↓	↓	↓	↓	Second harmonic
21(a)	Medium	↓	60	–	Angle of attack	
(b)	No	↓	60	↓	↓	
(c)	↓	↓	30	↓	↓	

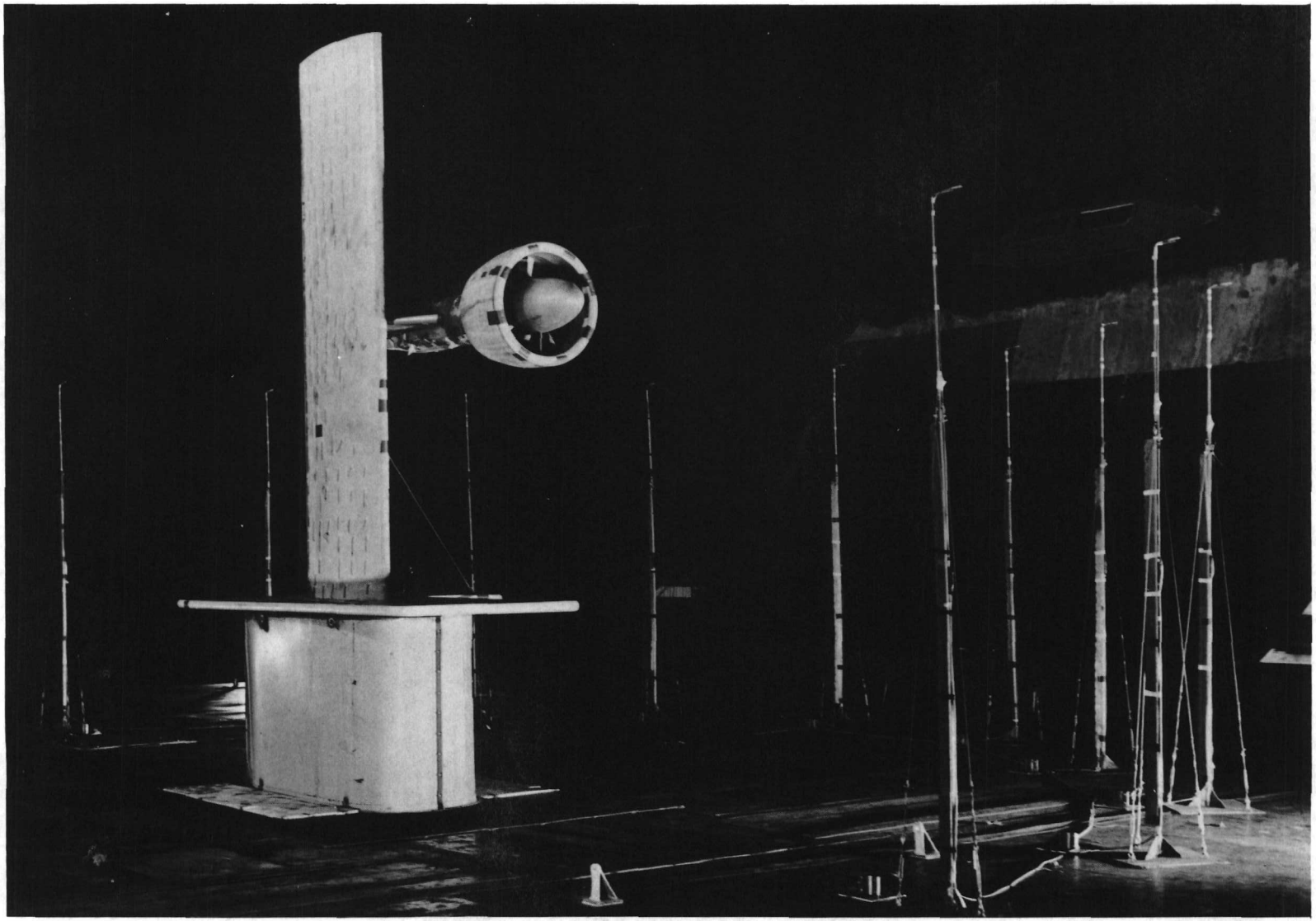

(a) Model installed in the wind tunnel

Figure 1.– Model installation.

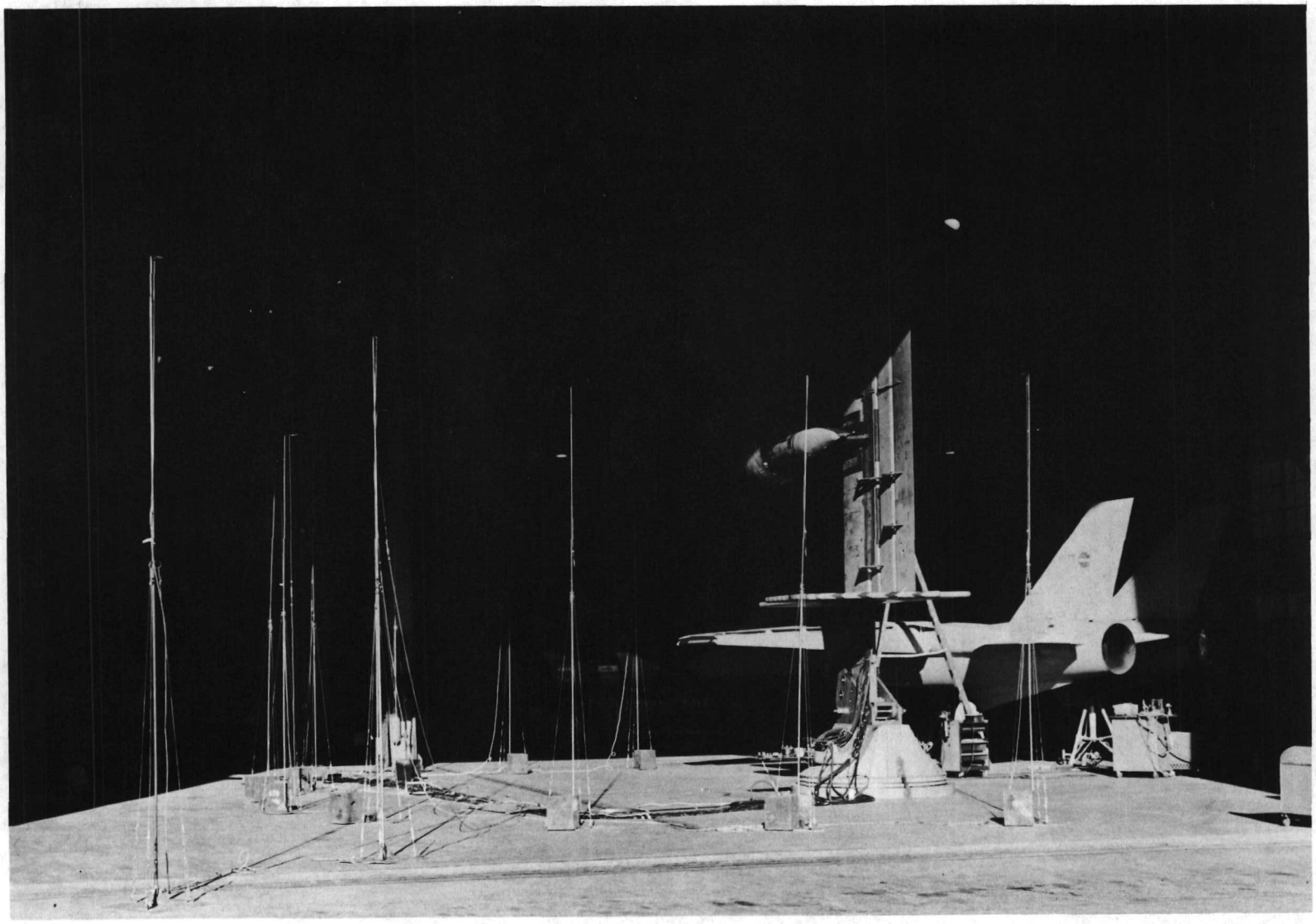

(b) Model installed in the model preparation area.

Figure 1.– Continued.

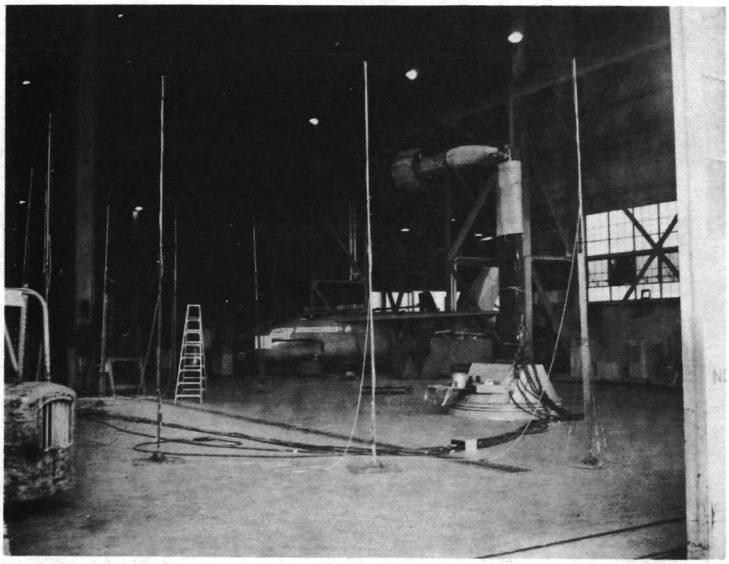

Three-quarter rear view.

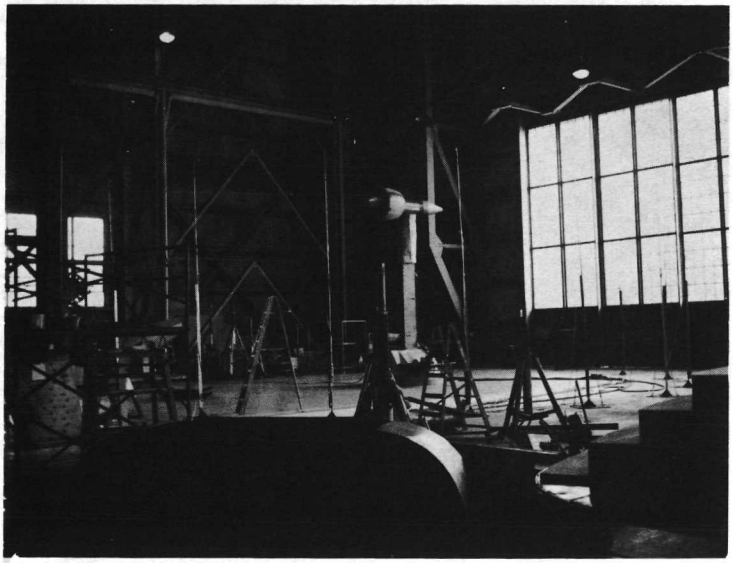

Three-quarter front view

(c) Isolated ducted fan installed in the model preparation area.

Figure 1.– Concluded.

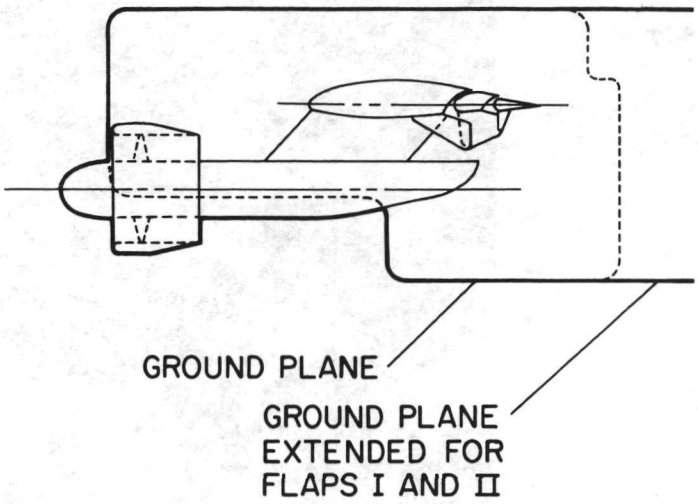

ALL DIMENSIONS IN METERS (INCHES)

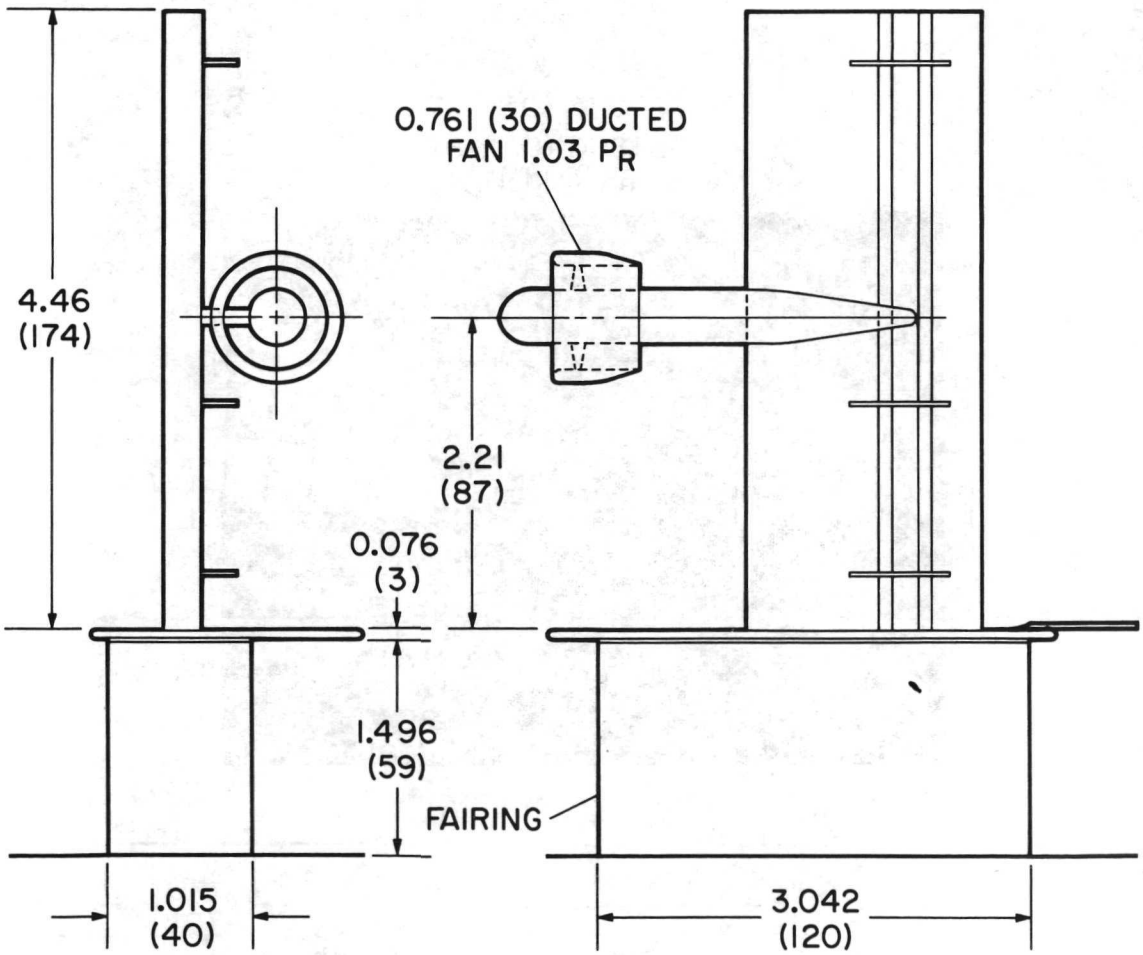

Figure 2.– Basic model geometry.

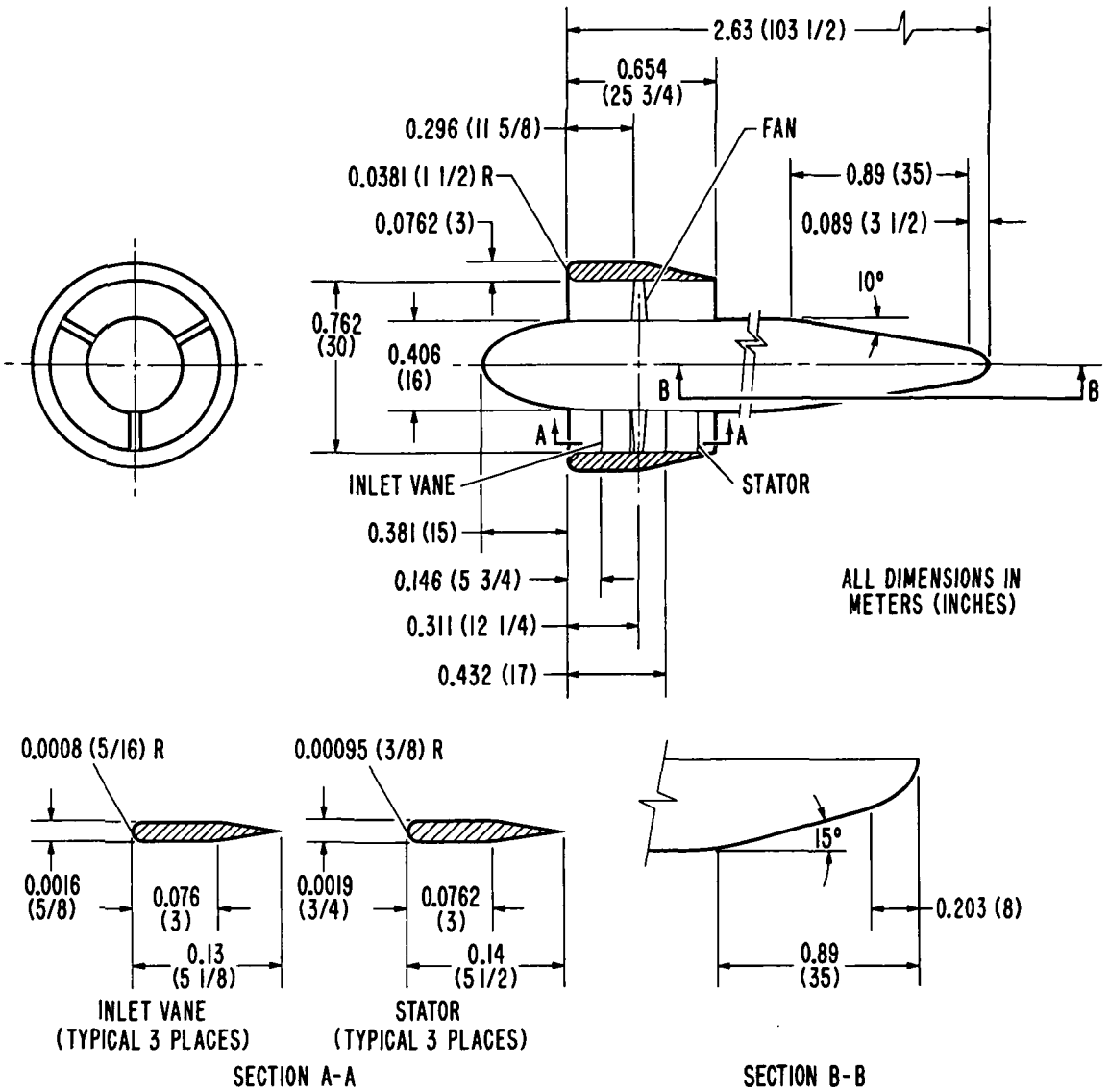

(a) Basic geometry.

Figure 3.—Ducted fan geometry and fan characteristics.

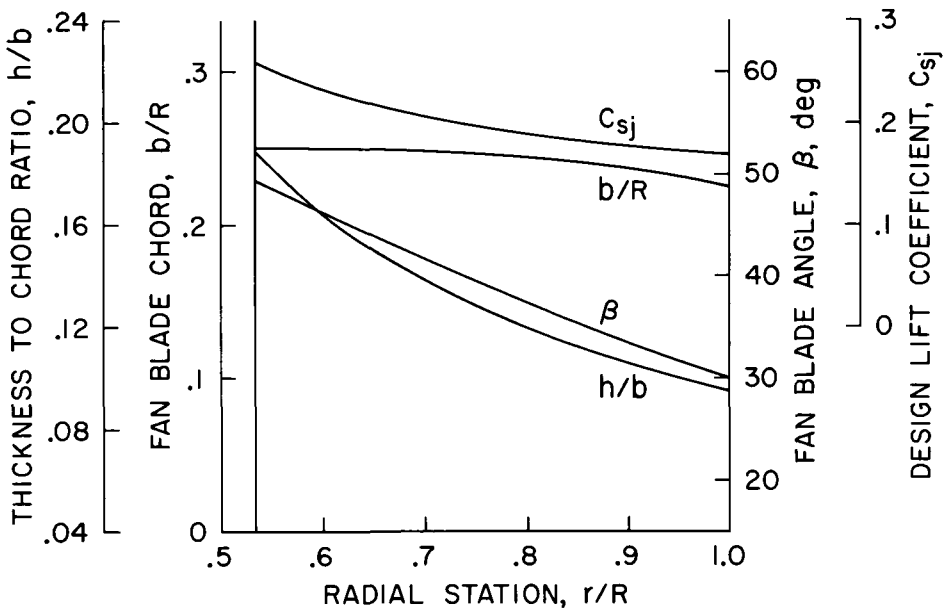

(b) Fan blade plan-form characteristics.

Figure 3.– Continued.

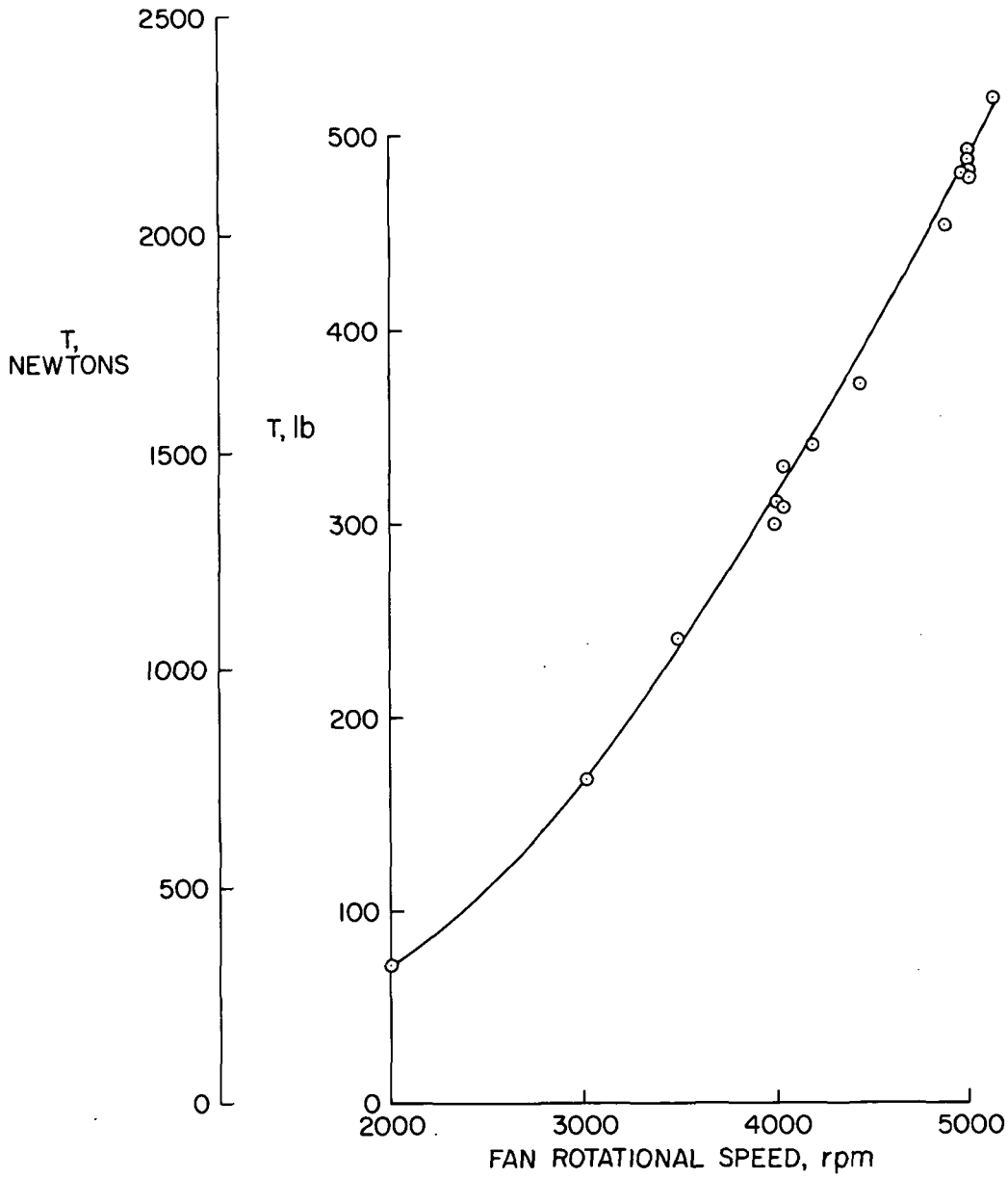

(c) Static thrust as a function of fan speed.

Figure 3.– Continued.

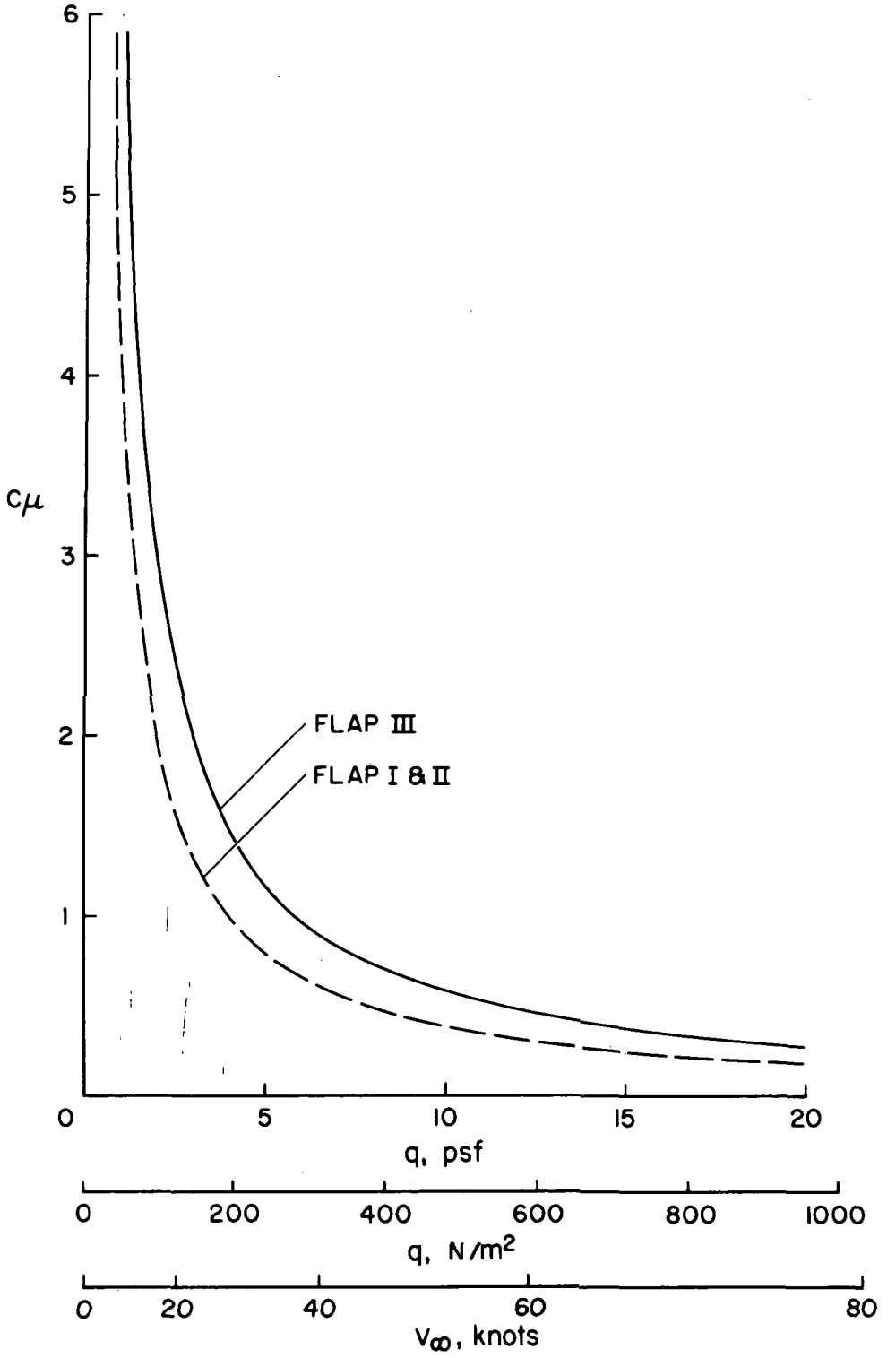

(d) Gross thrust coefficient as a function of α.

Figure 3.– Concluded.

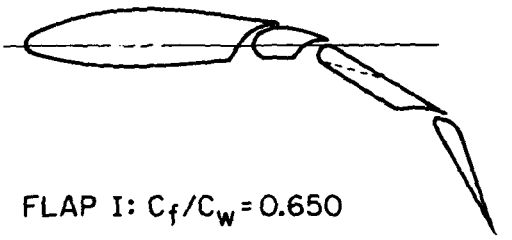

FLAP I: $C_f/C_w = 0.650$

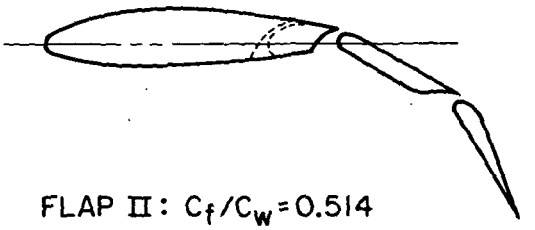

FLAP II: $C_f/C_w = 0.514$

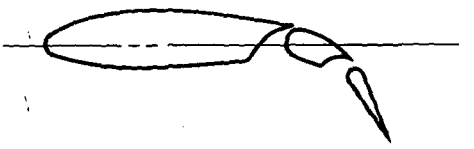

FLAP III: $C_f/C_w = 0.420$

(a) General characteristics.

Figure 4.– Geometry of the flap systems.

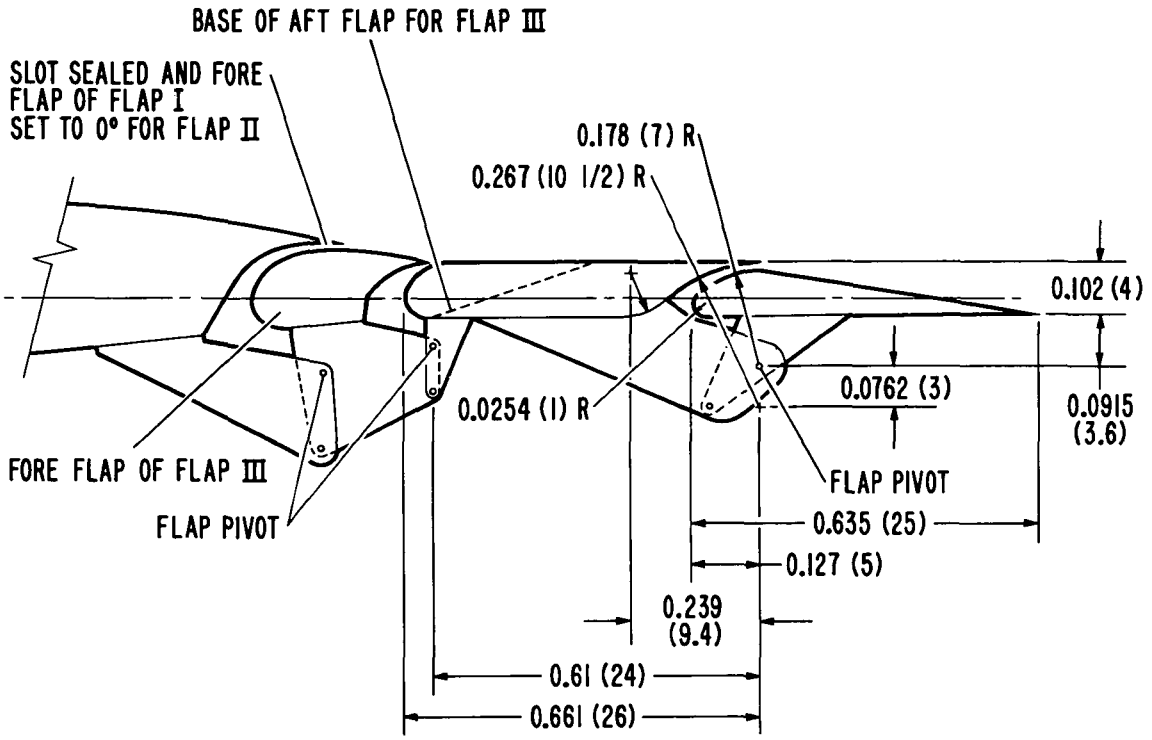

(b) Basic geometry of flaps I and II.

Figure 4.– Continued.

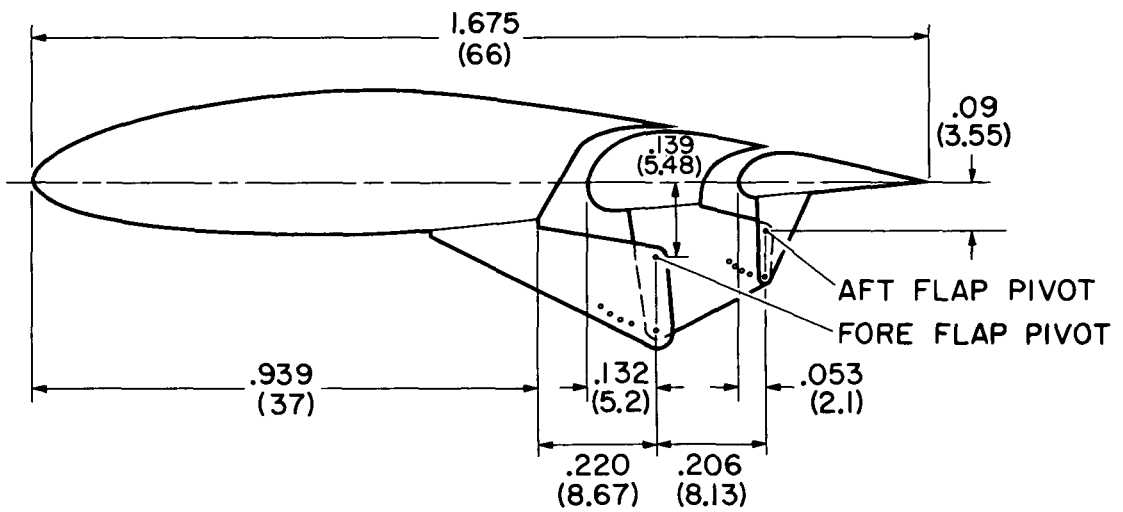

(c) Basic geometry of flap III.

Figure 4.– Concluded.

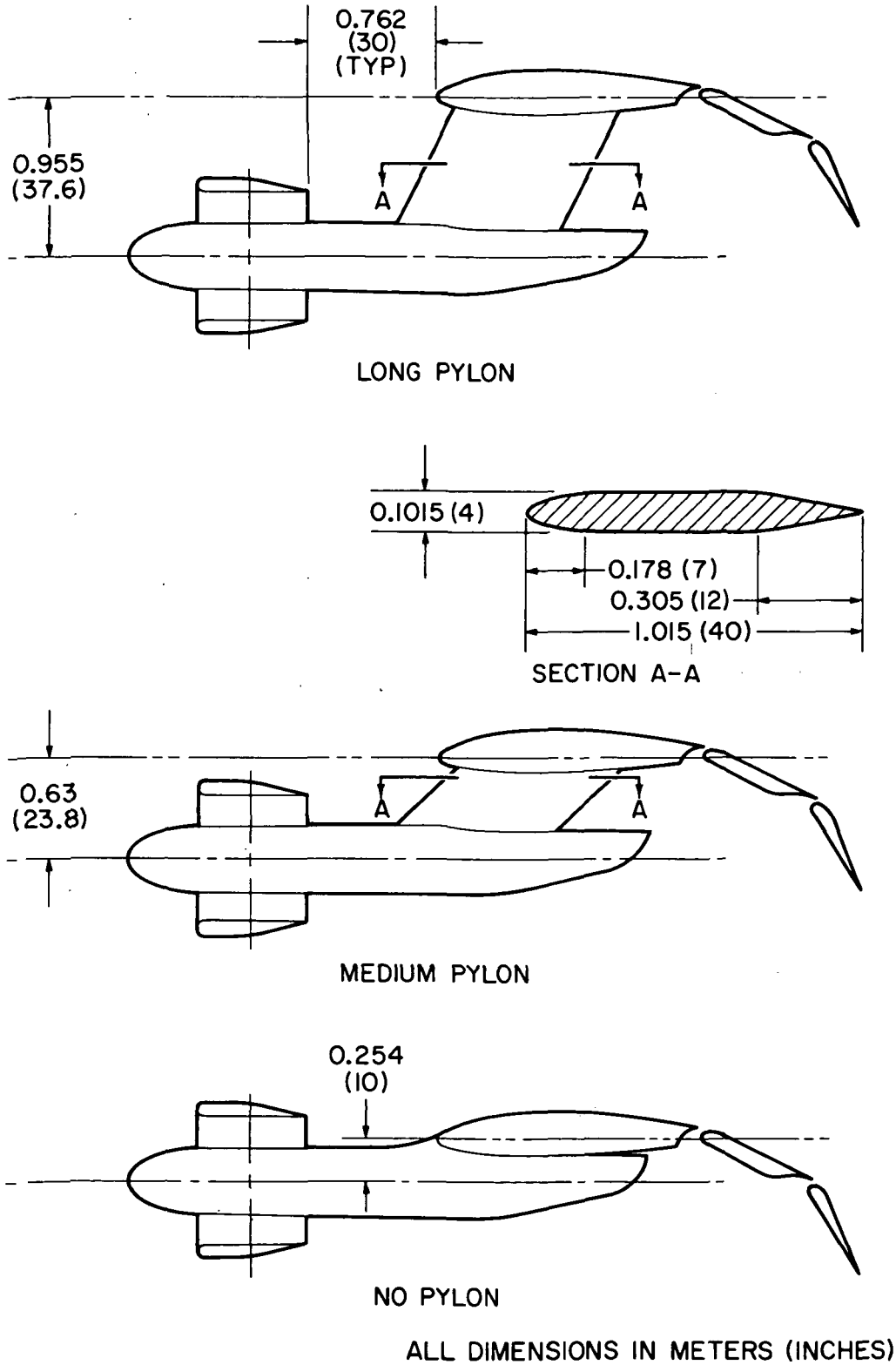

Figure 5.– Geometry of the ducted fan pylons.

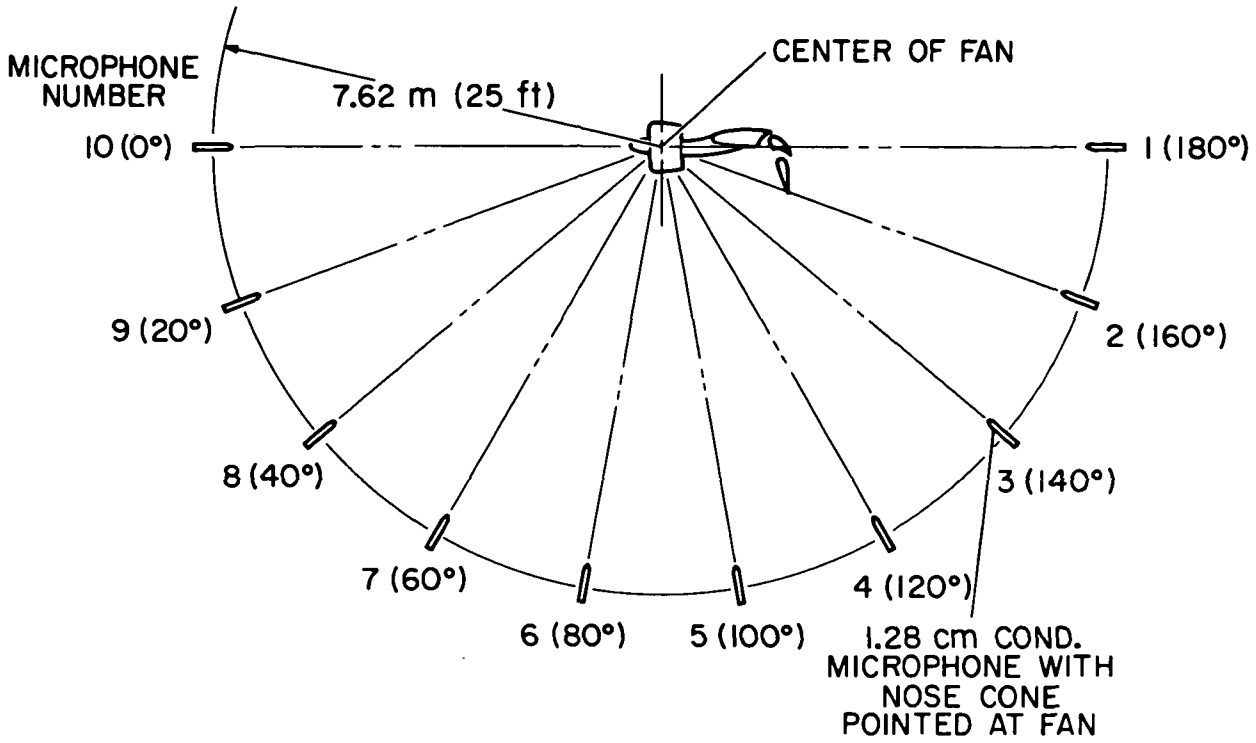

STATIC TEST MICROPHONE ARRANGEMENT

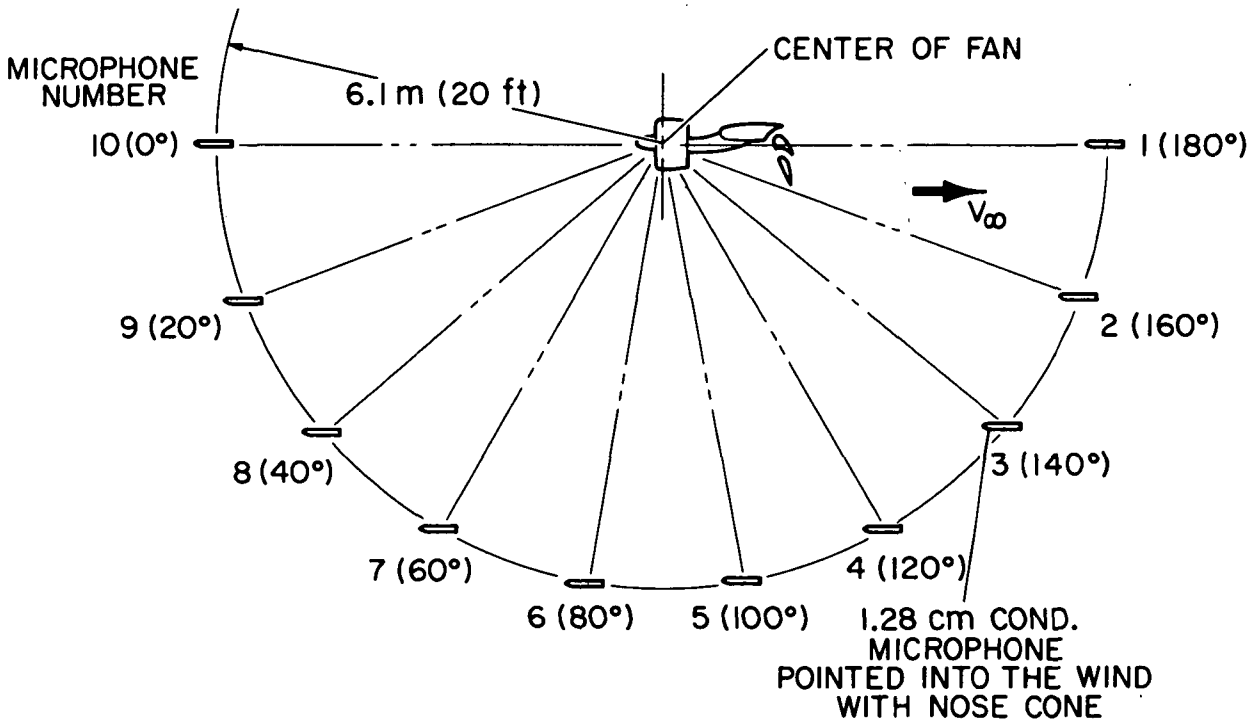

WIND TUNNEL TEST MICROPHONE ARRANGEMENT

Figure 6.– Wind tunnel and static test microphone arrangement.

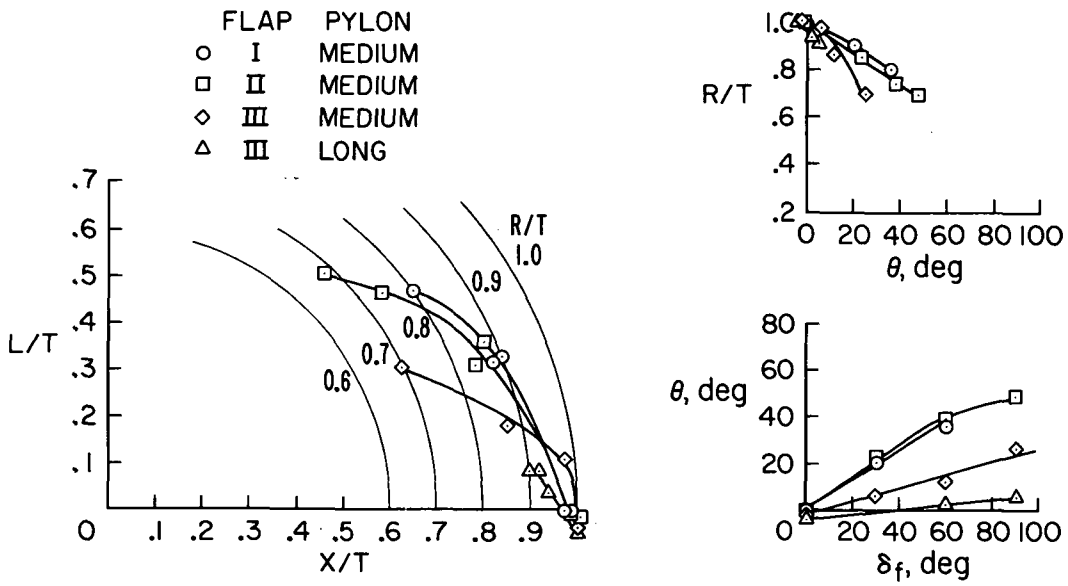

(a) Medium and long pylons.

Figure 7.– Static longitudinal aerodynamic characteristics.

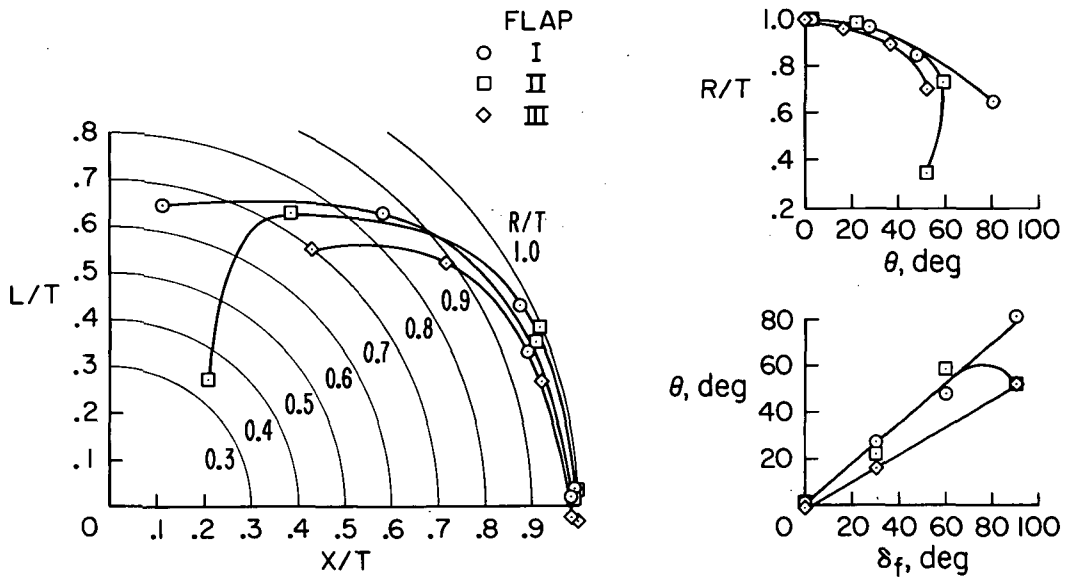

(b) No pylon.

Figure 7.– Concluded.

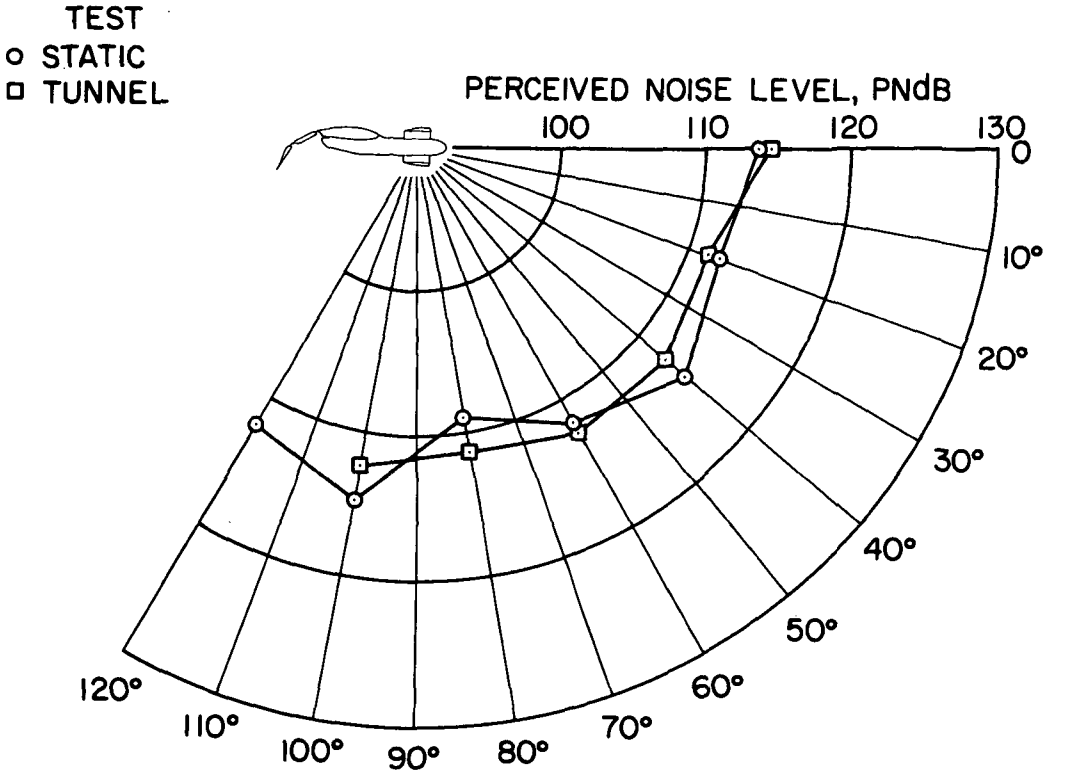

(a) Flap II, $\delta_f = 60°$, no pylon, 4000 rpm.

Figure 8.– Comparison of perceived noise level directivity of the static tests in the model preparation area and wind-tunnel test section.

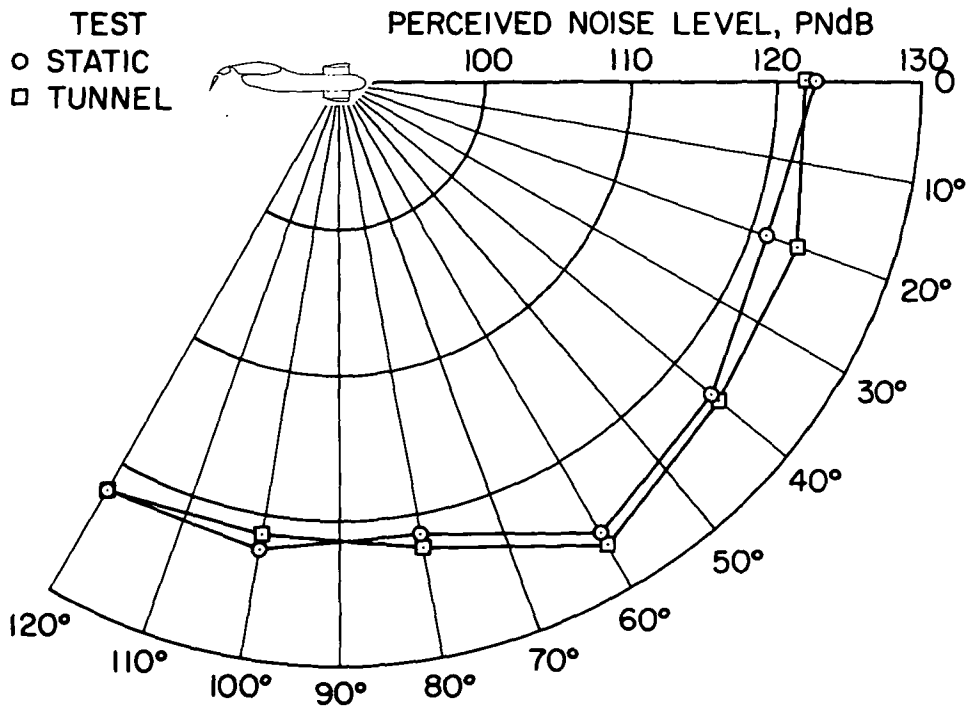

(b) Flap III, $\delta_f = 30°$, no pylon, 5000 rmp, q = 0 psf.

Figure 8.– Continued.

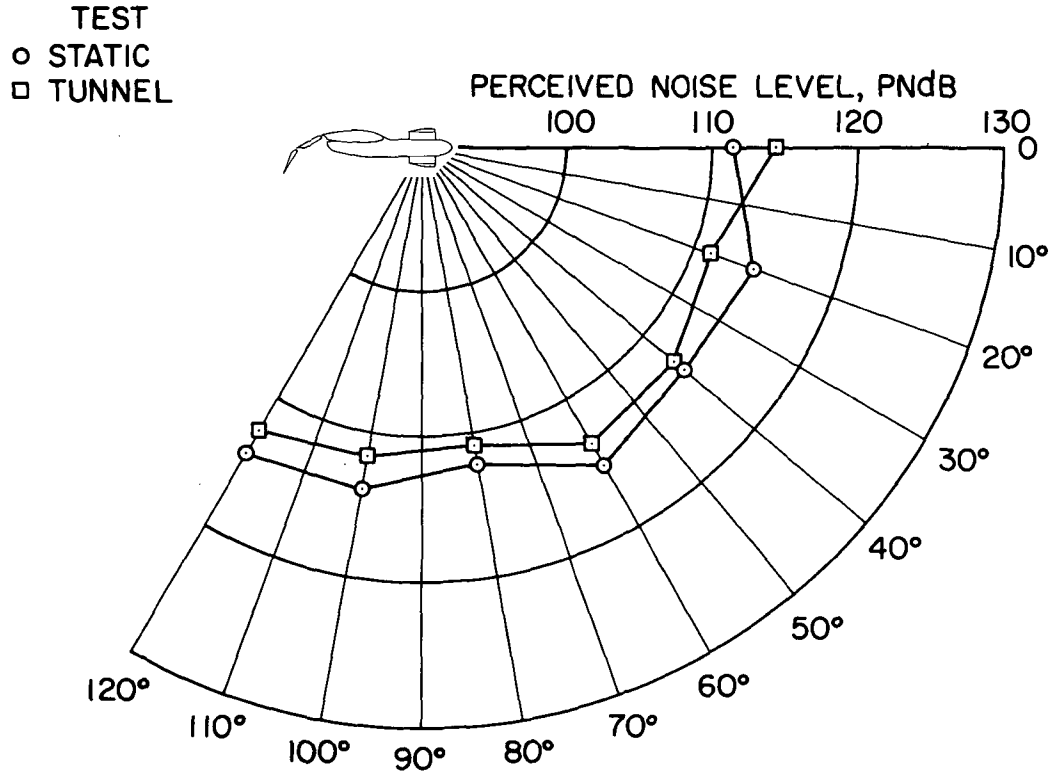

(c) Flap II, $\delta_f = 90°$, no pylon, 4000 rpm.

Figure 8.– Continued.

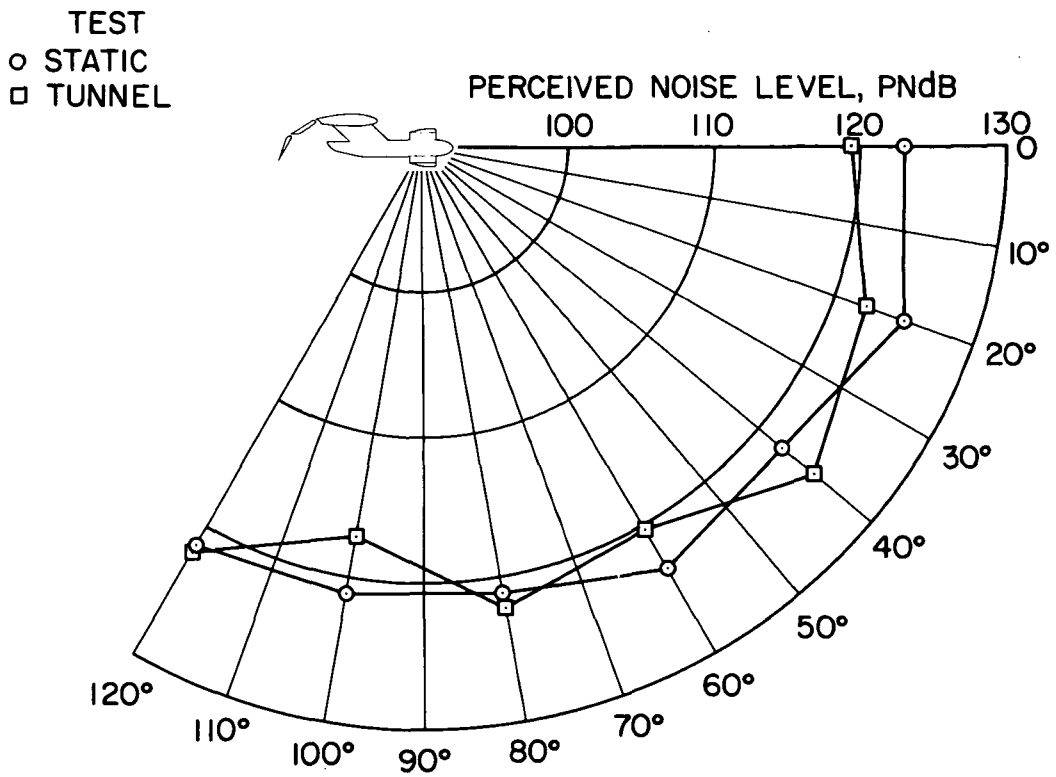

(d) Flap II, $\delta_f = 0°$, medium pylon, 5000 rpm.

Figure 8.– Continued.

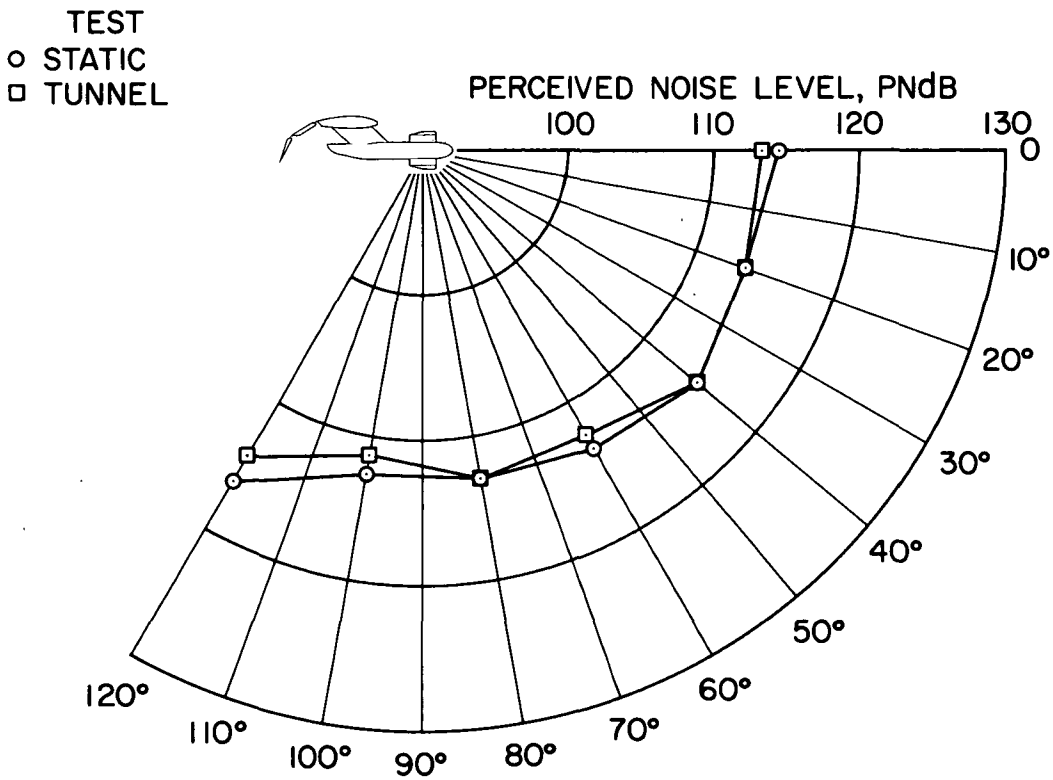

(e) Flap II, $\delta_f = 60^\circ$, medium pylon, 4000 rpm, q = 0 psf.

Figure 8.– Concluded.

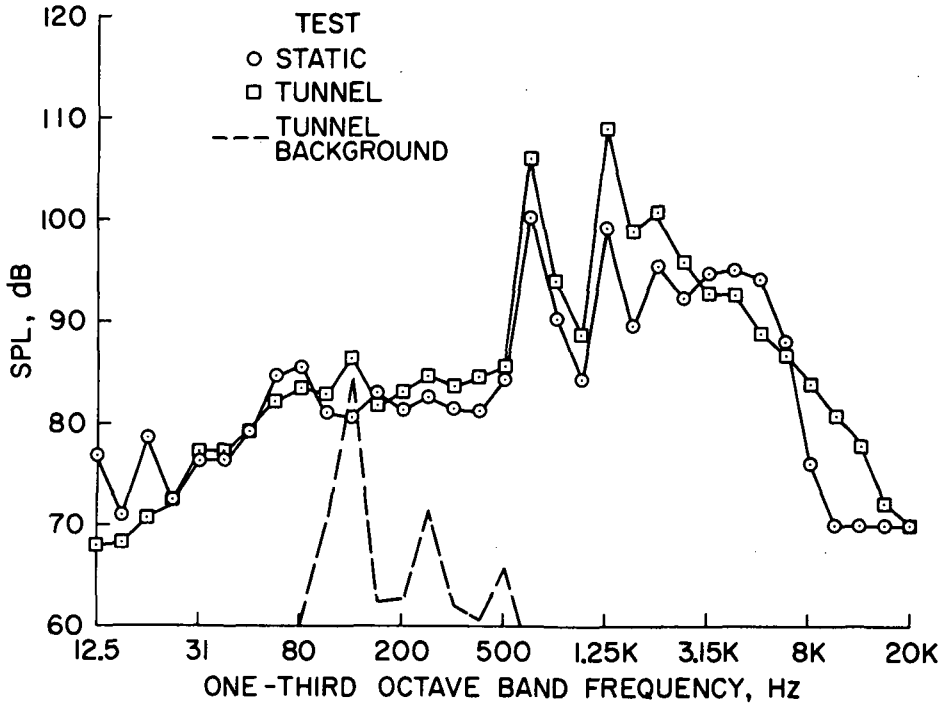

Figure 9.– Comparison of sound frequency spectrum of static tests in the model preparation area and the wind-tunnel test section,

(a) Flap II, $\delta_f = 30°$, no pylon, 5000 rpm, microphone position = 100°.

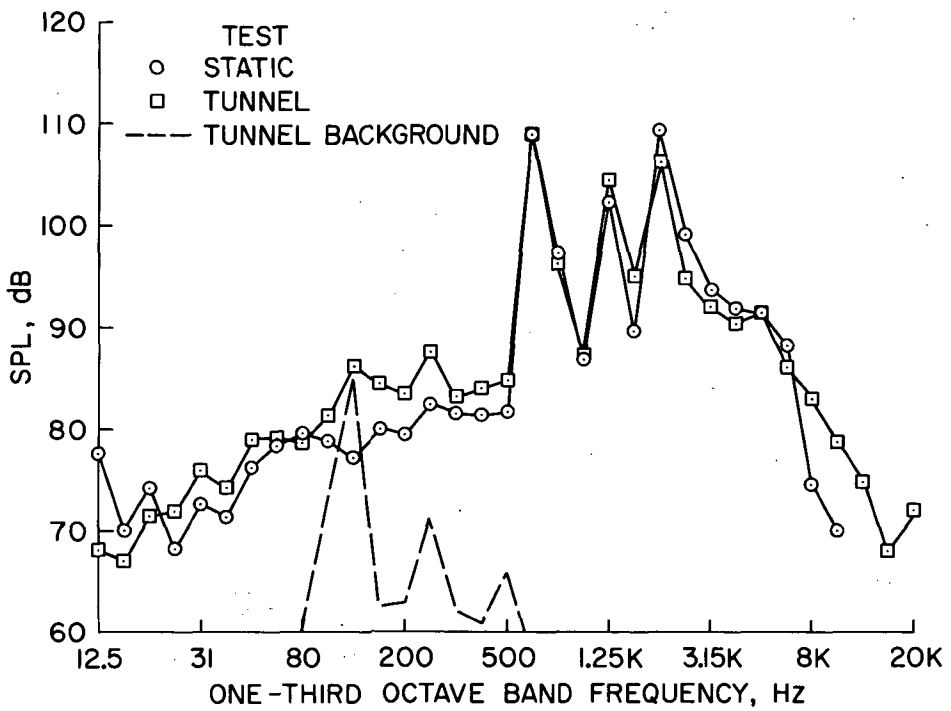

(b) Flap II, $\delta_f = 30°$, no pylon, 5000 rpm, microphone position = 60°.

Figure 9.– Continued.

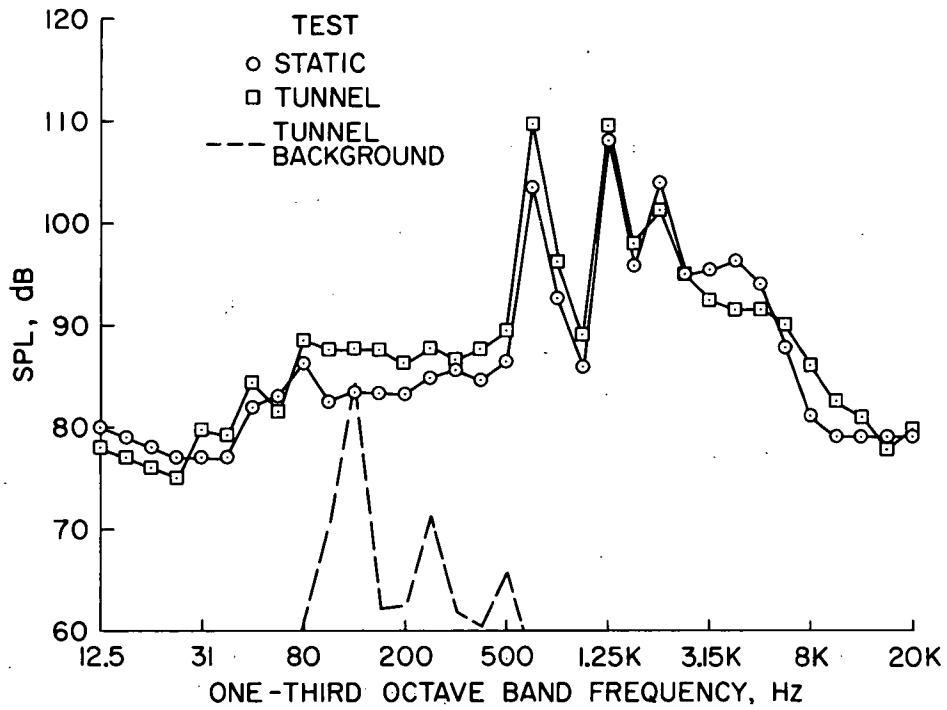

(c) Flap III, $\delta_f = 30°$, no pylon, 5000 rpm, microphone position = 120°.

Figure 9.– Continued.

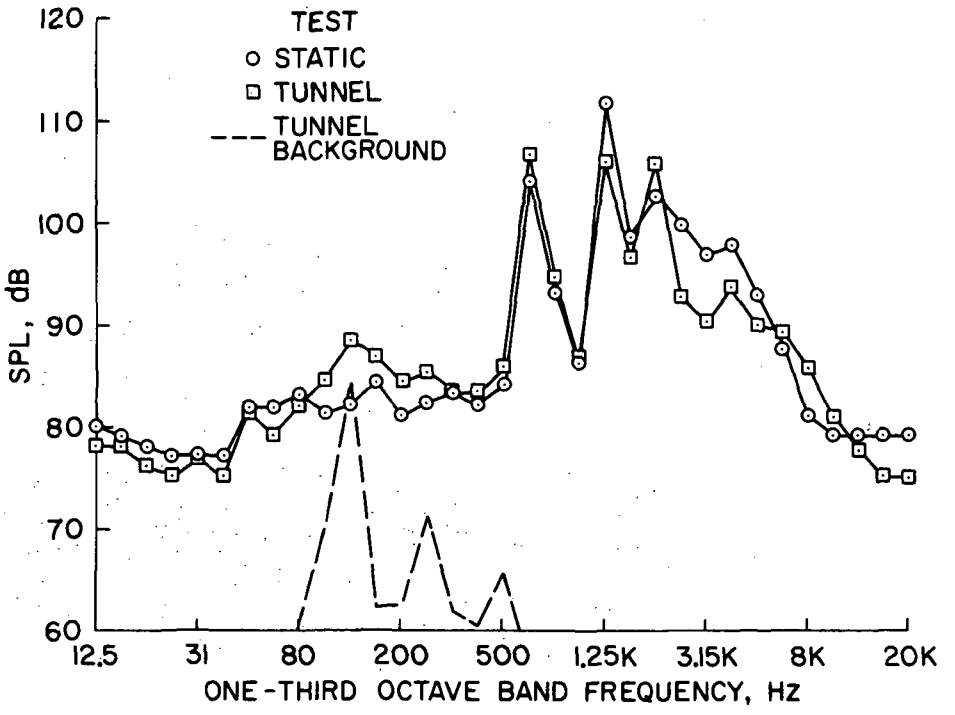

(d) Flap II, $\delta_f = 30°$, medium pylon, 5000 rpm, microphone position = 120°.

Figure 9.– Continued.

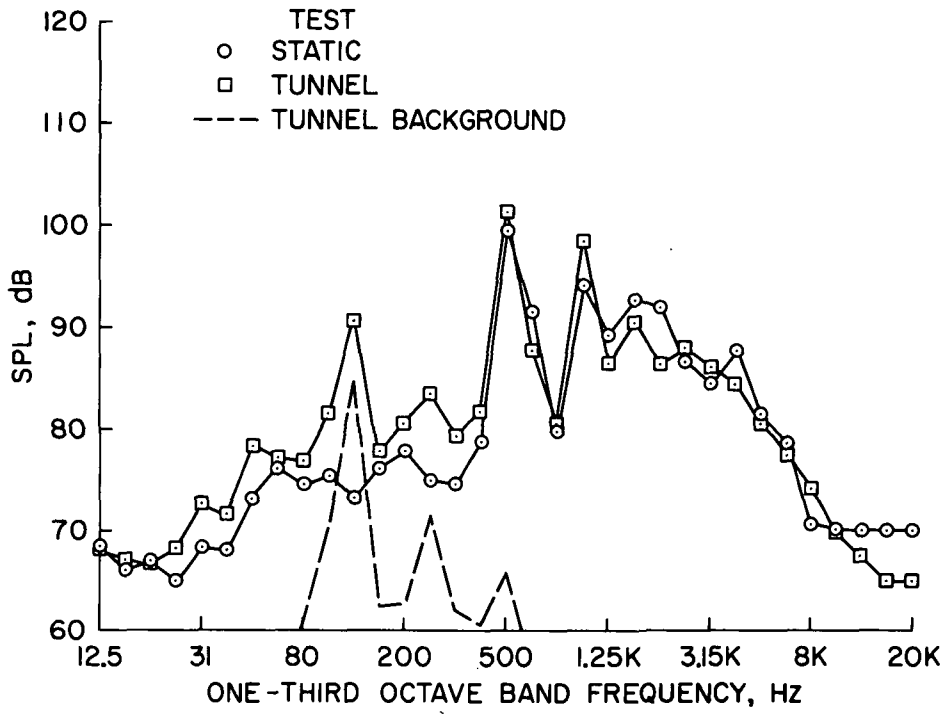

(e) Flap II, $\delta_f = 60°$, medium pylon, 4000 rpm, microphone position = 60°.

Figure 9.– Concluded.

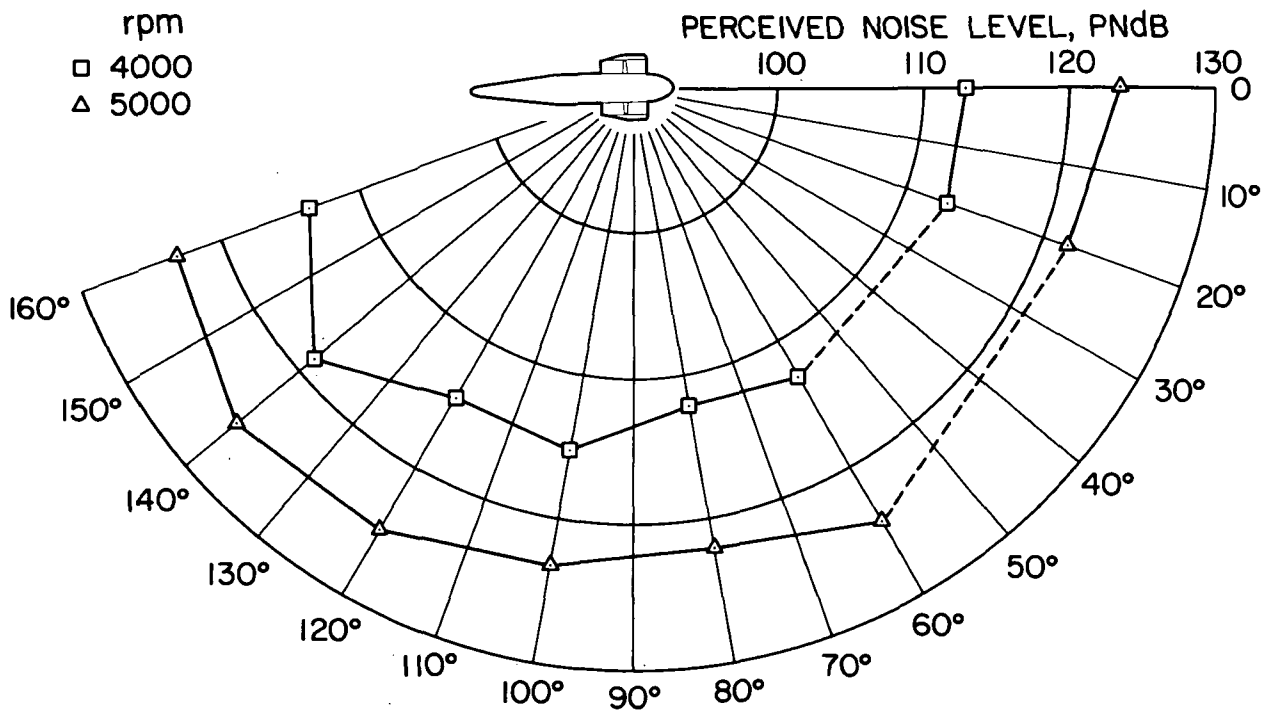

Figure 10.– Perceived noise level directivity pattern for the isolated ducted fan.

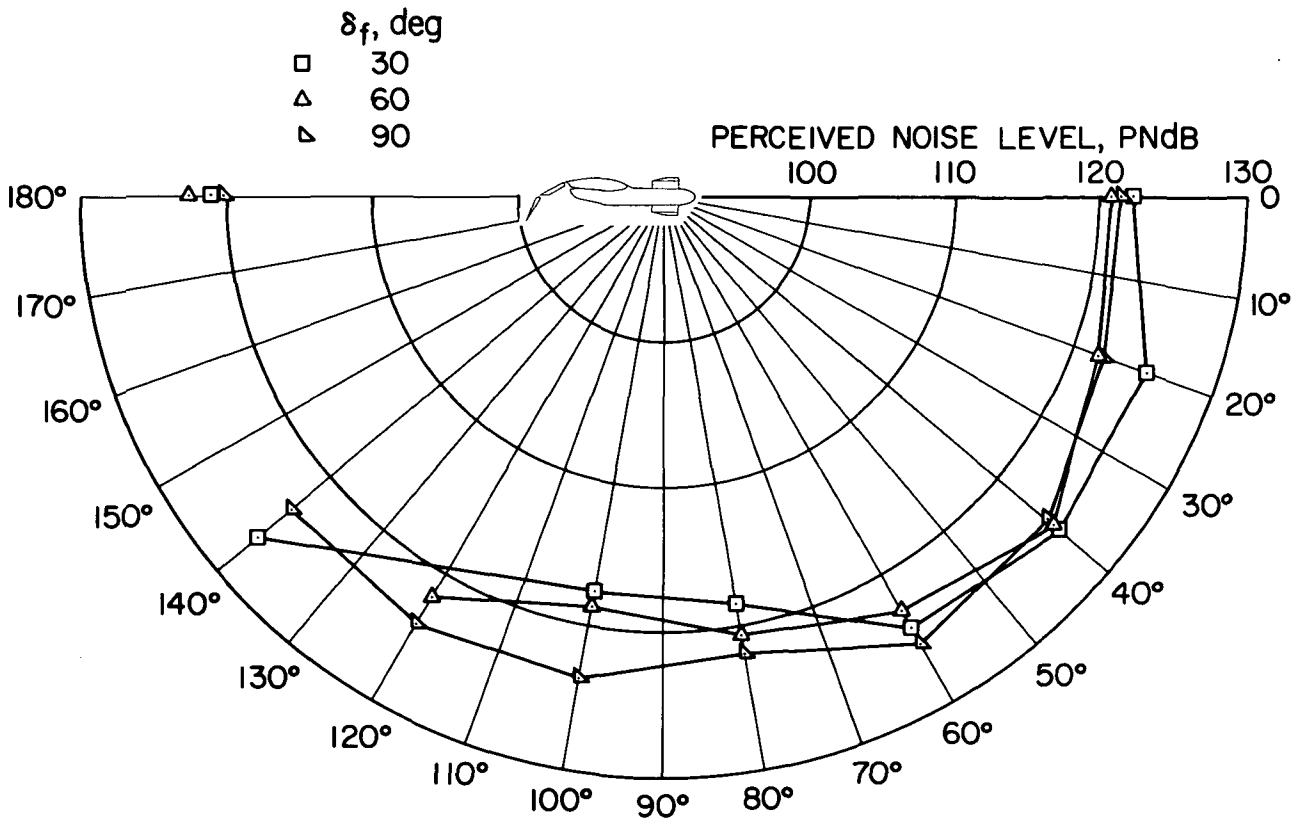

(a) Flap II, no pylon, 5000 rpm.

Figure 11.– Effect of flap deflection on the perceived noise level directivity pattern; static test, 5000 rpm.

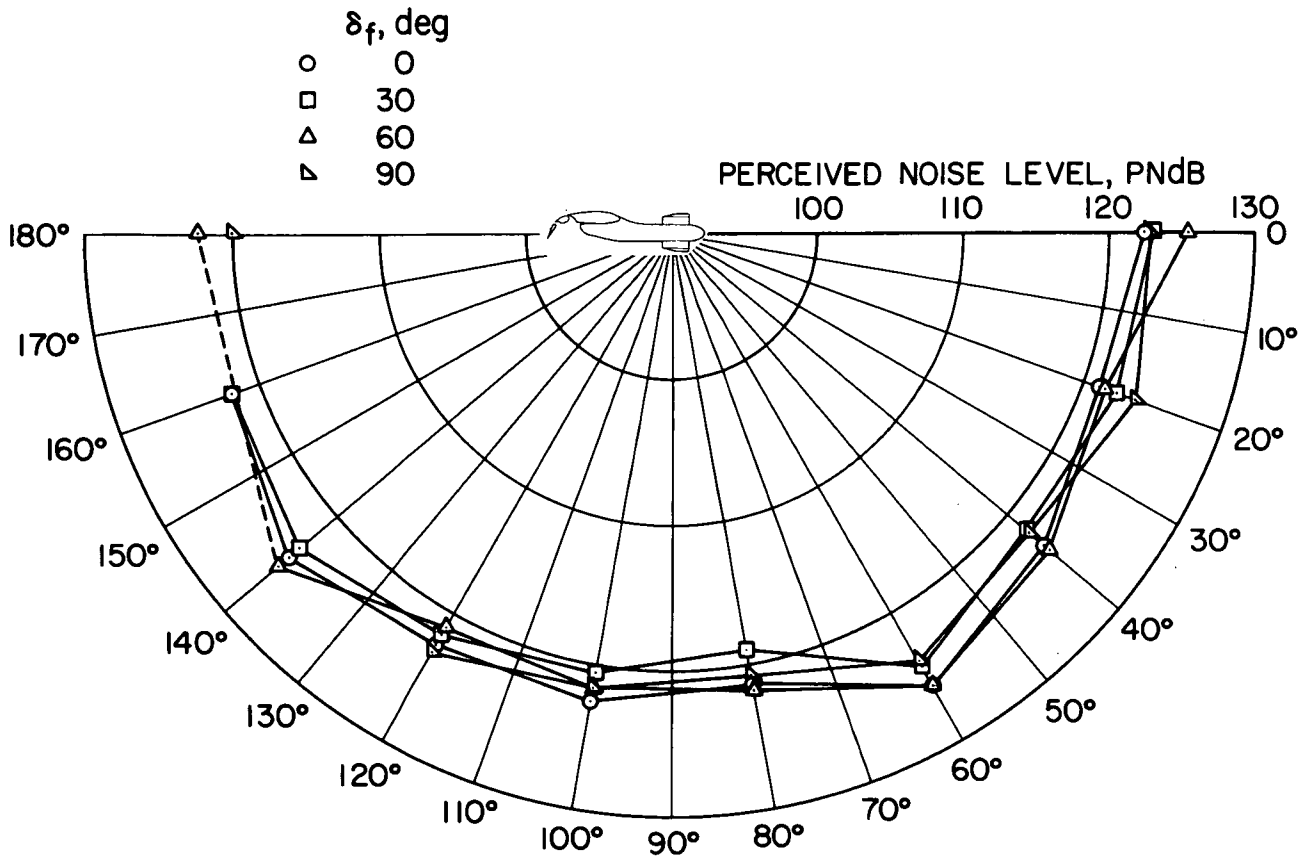

(b) Flap III, no pylon.

Figure 11.– Continued.

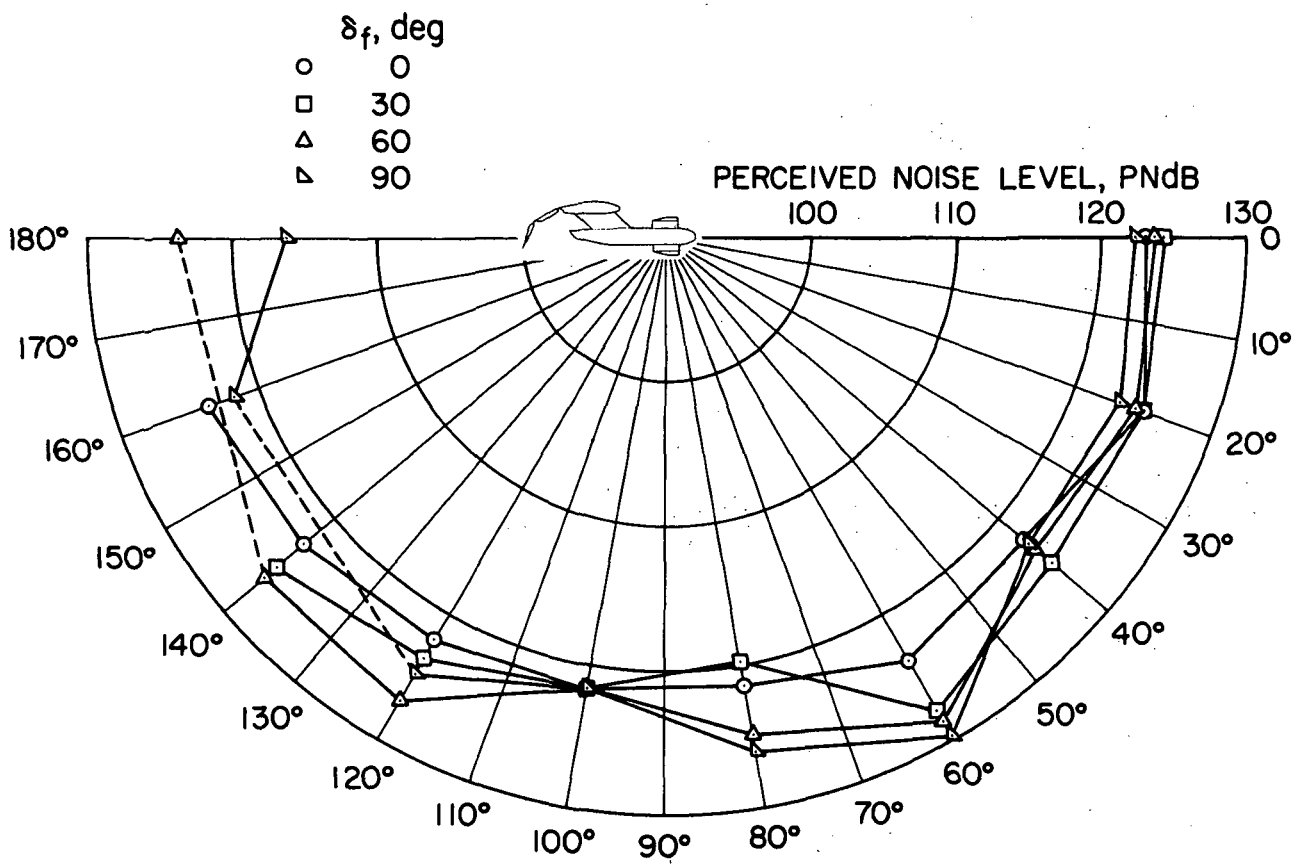

(c) Flap II, medium pylon.

Figure 11.– Continued.

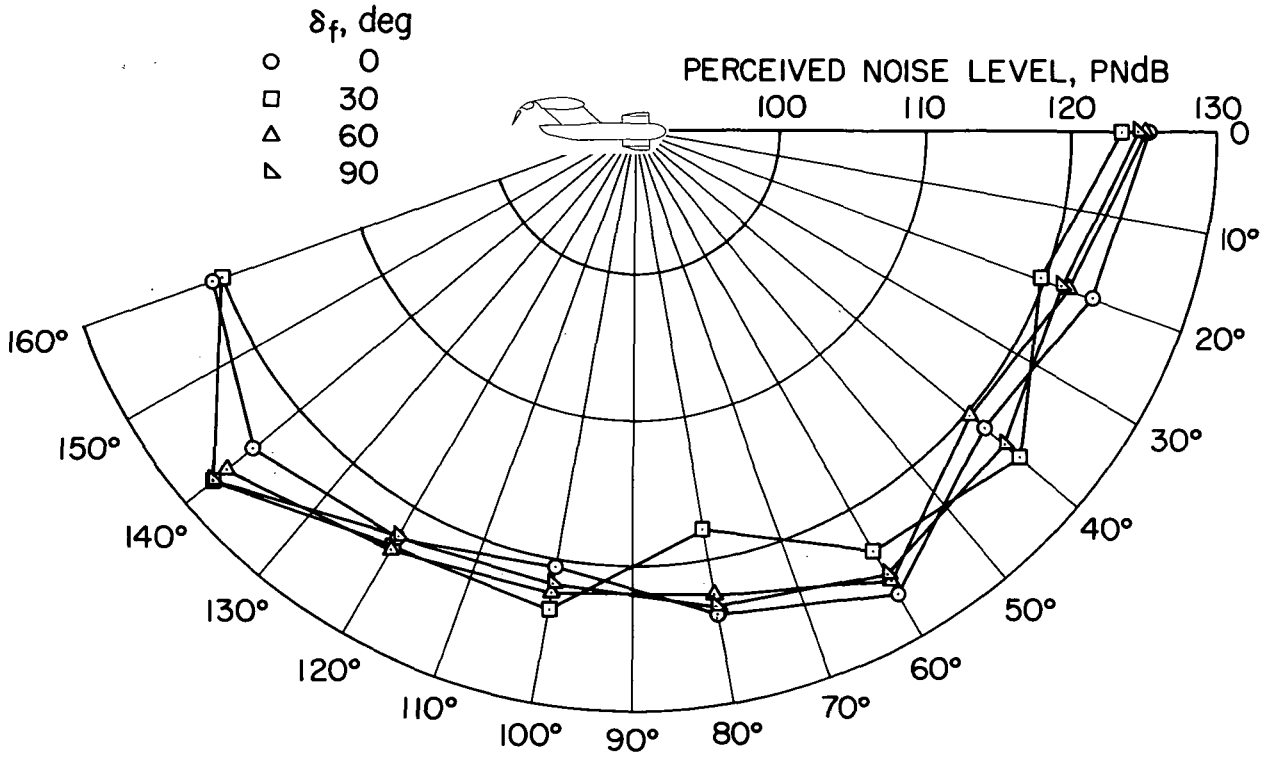

(d) Flap III, medium pylon.

Figure 11.– Continued.

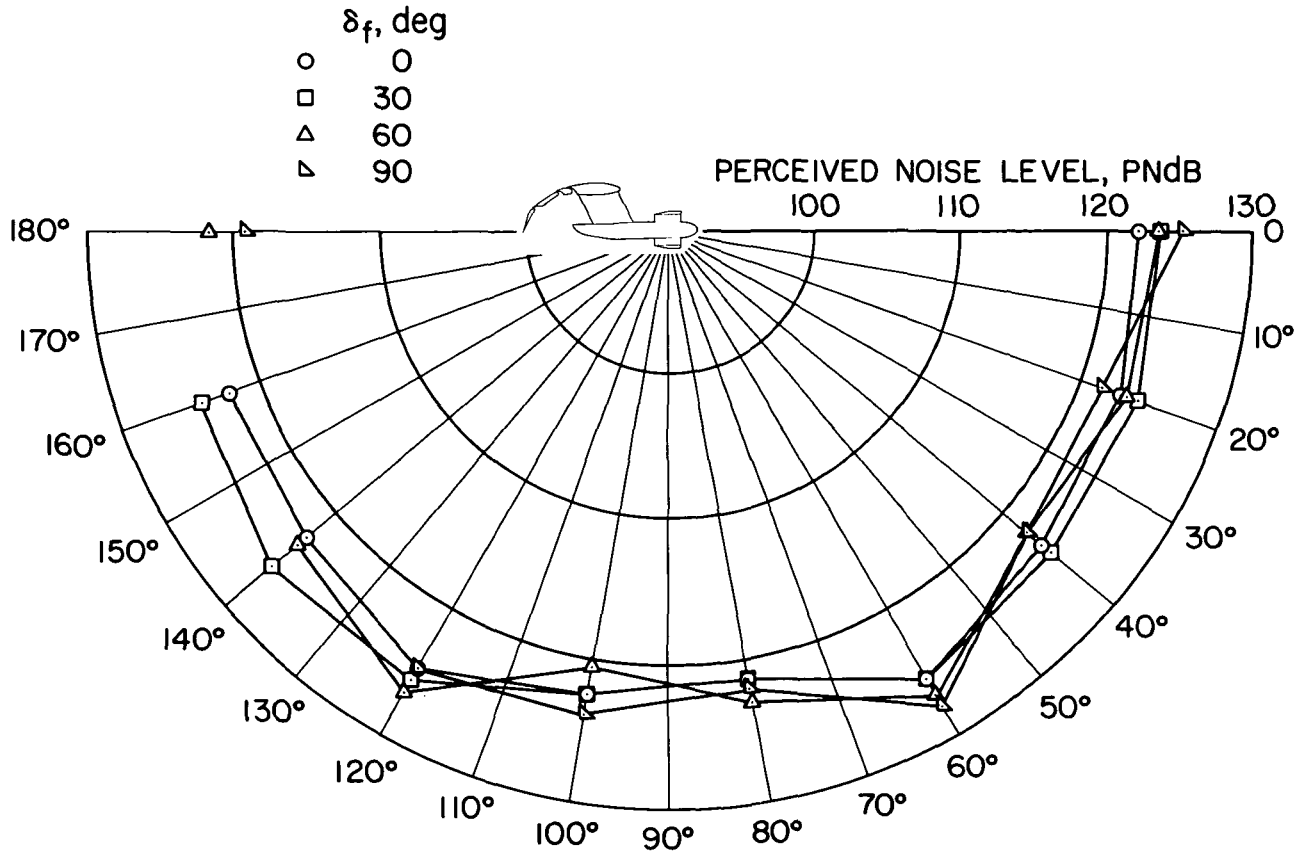

(e) Flap I, long pylon.

Figure 11.– Continued.

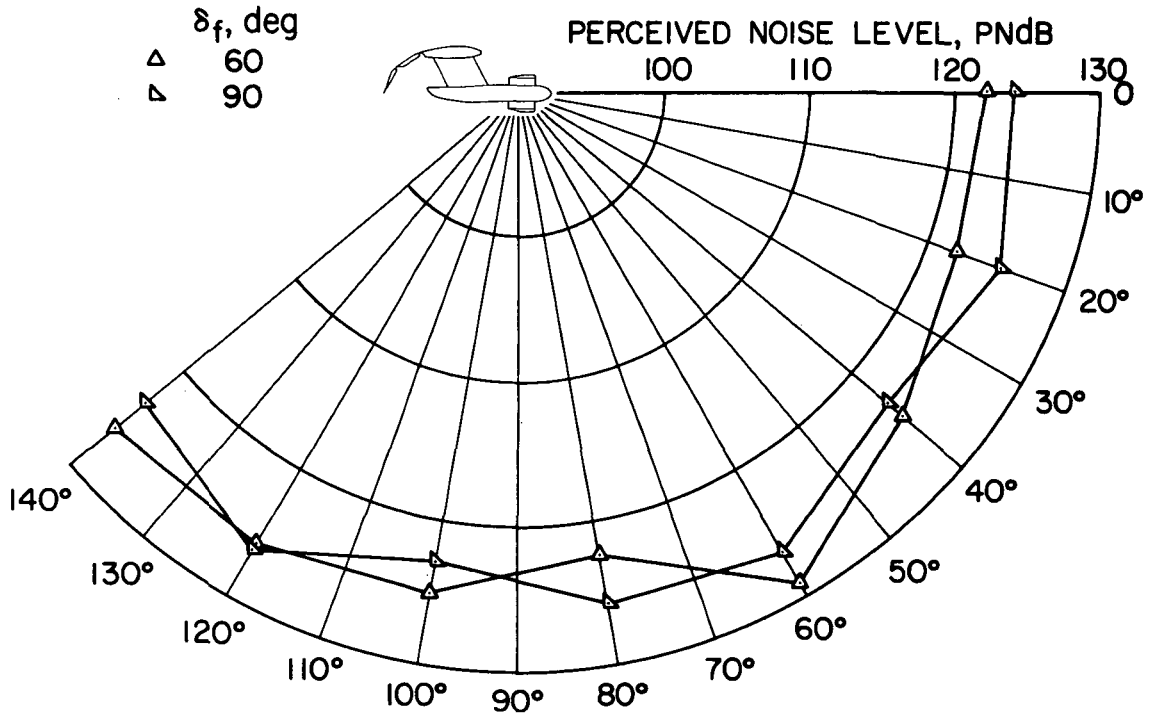

(f) Flap II, long pylon.

Figure 11.– Continued.

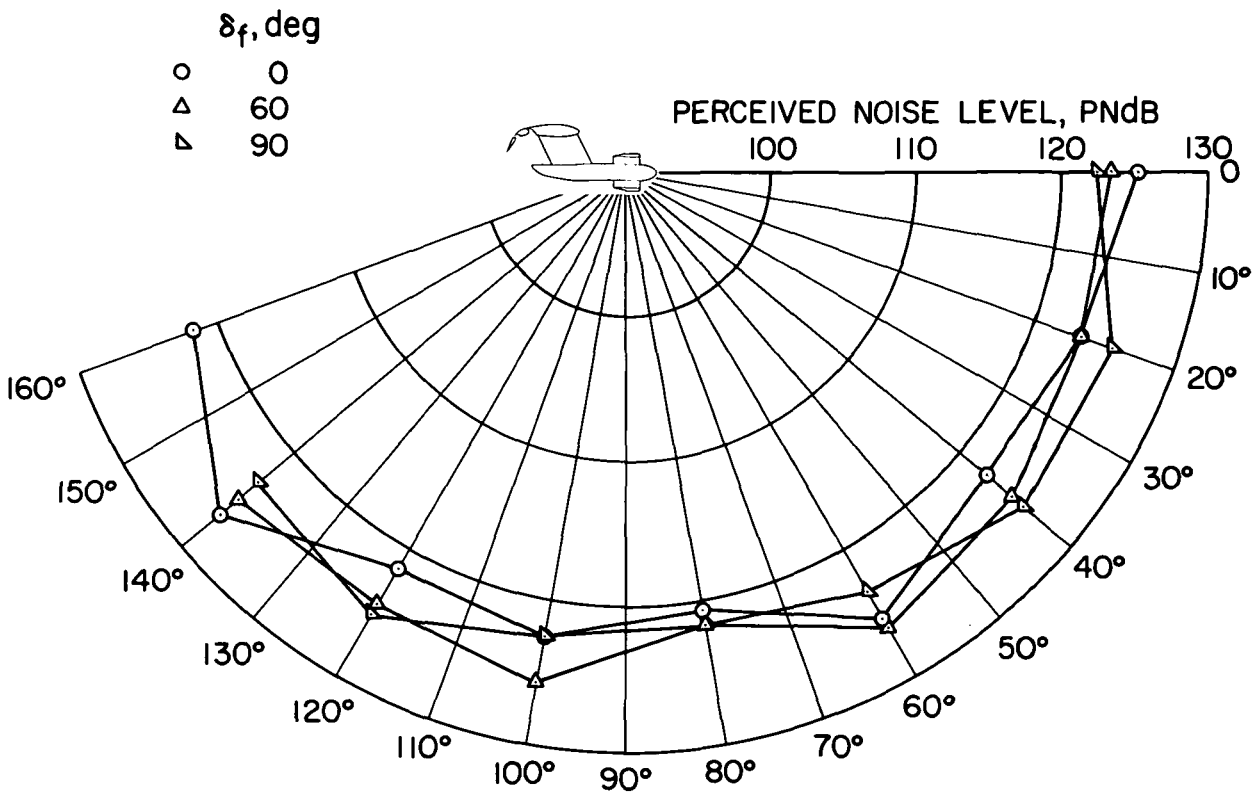

(g) Flap III, long pylon.

Figure 11.– Concluded.

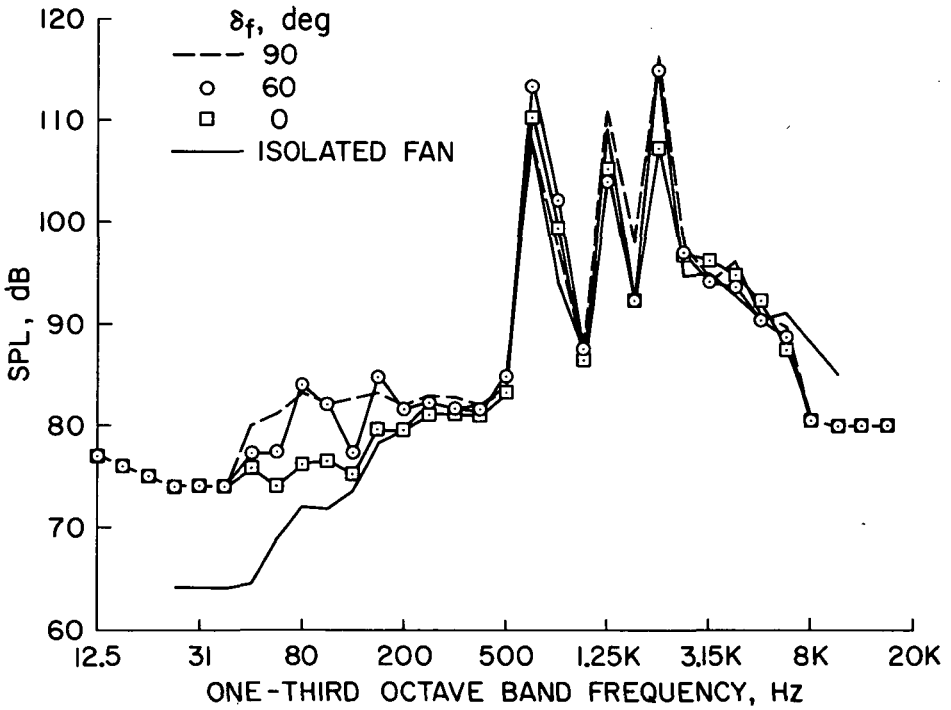

(a) Flap II, medium pylon.

Figure 12.– Effect of flap deflection on noise frequency spectrum; static test, 5000 rpm, microphone position = 60°.

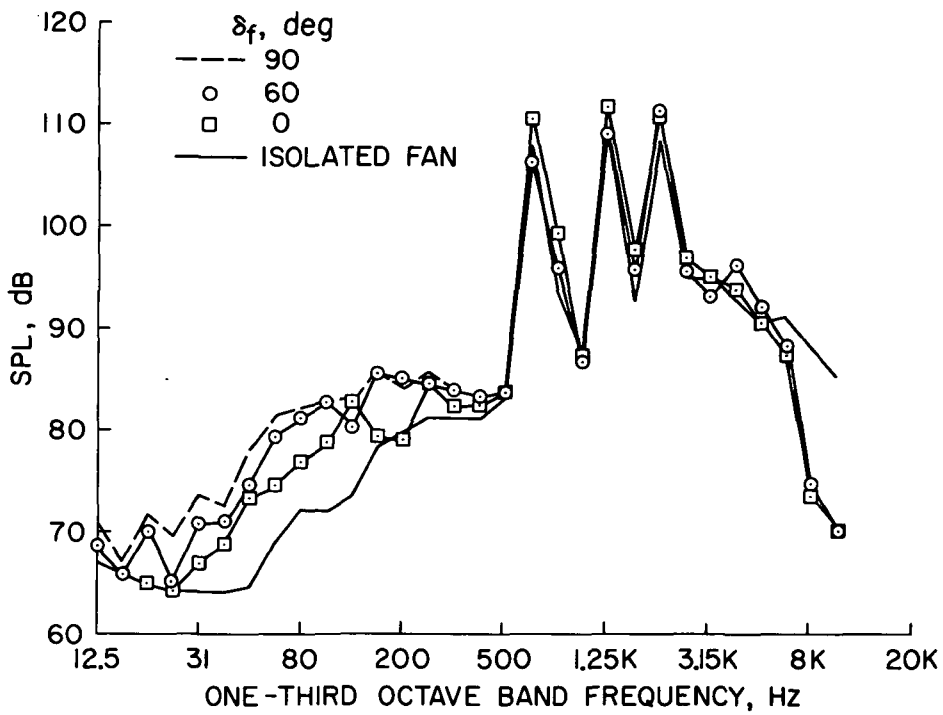

(b) Flap III, no pylon,

Figure 12.– Concluded.

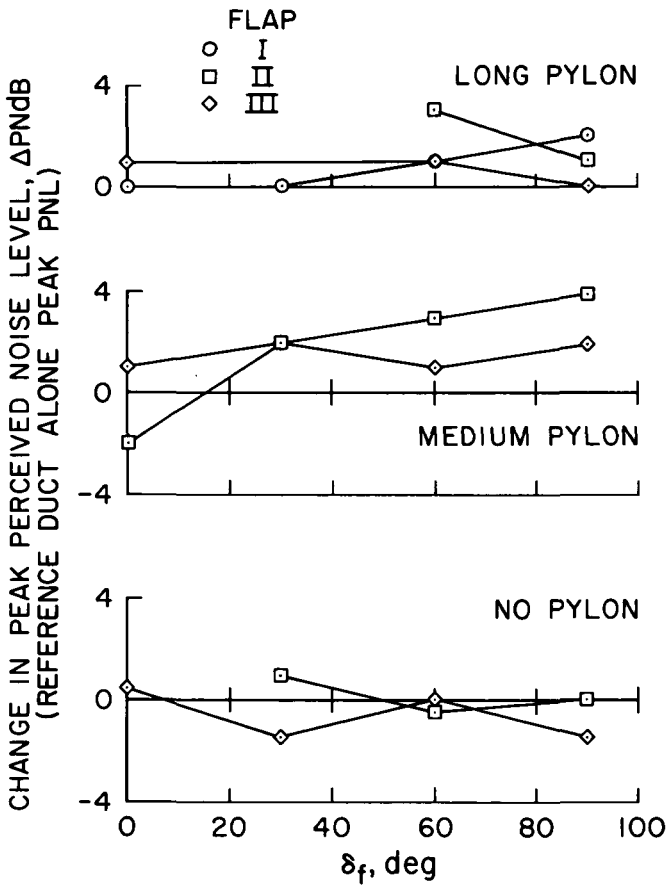

Figure 13.– Change in peak perceived noise level with flap deflection; static test, 5000 rpm.

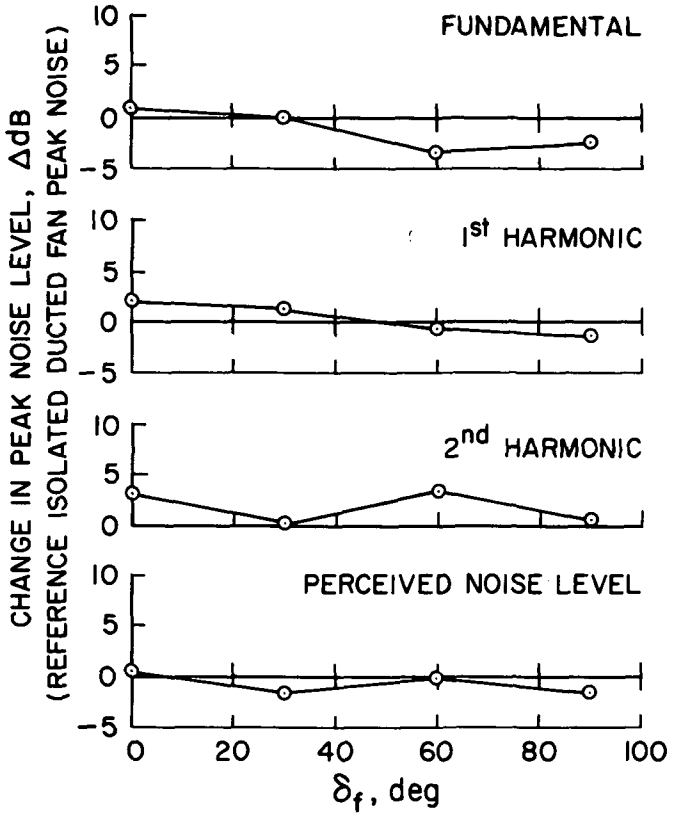

(a) Flap III, no pylon.

Figure 14.– Variation of the fundamental frequency and the first two harmonics of the peak perceived noise level with flap deflection; static test, 5000 rpm.

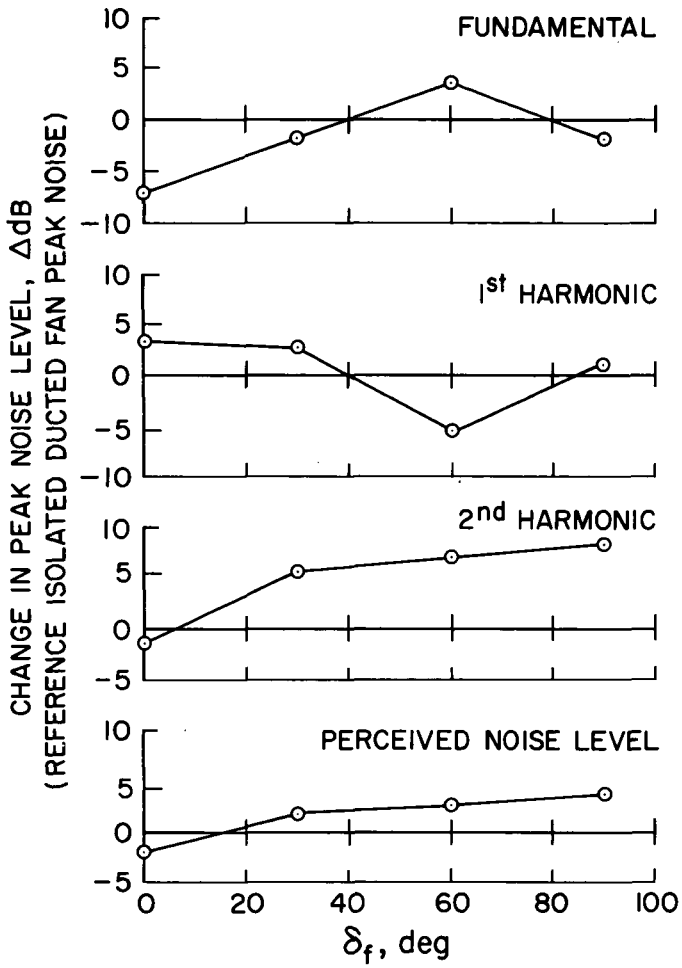

(b) Flap II, medium pylon.

Figure 14.– Continued.

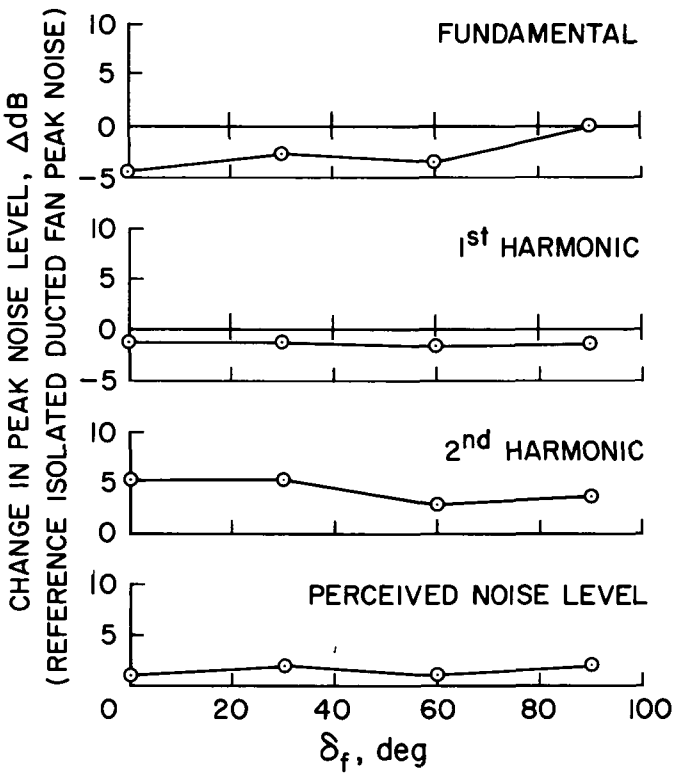

(c) Flap III, medium pylon.

Figure 14.– Continued.

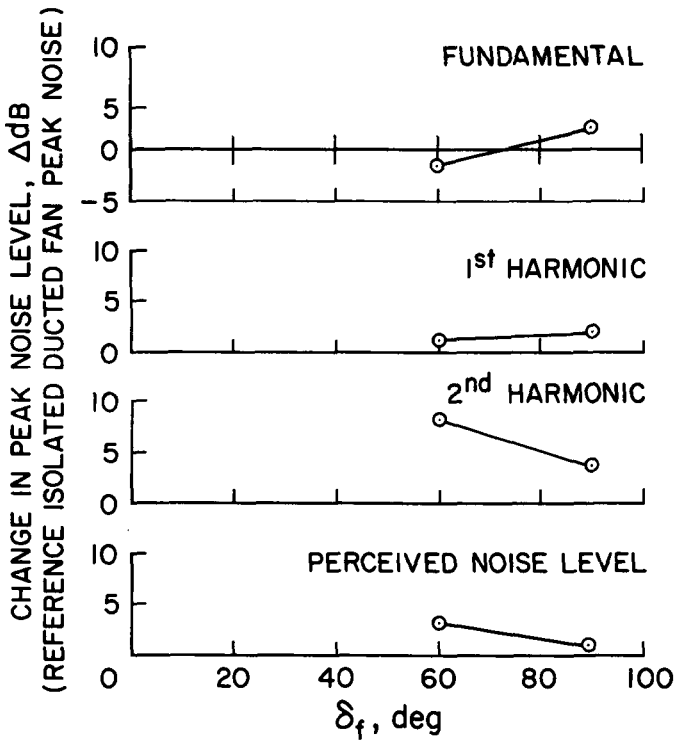

(d) Flap II, long pylon.

Figure 14.– Concluded.

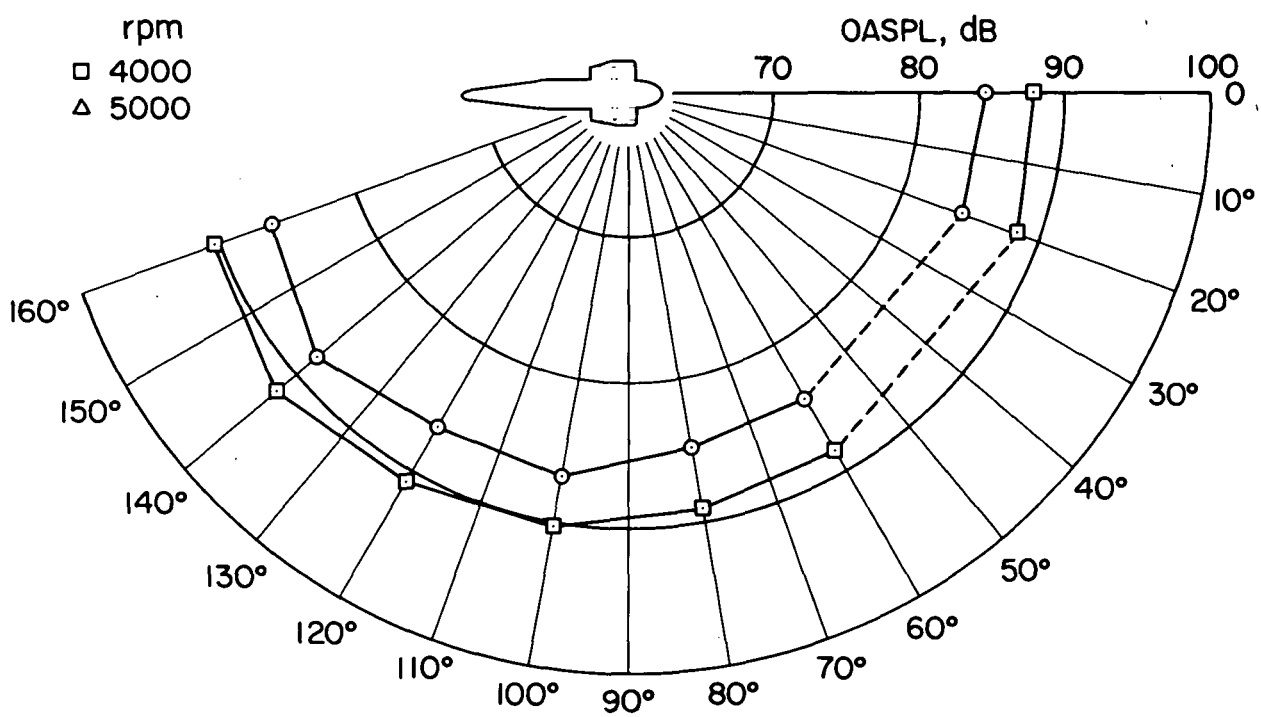

(a) Isolated ducted fan.

Figure 15.– Noise directivity pattern of the jet noise; static test, 5000 rpm, frequency range = 12.5–500 Hz.

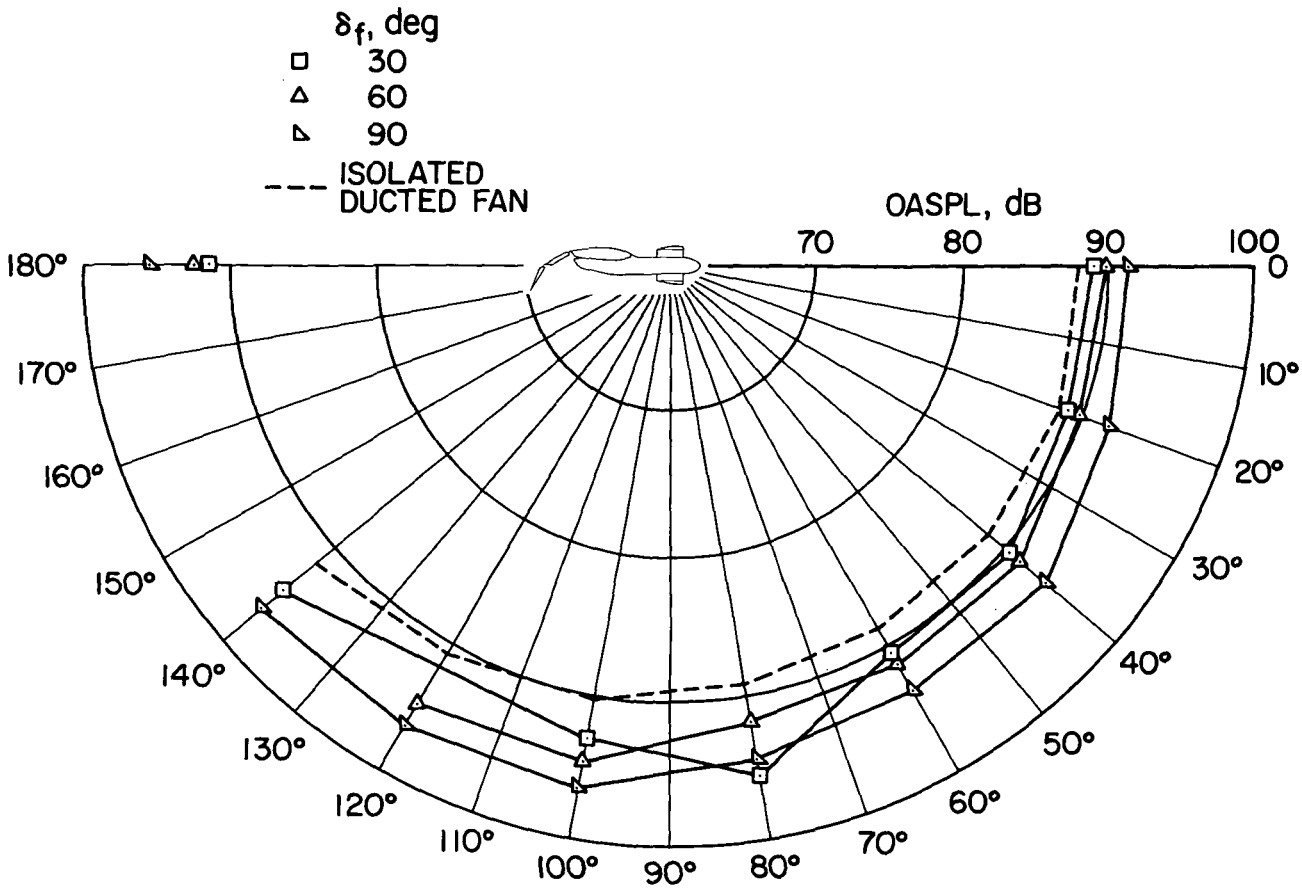

(b) Flap II, no pylon.

Figure 15.– Continued.

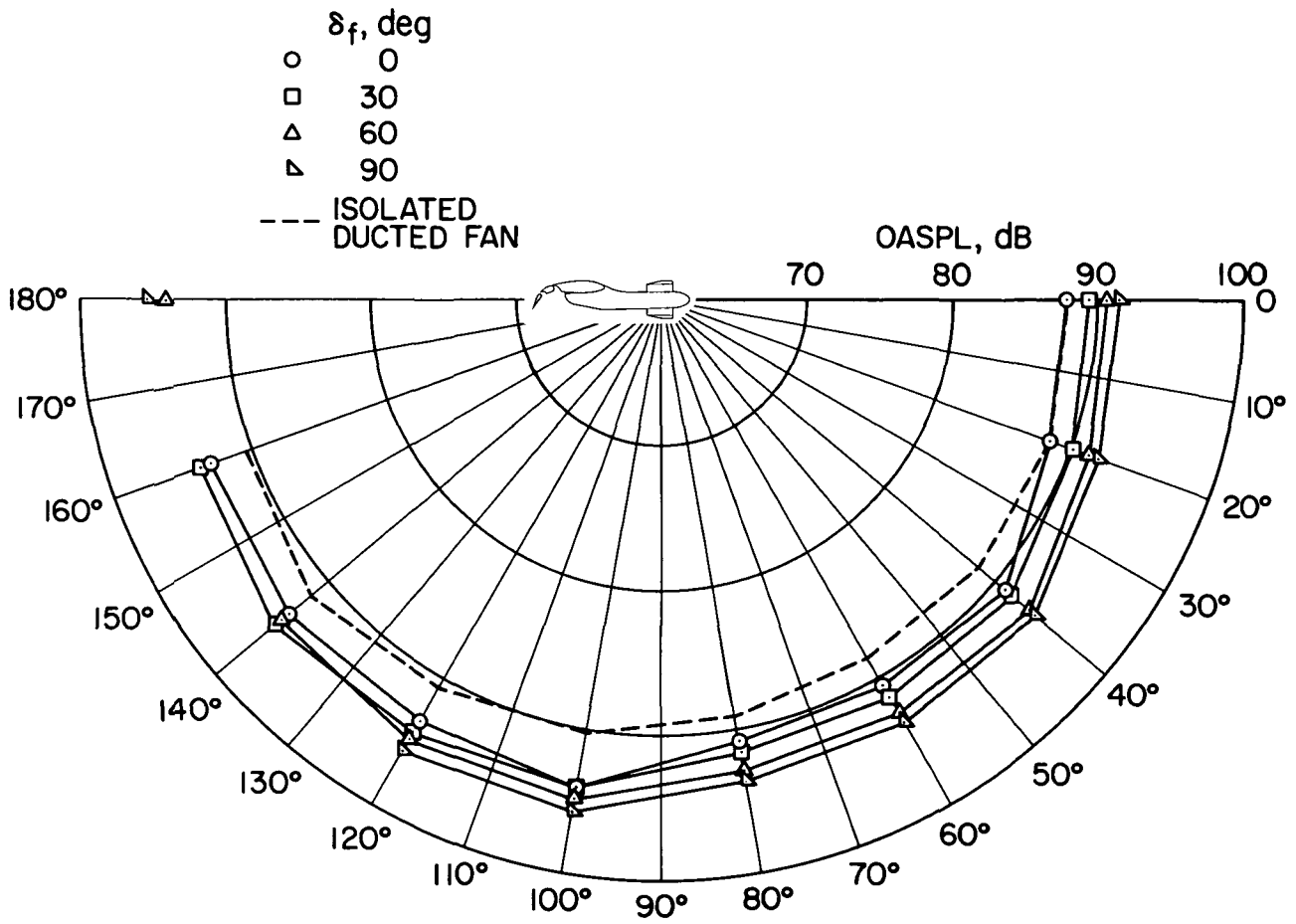

(c) Flap III, no pylon.

Figure 15.– Continued.

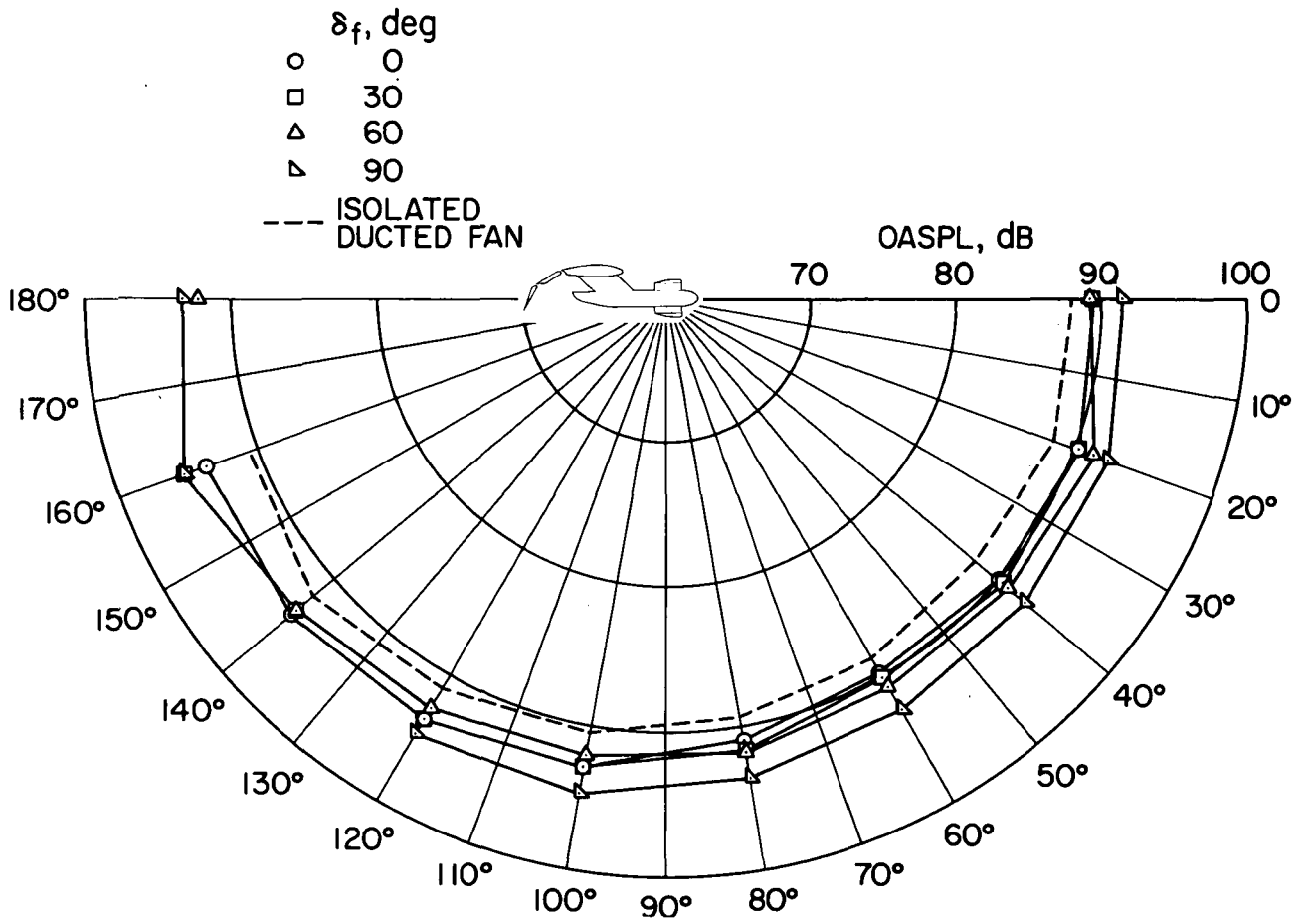

(d) Flap II, medium pylon.

Figure 15.– Continued.

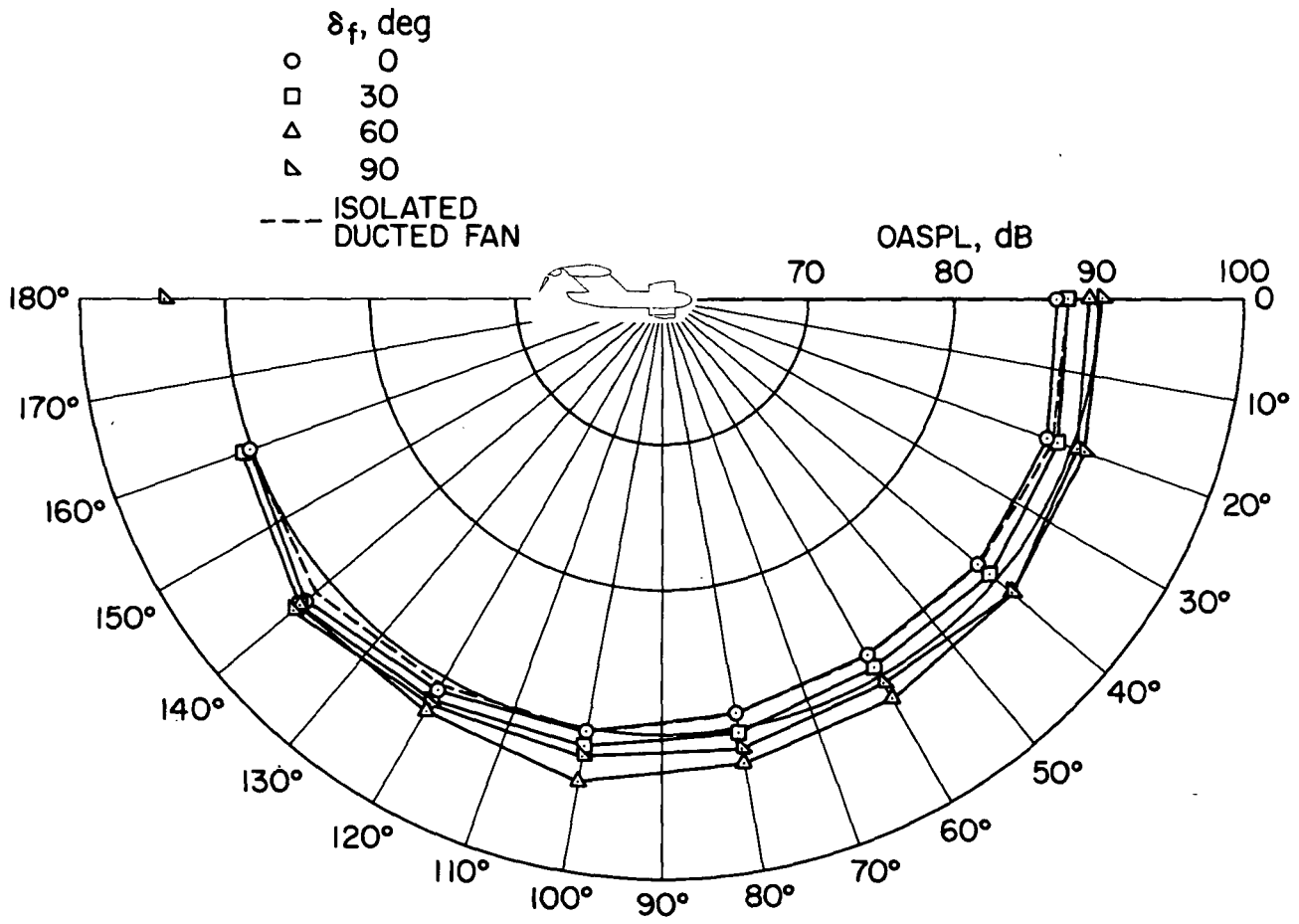

(e) Flap III, medium pylon.

Figure 15.– Continued.

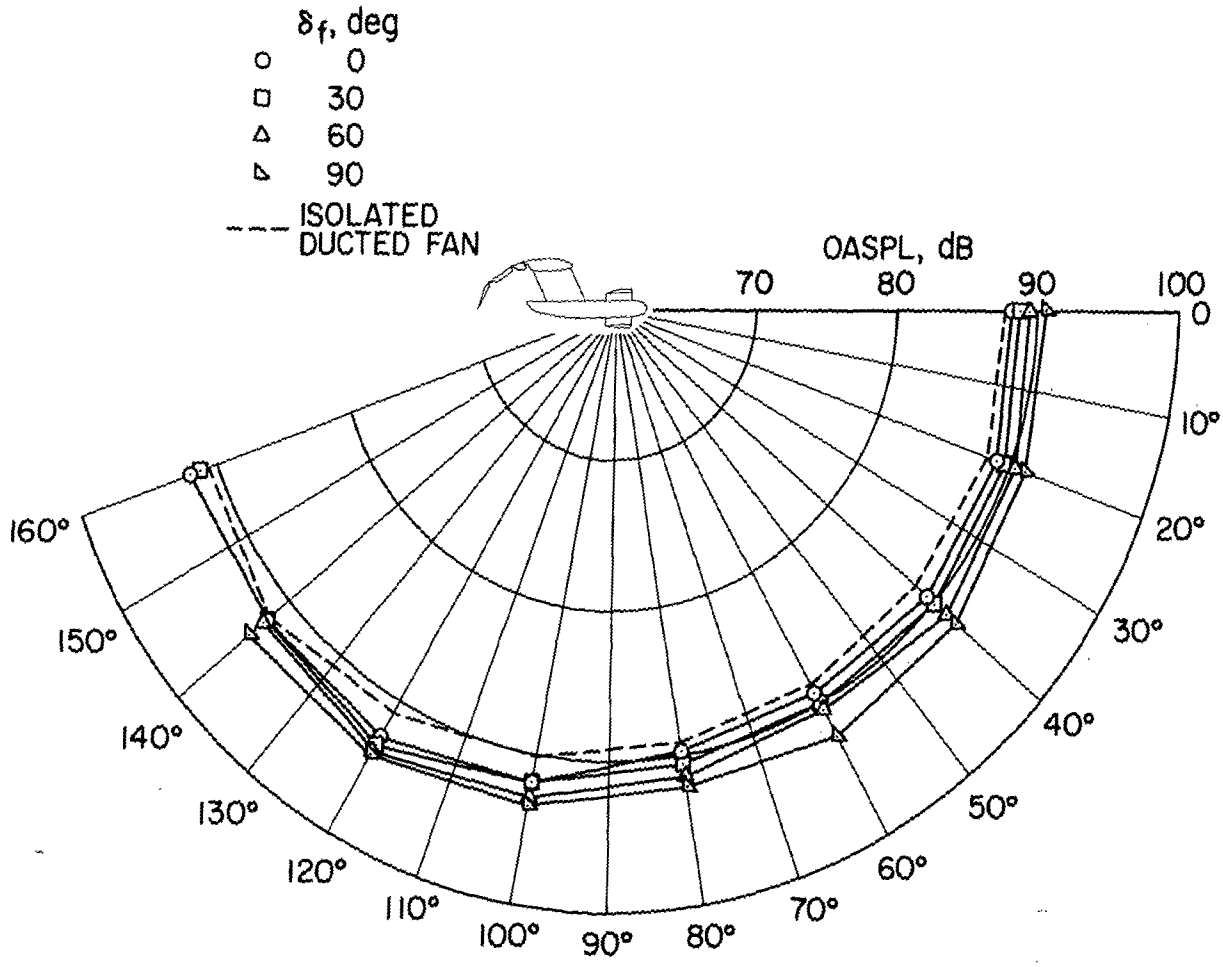

(f) Flap I, long pylon.

Figure 15.– Continued.

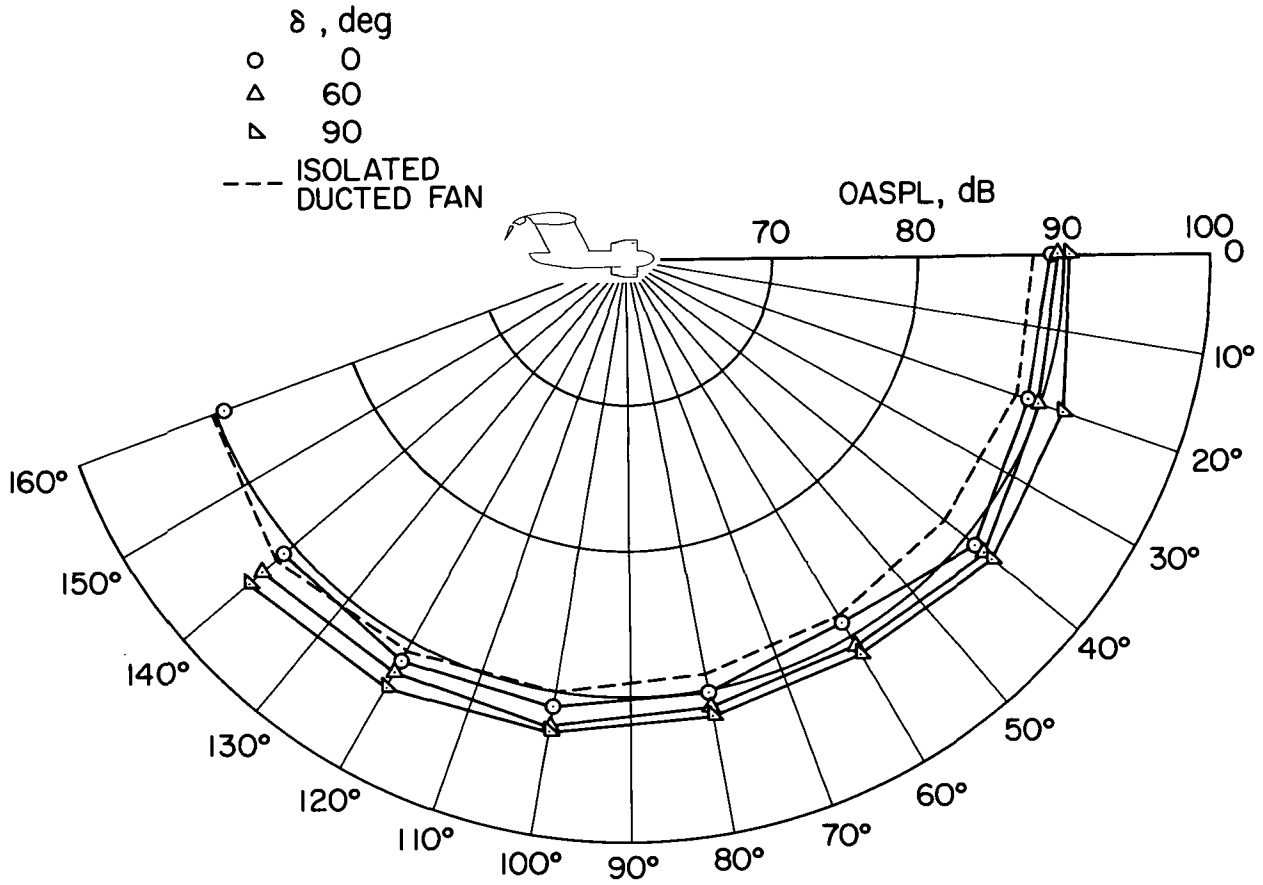

(g) Flap III, long pylon.

Figure 15.– Concluded.

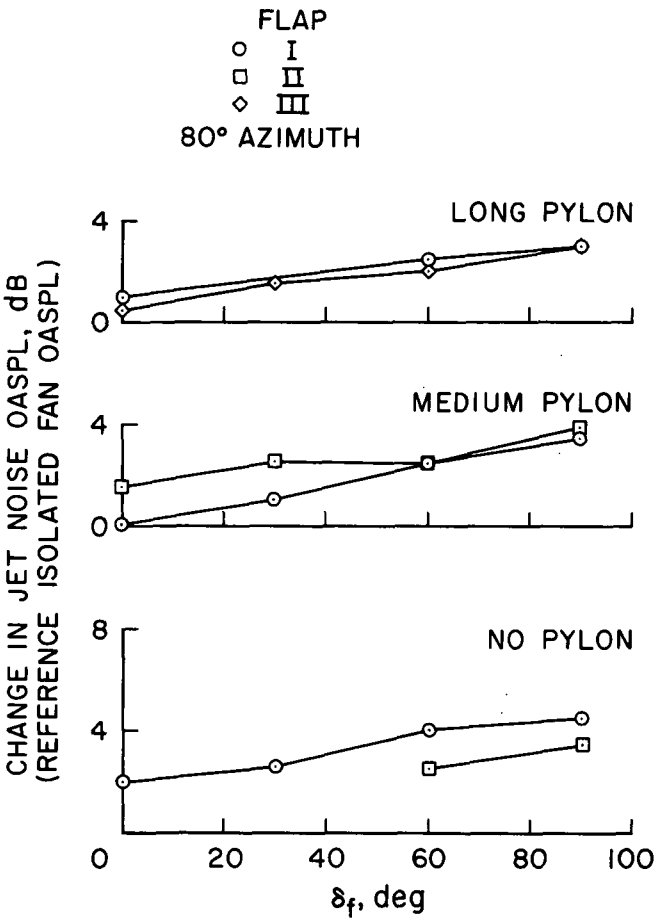

Figure 16.– Variation in the jet noise OASPL with flap deflection; static test, 5000 rpm, 80° azimuth, frequency range = 12.5–500 Hz.

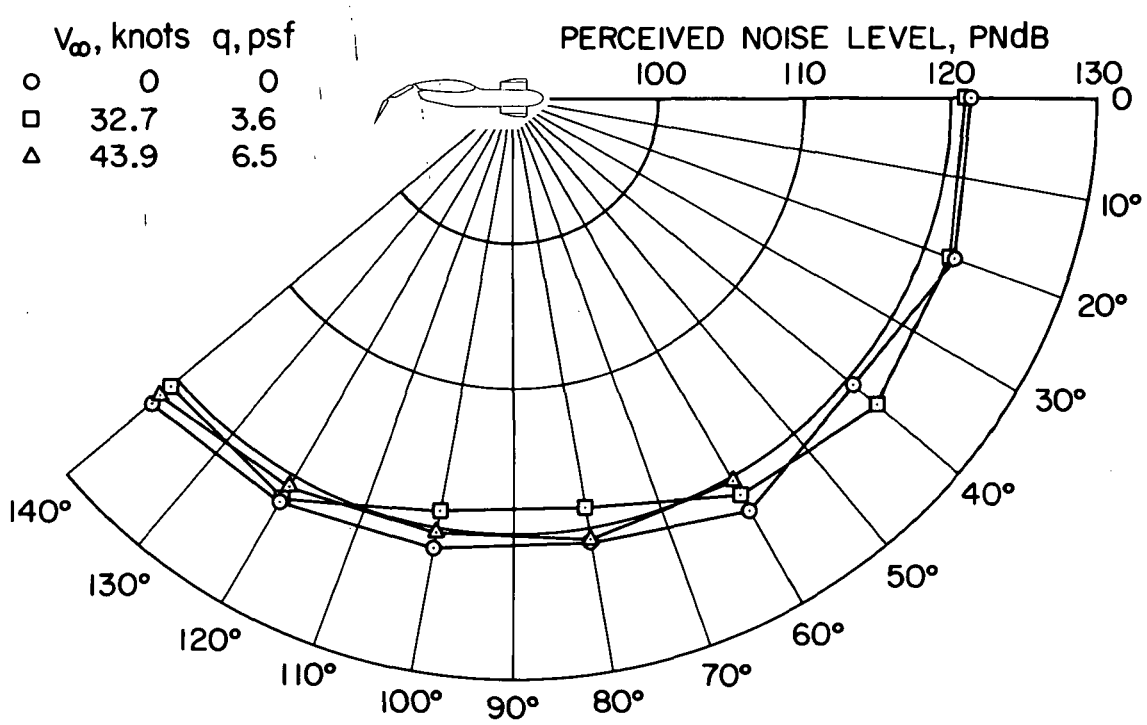

(a) Flap II, no pylon, 5000 rpm, $\delta_f = 30°$.

Figure 17.– Variation of perceived noise level directivity pattern with forward speed.

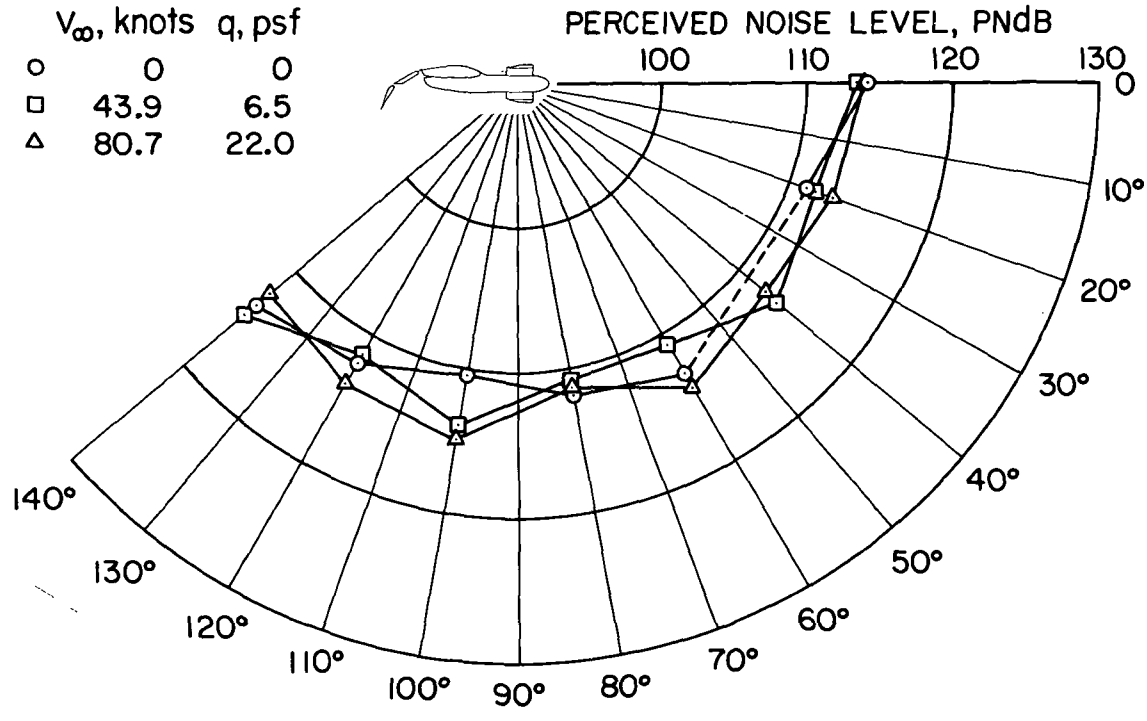

(b) Flap II, no pylon, 4000 rpm, $\delta_f = 30°$.

Figure 17.– Continued.

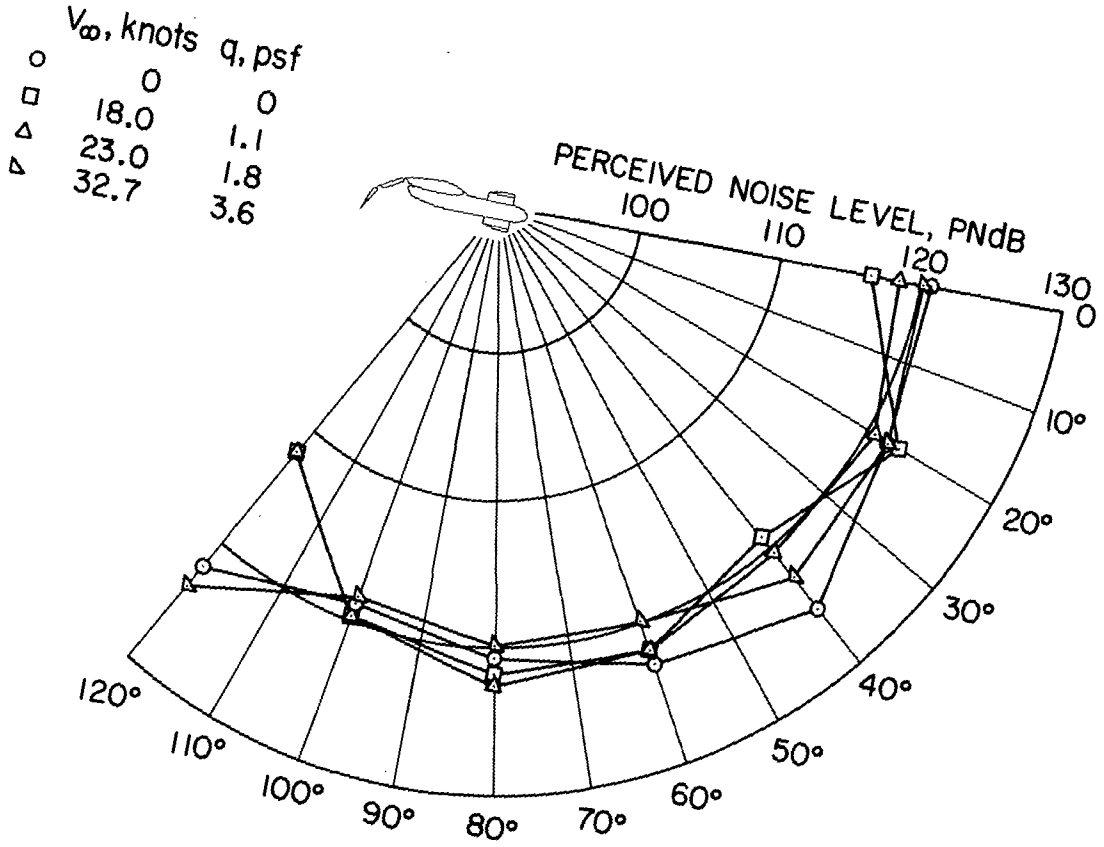

(c) Flap II, $\delta_f = 60°$, no pylon, 5000 rpm.

Figure 17.– Continued.

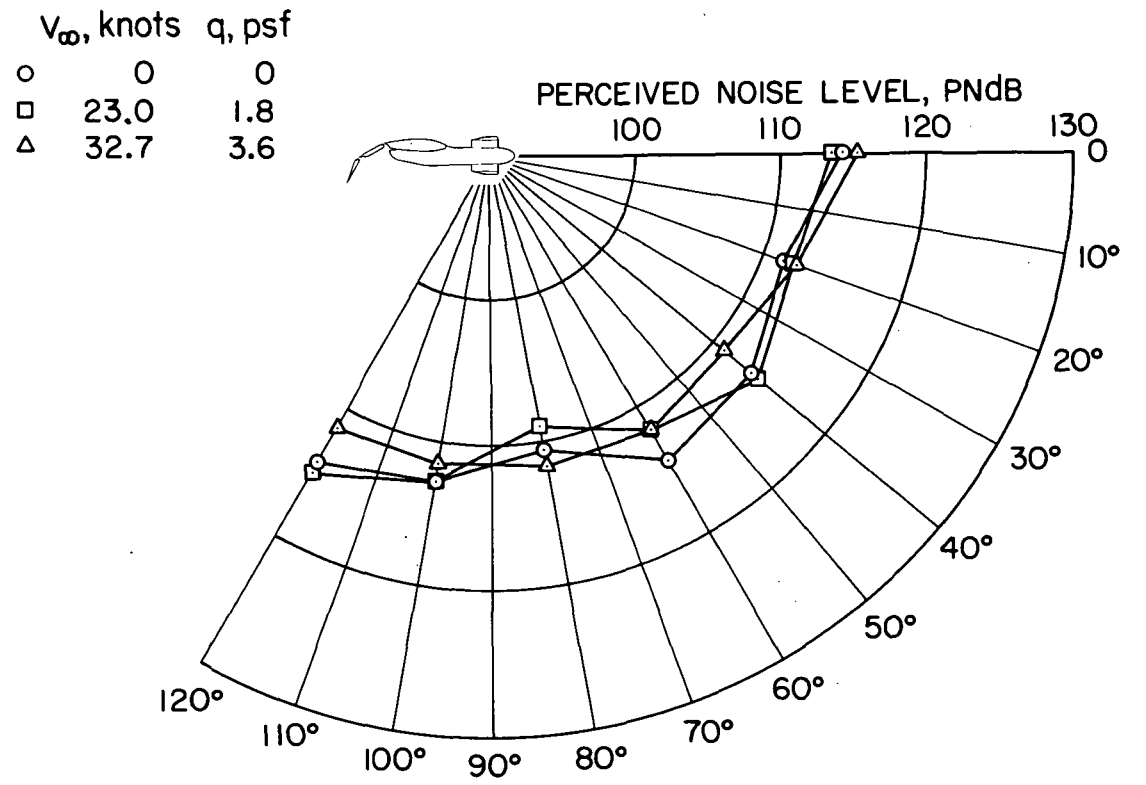

(d) Flap II, $\delta_f = 90°$, no pylon, 4000 rpm.

Figure 17.– Continued.

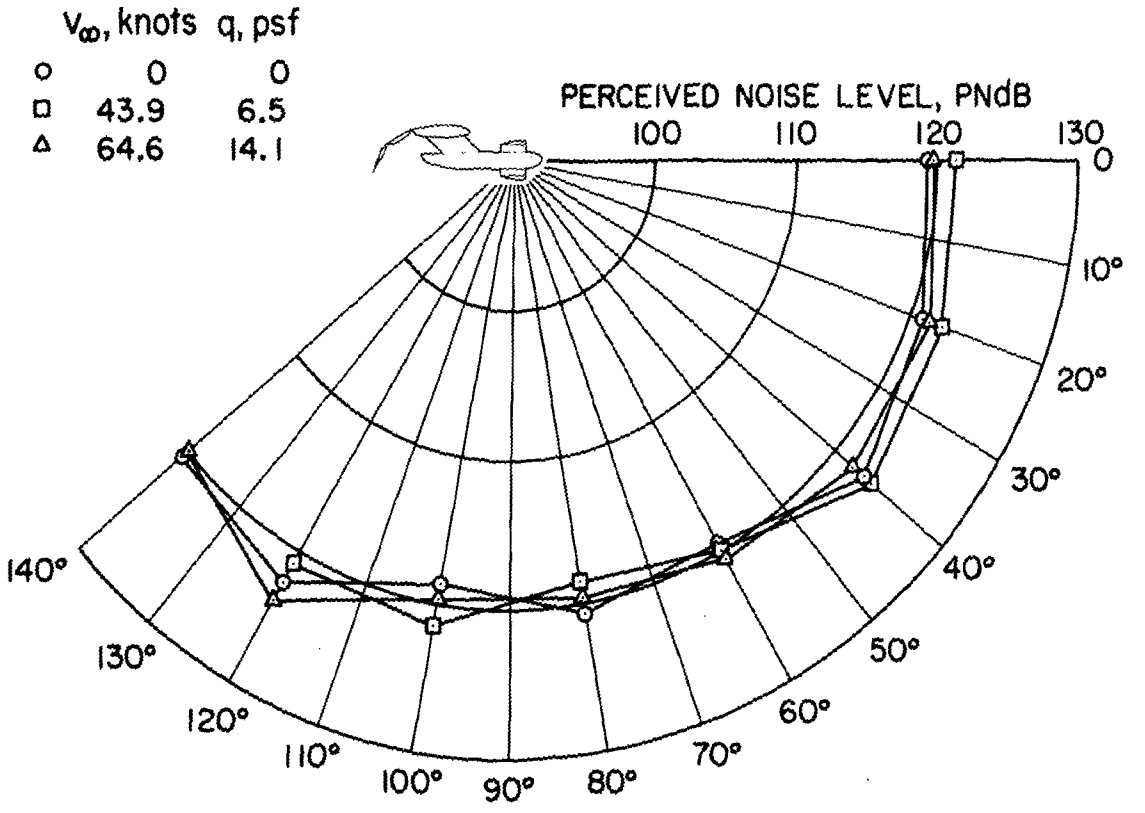

(e) Flap II, medium pylon, 5000 rpm, $\delta_f = 30°$.

Figure 17.– Continued.

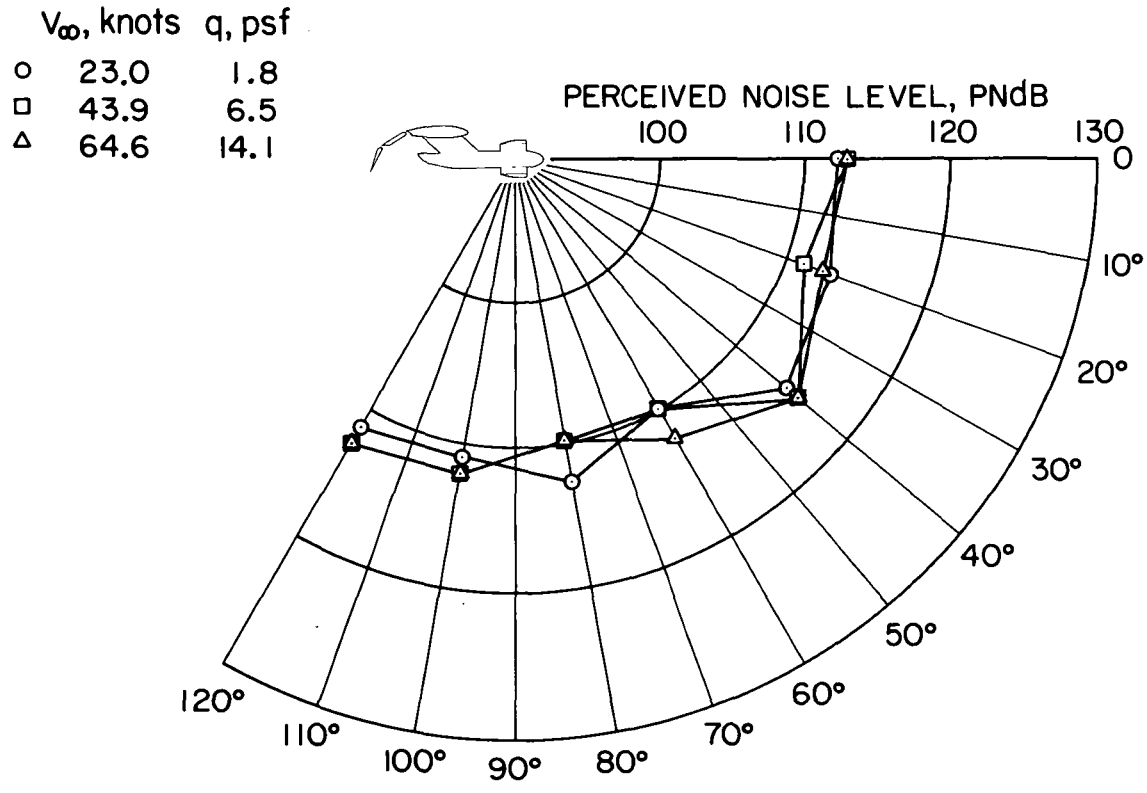

(f) Flap II, medium pylon, 4000 rpm, $\delta_f = 30°$.

Figure 17.– Continued.

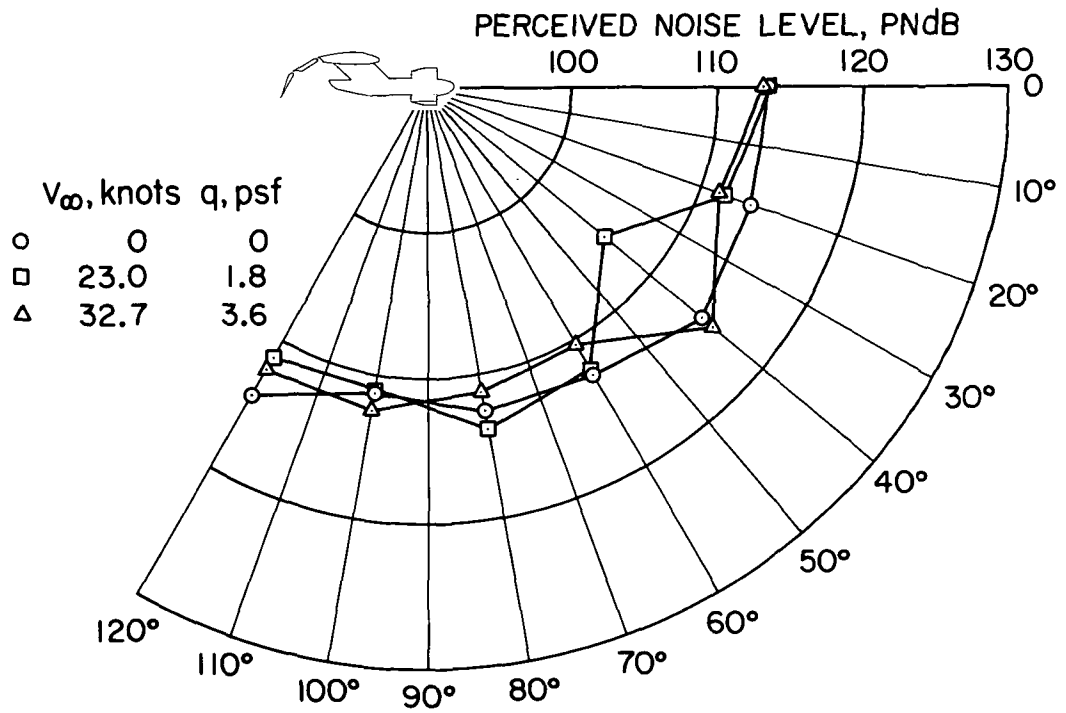

(g) Flap II, $\delta_f = 60°$, medium pylon, 4000 rpm.

Figure 17.– Continued.

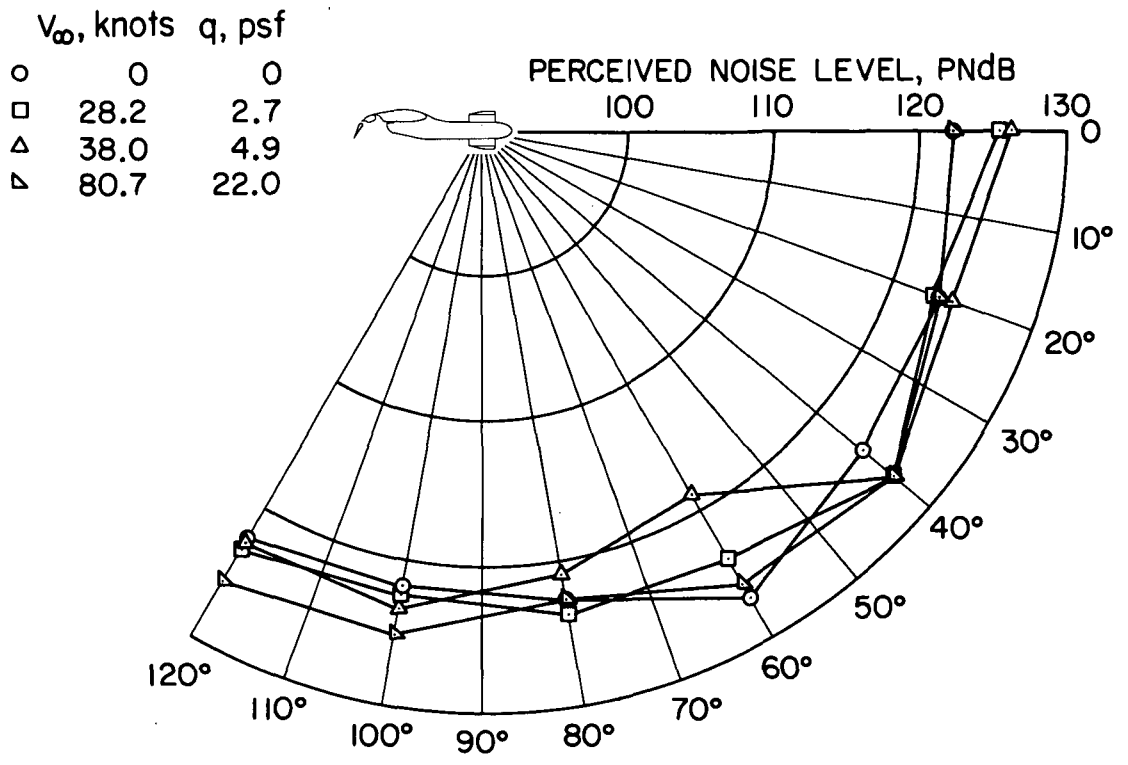

(h) Flap III, $\delta_f = 30°$, no pylon, 5000 rpm.

Figure 17.– Concluded.

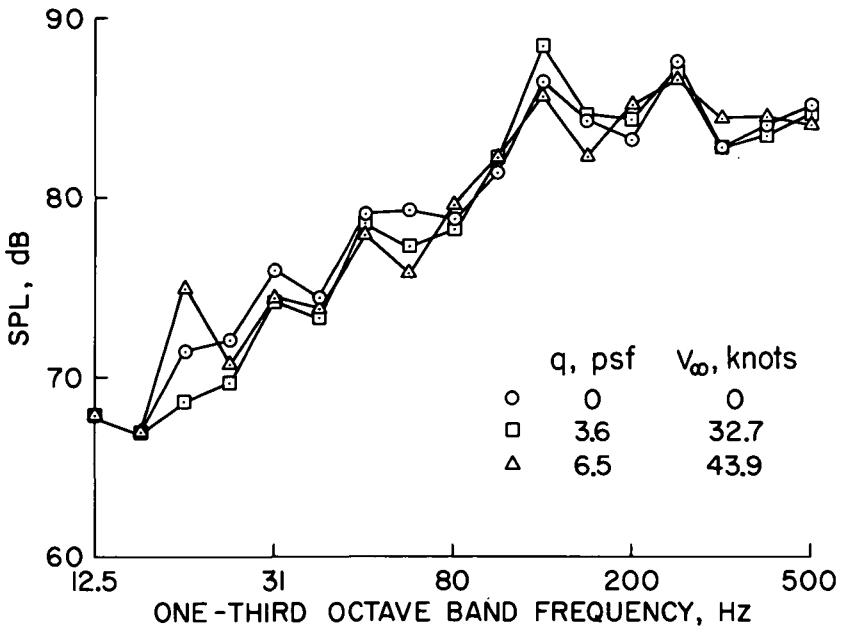

(a) Flap II, $\delta_f = 30°$, no pylon, 5000 rpm.

Figure 18.– Variation of broadband noise frequency spectrum with forward speed; microphone location = 60°.

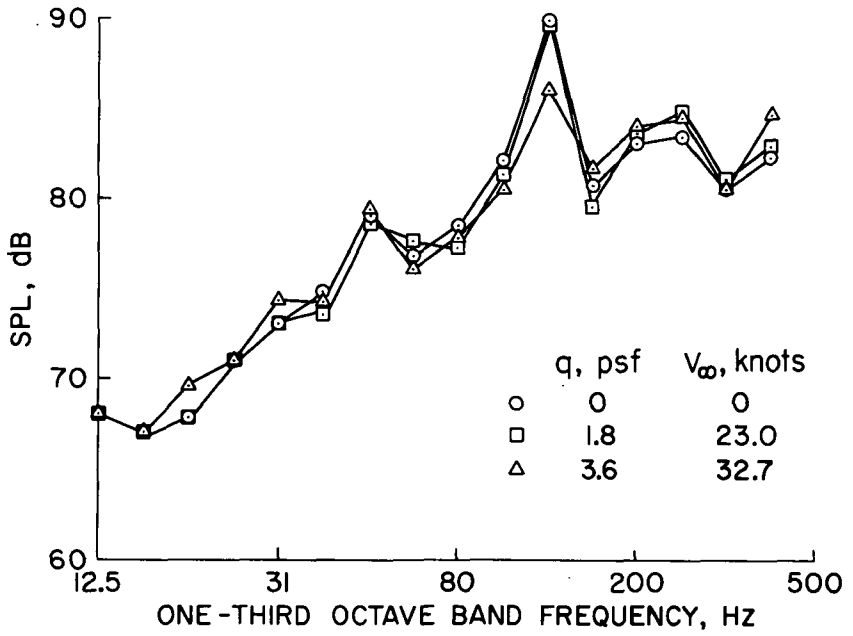

(b) Flap II, $\delta_f = 60°$, no pylon, 4000 rpm.

Figure 18.– Continued.

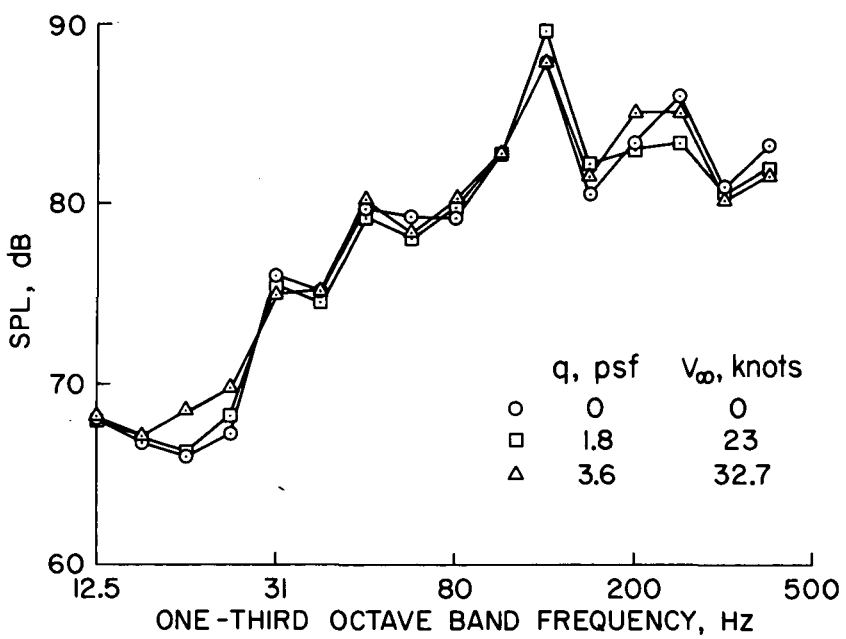

(c) Flap II, $\delta_f = 90°$, no pylon, 4000 rpm.

Figure 18.– Continued.

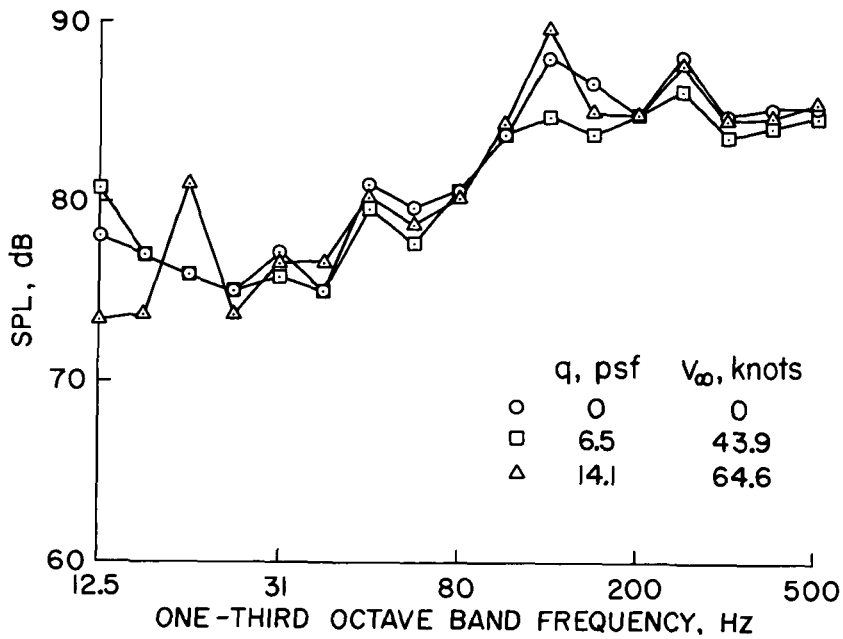

(d) Flap II, $\delta_f = 30°$, medium pylon, 5000 rpm.

Figure 18.– Continued.

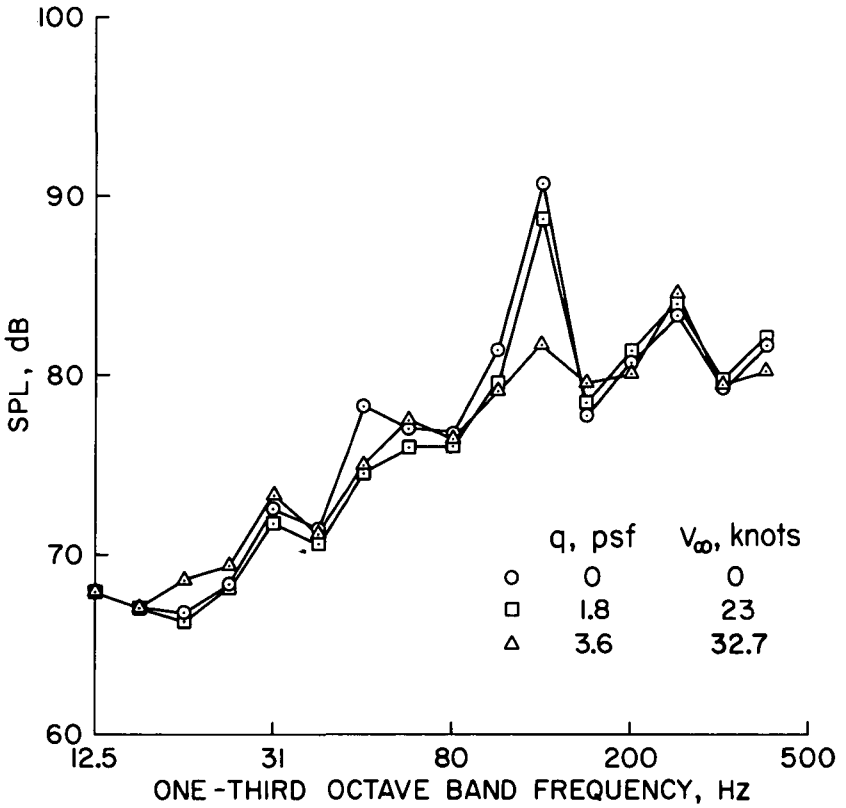

(e) Flap II, $\delta_f = 60°$, medium pylon, 4000 rpm.

Figure 18.– Continued.

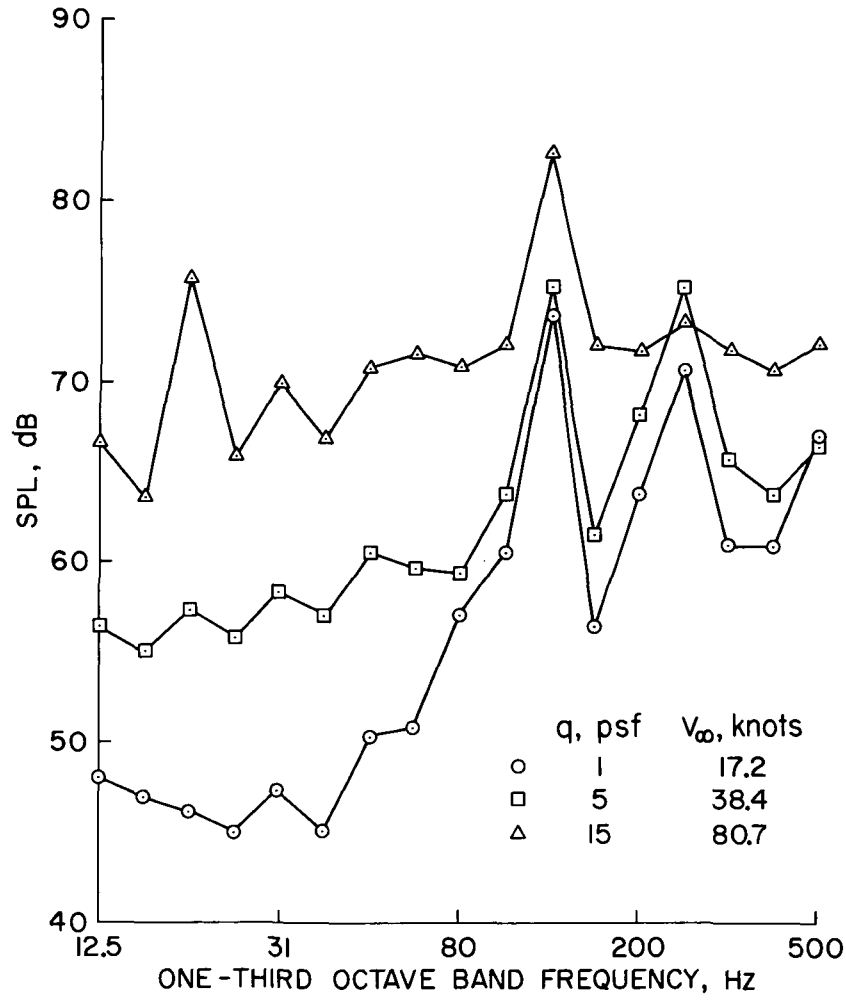

(f) Flap III, $\delta_f = 0°$, power off.

Figure 18.– Concluded.

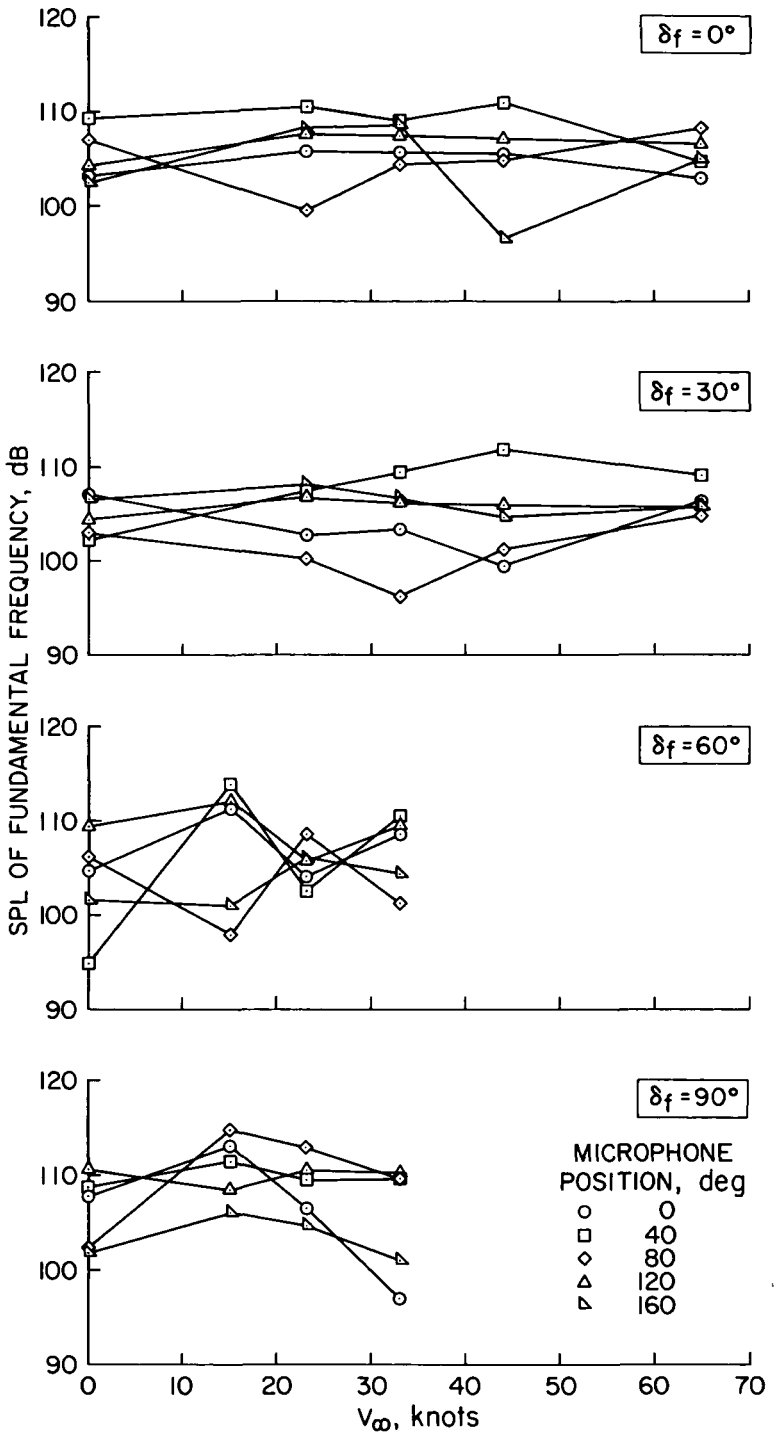

(a) Fundamental frequency.

Figure 19.– Variation of SPL of the fan tones with forward speed; flap II, medium pylon, 5000 rpm.

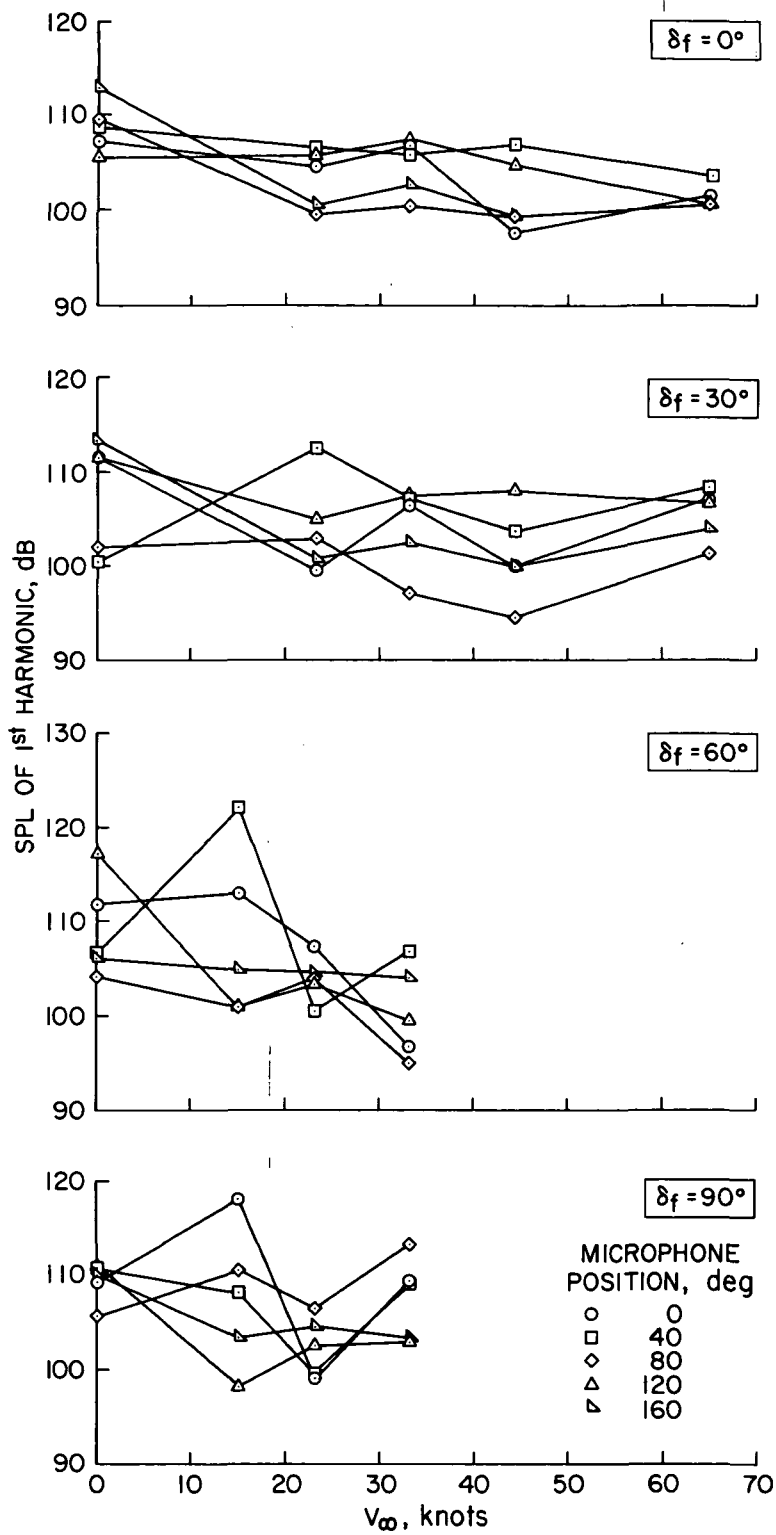

(b) First harmonic.

Figure 19.– Continued.

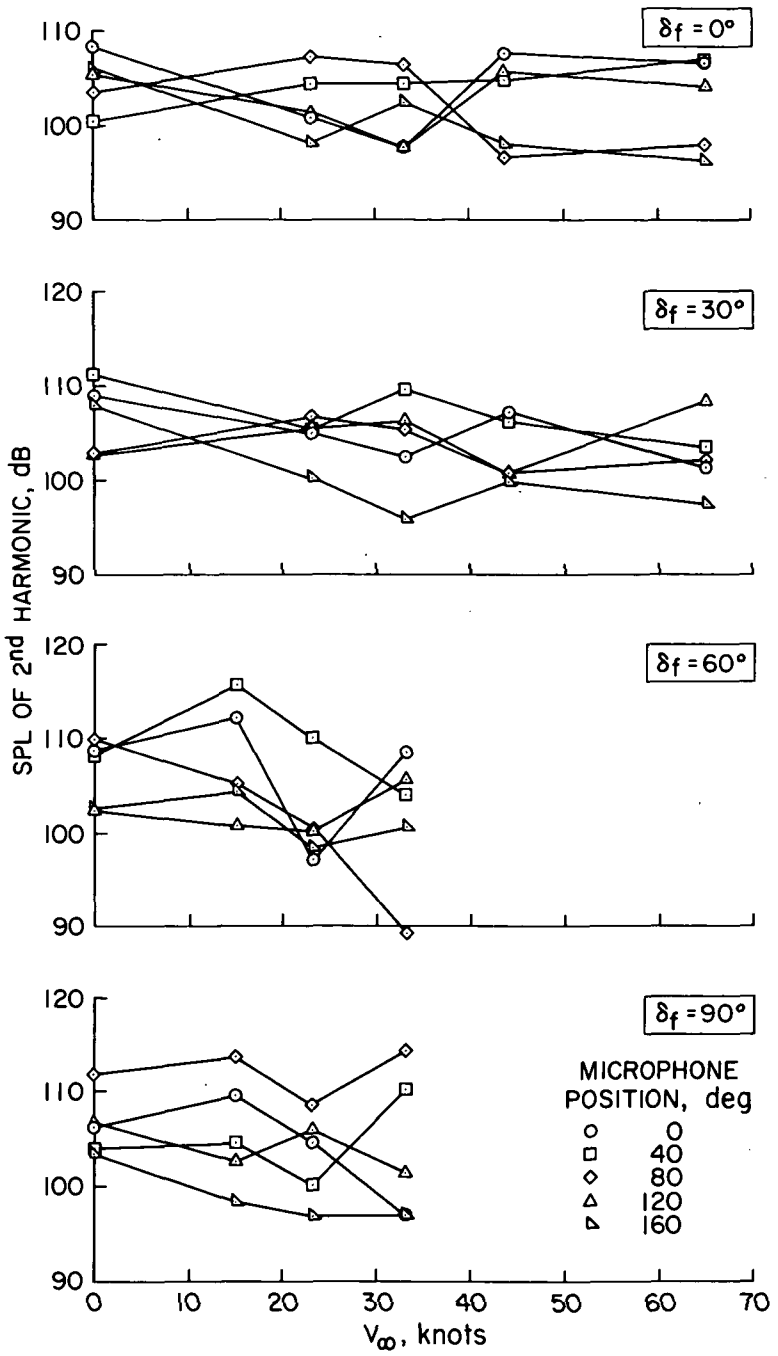

(c) Second harmonic.

Figure 19.– Concluded.

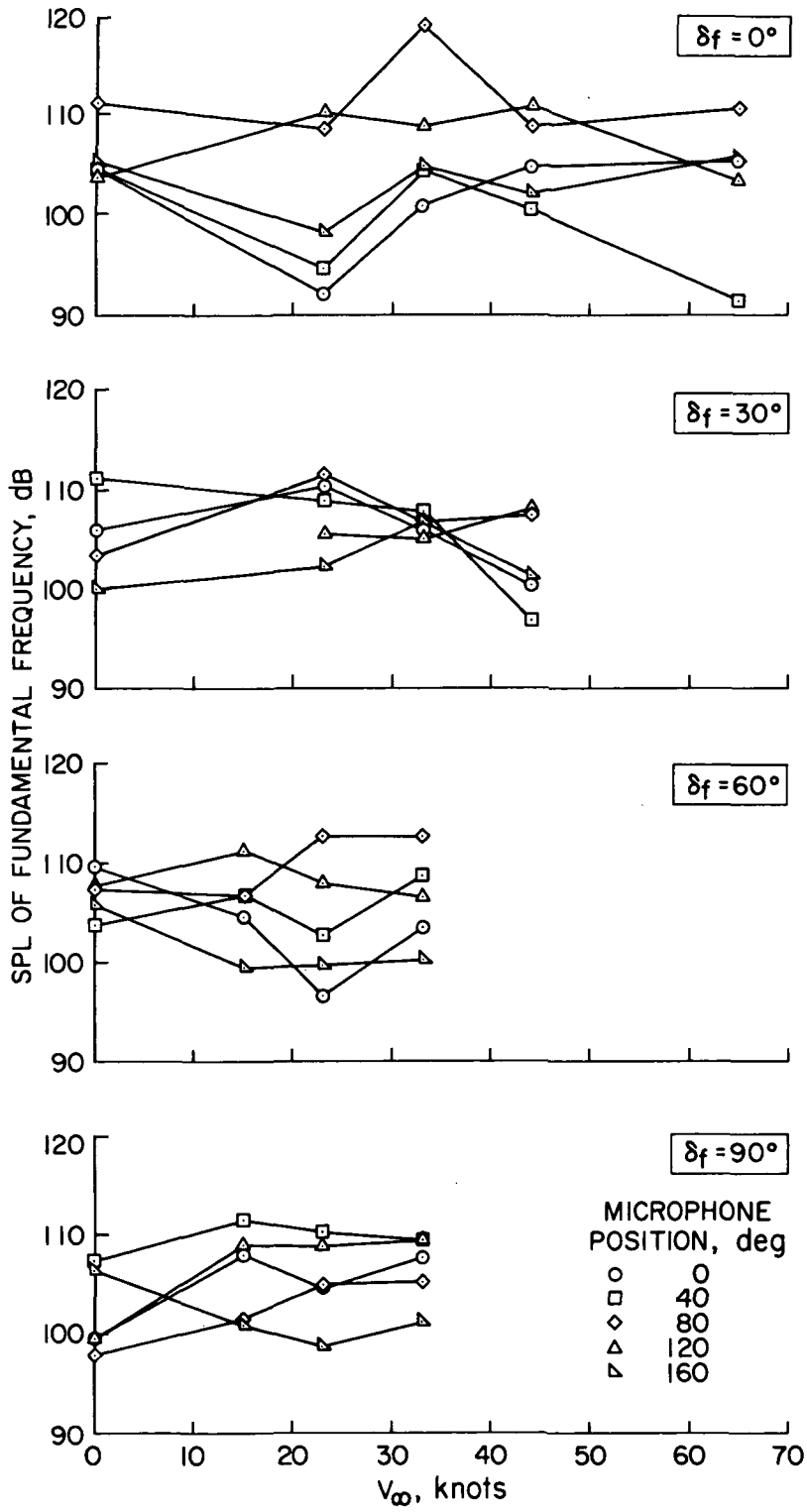

(a) Fundamental frequency.

Figure 20.– Variation of SPL of the fan tones with forward speed; flap II, no pylon, 5000 rpm.

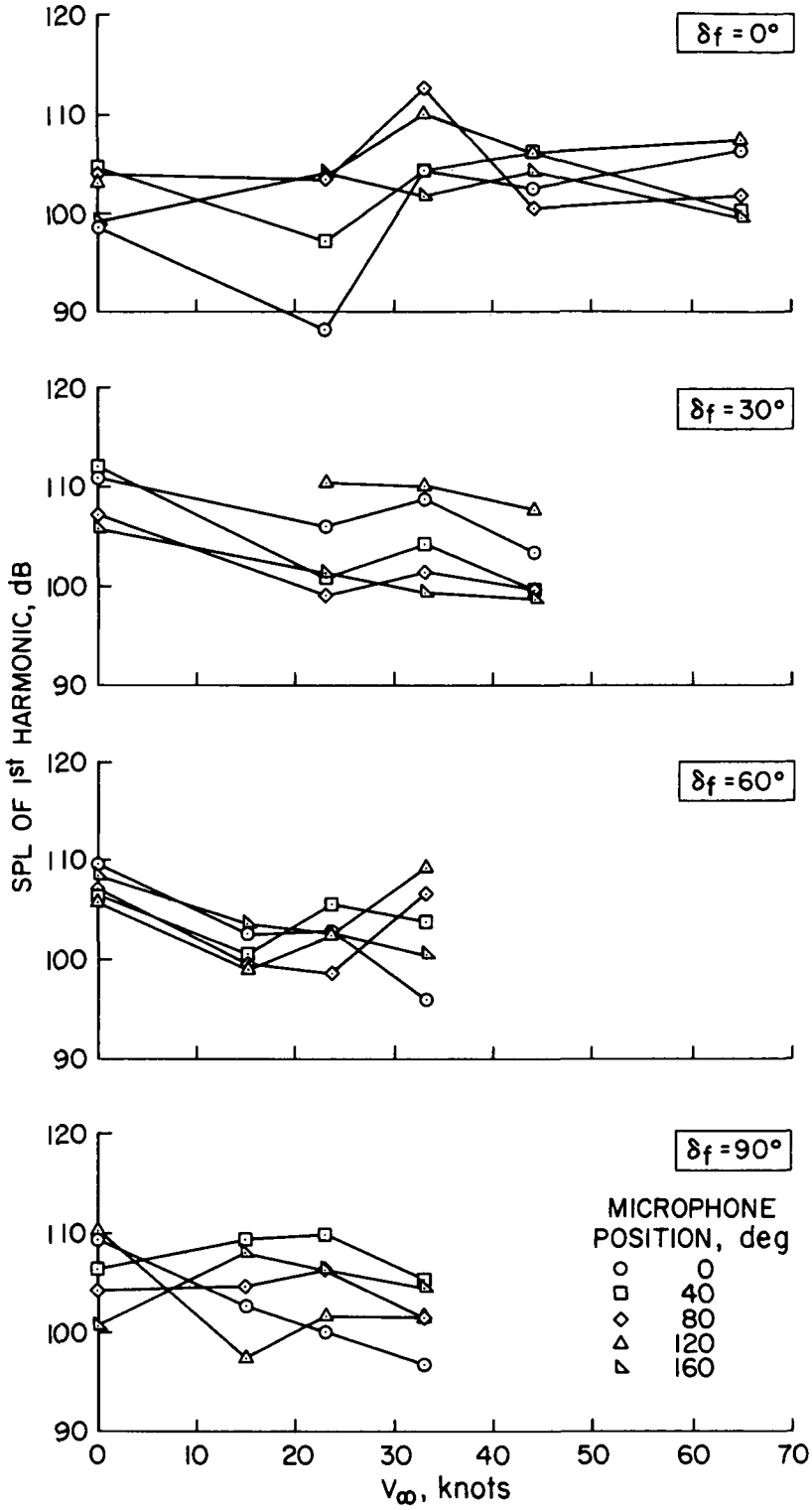

(b) First harmonic.

Figure 20.– Continued.

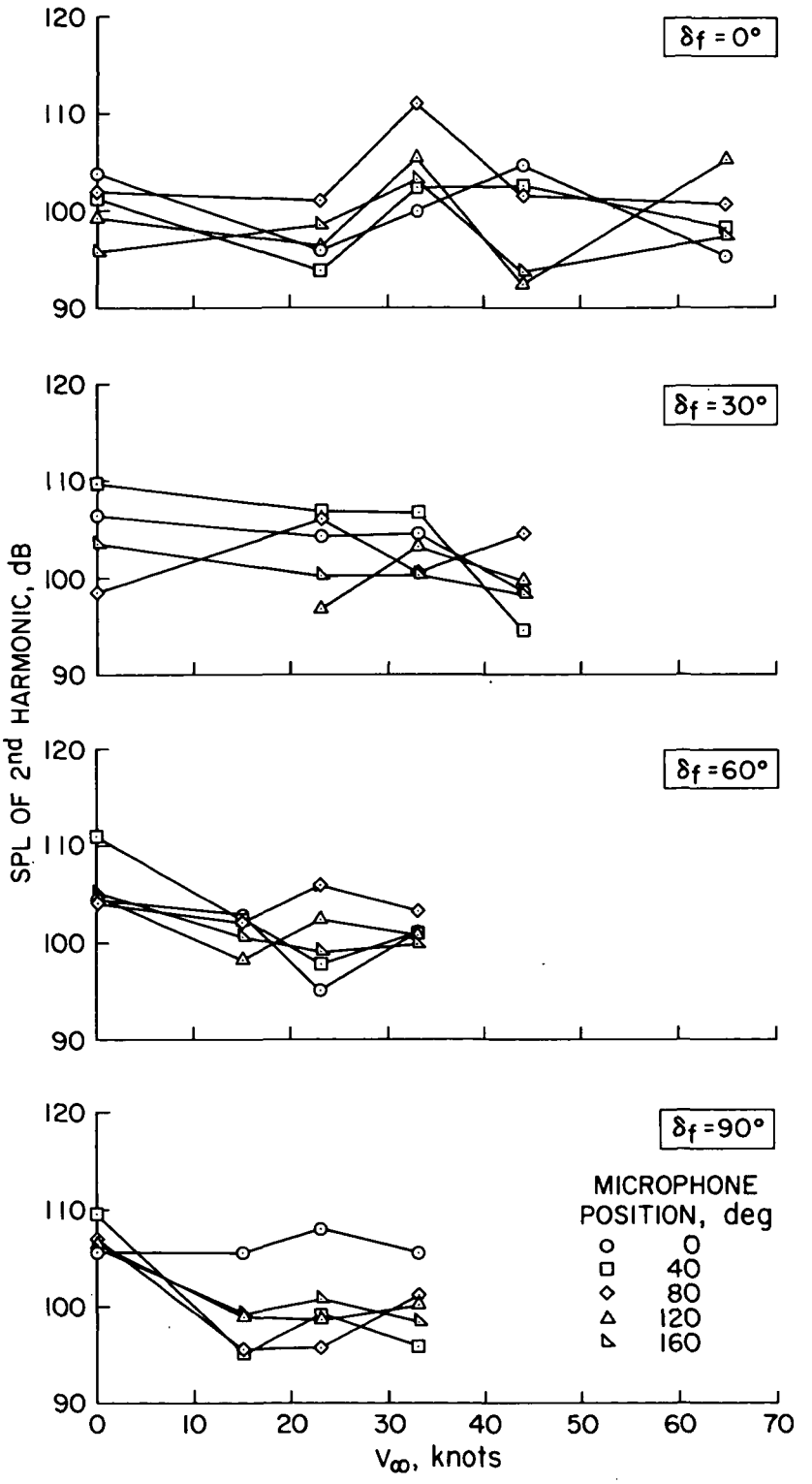

(c) Second harmonic.

Figure 20.– Concluded.

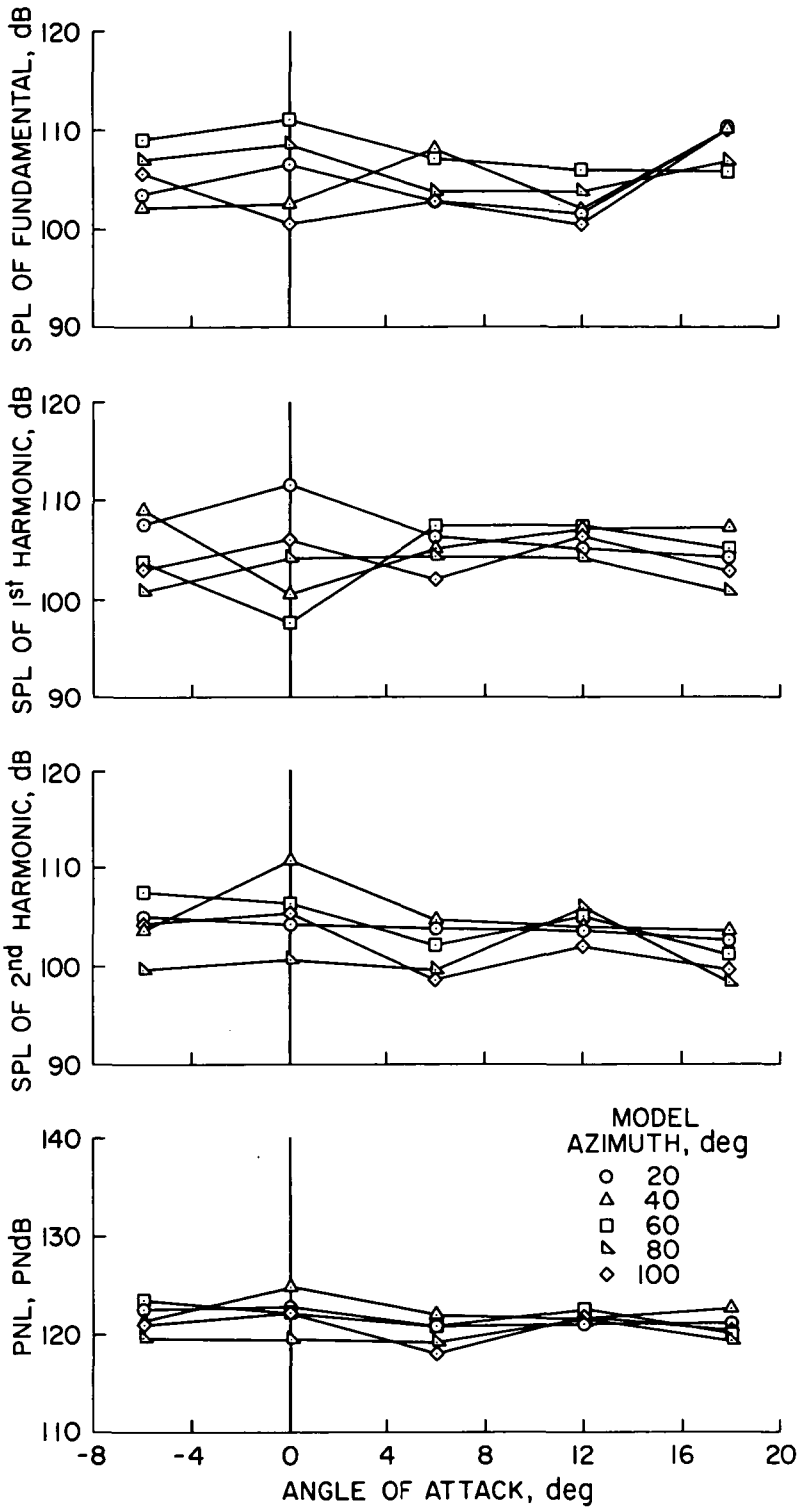

(a) Medium pylon, $\delta_f = 60°$.

Figure 21.– Variation of acoustic characteristics with angle of attack; flap II, $V_\infty = 23$ knots, 5000 rpm.

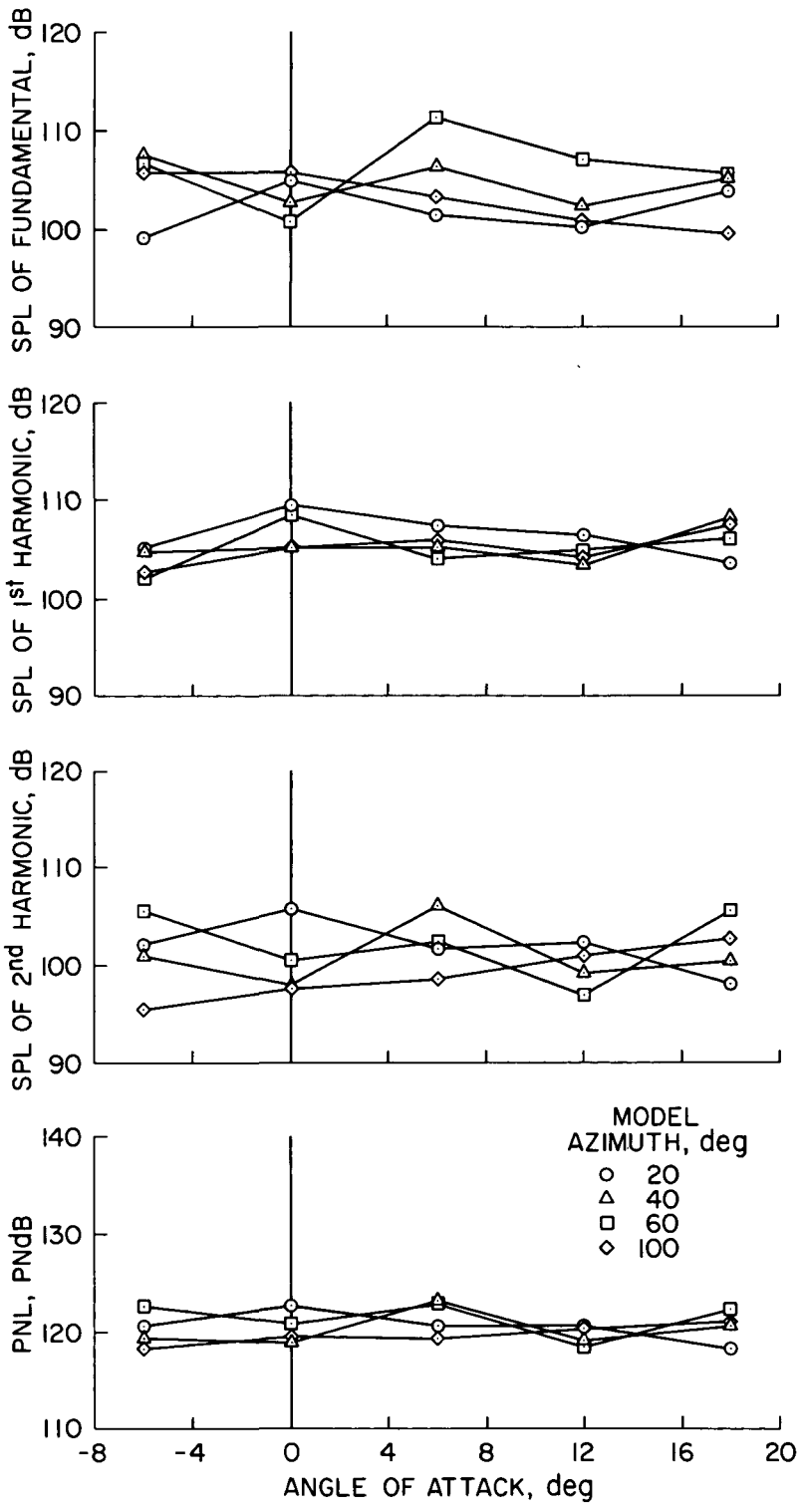

(b) No pylon, $\delta_f = 60°$.

Figure 21.– Continued.

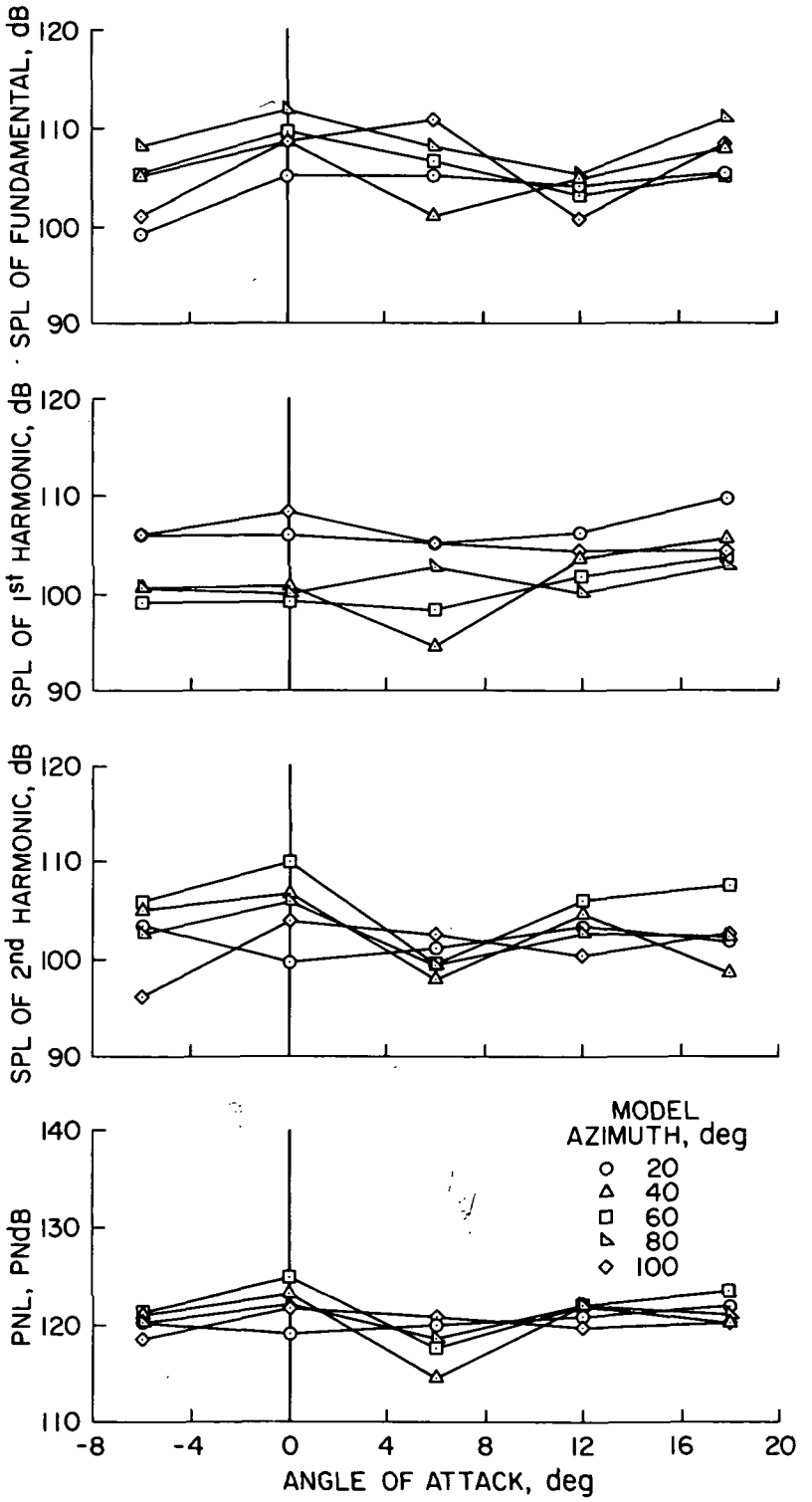

(c) No pylon, $\delta_f = 30°$.

Figure 21.– Concluded.

NATIONAL AERONAUTICS AND SPACE ADMINISTRATION
WASHINGTON, D.C. 20546

OFFICIAL BUSINESS
PENALTY FOR PRIVATE USE $300

SPECIAL FOURTH-CLASS RATE BOOK

POSTAGE AND FEES PAID
NATIONAL AERONAUTICS AND SPACE ADMINISTRATION
451

U.S.MAIL

POSTMASTER: If Undeliverable (Section 158 Postal Manual) Do Not Return

"The aeronautical and space activities of the United States shall be conducted so as to contribute . . . to the expansion of human knowledge of phenomena in the atmosphere and space. The Administration shall provide for the widest practicable and appropriate dissemination of information concerning its activities and the results thereof."

—NATIONAL AERONAUTICS AND SPACE ACT OF 1958

NASA SCIENTIFIC AND TECHNICAL PUBLICATIONS

TECHNICAL REPORTS: Scientific and technical information considered important, complete, and a lasting contribution to existing knowledge.

TECHNICAL NOTES: Information less broad in scope but nevertheless of importance as a contribution to existing knowledge.

TECHNICAL MEMORANDUMS: Information receiving limited distribution because of preliminary data, security classification, or other reasons. Also includes conference proceedings with either limited or unlimited distribution.

CONTRACTOR REPORTS: Scientific and technical information generated under a NASA contract or grant and considered an important contribution to existing knowledge.

TECHNICAL TRANSLATIONS: Information published in a foreign language considered to merit NASA distribution in English.

SPECIAL PUBLICATIONS: Information derived from or of value to NASA activities. Publications include final reports of major projects, monographs, data compilations, handbooks, sourcebooks, and special bibliographies.

TECHNOLOGY UTILIZATION PUBLICATIONS: Information on technology used by NASA that may be of particular interest in commercial and other non-aerospace applications. Publications include Tech Briefs, Technology Utilization Reports and Technology Surveys.

Details on the availability of these publications may be obtained from:

SCIENTIFIC AND TECHNICAL INFORMATION OFFICE

NATIONAL AERONAUTICS AND SPACE ADMINISTRATION

Washington, D.C. 20546